AN INVESTIGATION OF TWO MODES OF PLANT PROTECTION BY THE BIOCONTROL AGENT *Trichoderma virens*

A Dissertation

by

FRANKIE KAY CRUTCHER

Submitted to the Office of Graduate Studies of
Texas A&M University
in partial fulfillment of the requirements for the degree of

DOCTOR OF PHILOSOPHY

December 2011

Major Subject: Genetics

An Investigation of Two Modes of Plant Protection by the

Biocontrol Agent *Trichoderma virens*

AN INVESTIGATION OF TWO MODES OF PLANT PROTECTION BY THE BIOCONTROL AGENT *Trichoderma virens*

A Dissertation

by

FRANKIE KAY CRUTCHER

Submitted to the Office of Graduate Studies of
Texas A&M University
in partial fulfillment of the requirements for the degree of

DOCTOR OF PHILOSOPHY

Approved by:

Chair of Committee,	Charles M. Kenerley
Committee Members,	Daniel J. Ebbole
	Alan E. Pepper
	Won Bo Shim
Intercollegiate Faculty Chair,	Craig J. Coates

December 2011

Major Subject: Genetics

ABSTRACT

An Investigation of Two Modes of Plant Protection by the Biocontrol Agent *Trichoderma virens*. (December 2011)

Frankie Kay Crutcher, B.S., Montana State University

Chair of Advisory Committee: Dr. Charles M. Kenerley

The biocontrol fungus *Trichoderma virens* is an avirulent symbiont with the ability to control plant disease by the production of antibiotic compounds, induction of plant resistance to pathogens, and mycoparasitism of other fungi. In this document, the analysis of a putative terpene biosynthesis gene cluster (vir cluster) in *T. virens* is described. The vir cluster contains genes coding for four putative cytochrome P450s, an oxidoreductase, MFS transporter, and a terpene cyclase. To determine the function of this cluster in secondary metabolism biosynthesis, a strain of *T. virens* with a deletion of the putative cyclase, *vir4*, was constructed. Deletion mutants were deficient in the synthesis of sesquiterpene volatiles and complementation of *vir4* restored this loss in transformants, albeit at a lower level of production. An analysis of phenotypic characteristics between mutant and wild-type strains did not identify any differences when the strain interacted with other fungi, bacteria, or *Arabidopsis* seedlings.

Paralogs of the gene encoding the elicitor SM1 were examined as genetic sources for potential elicitors to induce systemic resistance in plants. A search of the *T. virens* genome revealed the presence of three paralogs of *sm1*. One paralog, *sm3*, was found to

be expressed when grown in association with plant roots and in still-culture. The *Pichia pastoris* protein expression system was used to generate sufficient quantities of SM3 to allow characterization of its function. The purified protein from the yeast system (picSM3) was shown to be glycosylated and to increase expression of a plant defense gene in maize seedlings. Mutant strains in which *sm3* was either deleted or over-expressed were constructed to further explore the potential of *sm3* as an elicitor of ISR. The differential production of SM1 and SM3 by these strains suggested that SM1 and SM3 may be co-regulated and native SM3 may be glycosylated.

To further understand the role of a putative glycosylation site as a mechanism to prevent dimerization and subsequent elicitor activity, a point mutation was created in a *sm1* deletion strain. Analysis of the behavior of the protein demonstrates that the putative glycosylation site is not involved in protein aggregation and deletion of this site does not prevent the protein from testing positive for glycosylation. We propose that SM1is not glycosylated but instead may interact with an oligosaccharide or other small molecule. However, the mechanism of dimerization in SM1 remains unknown.

DEDICATION

To my mother Laurie and my sister Melissa, for their love and support. Without your endless patience and encouragement none of this would have been possible.

ACKNOWLEDGEMENTS

I would like to thank my major advisor, Dr. Charles Kenerley, for his attention and guidance throughout my time in graduate school. I sincerely thank him for always pointing me in the right direction and providing an environment in which creative thinking and independence are encouraged. I believe my time in his laboratory has made me a better scientist and this work would not have been possible without him.

I would also like to thank the members of my committee, Dr. Daniel Ebbole, Dr. Won Bo Shim, and Dr. Alan Pepper for their time and effort during the course of my research. They forced me to face a tough lesson but I am all the better for it.

I would like to acknowledge Dr. Rustem Omarov and Dr. Lawrence Dangott for assistance with the protein work presented here and Ms. Suzanne Segner for providing some of the fungal strains. I would also like to thank Dr. Dennis Gross and Dr. Jessica Greenwald for providing the *Pseudomas syringae* strains and protocols.

A special thanks to Julie Campbell, Jessica Ciomperlik, and Dr. Veronica Ancona for their encouragement and emotional support these five years. To Martha Wight and Carlos Ortiz, thank you for the discussion, help, and much needed hugs throughout the writing of this manuscript. I am also grateful to my present and former lab mates Dr. Slavica Djonovic, Dr. Walter Vargas, Gloria Vittone Echeverria, Dr. Prasun Mukherjee, James Hurley, Cathryn Formichella, Mary Walker, David Laughlin, Dr. Natthiya Buensanteai, Dr. Maria Eugenia Moran Diez, and Dr. Sheng Li Ding for their friendship, endless discussions, and assistance with my research.

I also show special appreciation to the Department of Plant Pathology and Microbiology for all the help during the course of my time at Texas A&M University. I believe that at some point I have asked every single member of this department for their guidance or assistance, and their willingness to help and share their knowledge will always be appreciated.

This work was supported by the National Research Initiative Competitive Grants Program (grant no. 2008-35319-04470) from the USDA National Institute of Food and Agriculture, and the Texas Department of Agriculture and the US-Israel Binational Agricultural Research and Development Fund (grant no. TB-8031-08). Three years of fellowship support was also provided by a USDA National Needs Fellowship.

I am grateful for my family and friends who have supported me through every step of my journey and I hope to one day to give back all the inspiration you have given me. To my Sunday night grilling crew, Robert Vaughn, Sabrina Allen, Ashley Navarrette, Evan Blevins, and the Metzes, thanks for the food, the stress relief and the great conversation.

Most importantly I want to thank my mother and sister. There was never a time in which you did not believe in me, and I know with your love and encouragement I can accomplish the impossible. I would not be standing here today without you.

TABLE OF CONTENTS

CHAPTER Page

LIST OF FIGURES

FIGURE Page

LIST OF TABLES

CHAPTER I

INTRODUCTION

Members of the genus *Trichoderma* (the anamorphic form of *Hypocrea*) are ubiquitous soil fungi characterized by rapid growth, proliferation of conidia from highly branched conidiophores, conidia contained within green liquid, and production of chlamydospores. The ascospores where present are described as globose to subglobose, dark green, warted, two celled and contained within an ascus inside a perithecium (38). Although well known for their use in the generation of biofuels, food and industrial enzyme production, bioremediation of toxic compounds, and plant growth promotion (9, 75, 78, 112), *Trichoderma* ssp. are now known for their abilities as avirulent plant symbionts (44, 46). These beneficial fungi are currently employed as biocontrol agents in about 60 countries over 5 continents (75) resulting in a minimum impact on the environment and increased ecosystem sustainability (22, 75).

Trichoderma virens (telomorph *Hypocrea virens*) is an effective and commercially available biocontrol agent with activity against soilborne plant pathogens such as *Rhizoctonia solani*, species of *Pythium*, and *Sclerotinia rolfsii* (76, 134). The success of *T. virens* as a biocontrol agent is due to its ability to produce diverse antimicrobial secondary metabolites, parasitize plant pathogenic fungi, synthesize fungal cell wall degrading enzymes, rapidly and extensively colonize plant roots, and produce proteinaceous elicitors responsible for increased defense responses to pathogens in plants (28, 29, 49, 63, 76). These descriptions are similar for a few other species of

---

This dissertation follows the style of Applied and Environmental Microbiology.

Trichoderma; however, a genomic comparison with *T. atroviride* and *T. reesei* revealed that *T. virens* is genetically specialized for active predation of other fungi (31, 63). The use of antifungal secondary metabolites and cell wall degrading enzymes is distinct from *T. atroviride*, which uses parasitism as the primary mechanism and *T. reesei*, which essentially has lost the ability to parasitize other fungi. Additionally, the elicitors involved in inducing plant disease resistance appear to be different between *T. virens* and *T. atroviride*. The elicitor SM1 is primarily responsible for plant defense responses induced by *T. virens* (29, 30). The closely related homolog, EPL1, does not act as an elicitor, and the primary mechanism for inducing plant resistance to pathogens is still unknown in *T. atroviride* (115, 130). These significant differences in biocontrol activity between *T. virens* and other species of *Trichoderma* provide an opportunity to develop a deeper understanding of the complicated mechanisms by which biocontrol agents interact with plant hosts.

Biocontrol of plant pathogens by fungal antagonists at a commercial scale is a complex process and has been developed through direct and indirect approaches (20, 47, 134). The direct approach uses antagonistic fungi to compete with potential pathogens. This method requires the antagonist to interact with the pathogen or alter the potential substrate of the pathogen. In one case, the antagonist is selected based on its ability to rapidly colonize roots and compete with the pathogen in the rhizosphere for resources. The biocontrol agent may also produce antibiotics that inhibit growth or are toxic to the competing pathogen. And lastly, the antagonist may mycoparasitize the pathogen to obtain nutrients and destroy the pathogen inoculum. Indirect mechanisms involve

enhancing growth of the plant and/or inducing resistance to the pathogen through physical and chemical responses within the plant. *Trichoderma virens* is a model system for the study of biocontrol because of its ability to synergistically employ both direct and indirect strategies to manage plant disease (20, 46, 64).

Competition between biocontrol fungi and plant pathogens occurs for nutrients that are secreted by roots or in decaying organic matter on the root surface (rhizoplane), in small distances around the root (rhizosphere), and within discrete nutrient bundles in bulk soil. One of the most important of these nutrients is iron, which is limiting within the soil and important for fungal development. In the soil, iron can be chelated and absorbed by the secretion of microbial siderophores into the surrounding environment (90). Competition for iron was recently shown to be a key factor in biocontrol activity of *T. asperellum* against *Fusarium oxysporum f.sp. lycopersici*, the cause of wilt disease in tomato (113). In addition, the deletion of the intracellular siderophore, ferricrocin, lead to increased susceptibility to oxidative stress in *T. virens* (Mukherjee and Kenerley, unpublished). However, the role of intra- and extracellular siderophores in the biocontrol activity of *T. virens* has yet to be defined. Other compounds competed for by microbes in the soil environment are plant produced sucrose and other carbohydrates (10, 131). *Trichoderma virens* has developed a system to take advantage of the available sucrose secreted by plants that includes a intracellular invertase (*tvinv*) (131) and a sucrose transporter (*tvsut*) (129). Characterization of these two genes demonstrated that plant derived sucrose is crucial in the initiation of root colonization and led to the hypothesis

that a sucrose-independent signaling network is responsible for regulating symbiotic processes within *T. virens* (44, 129).

Species of *Trichoderma*, including *T. virens*, are well documented producers of numerous secondary metabolites with many of these possessing antibiotic activity (102, 119). Several of these, including peptaibols and gliotoxin, are biosynthesized by the action of nonribosomal peptide synthetases (NRPSs) (135, 141). In addition, *T. virens* secretes a number of cell wall degrading enzymes (CWDEs), such as chitinases, proteinases, and glucanases (28, 99), that may act synergistically with secondary metabolites to break down fungal cell walls (74, 98) and inhibit conidial germination of fungal plant pathogens (3).

Volatile secondary metabolites can also have inhibitory effects on plant pathogenic fungi (18, 56). The volatile organic compounds (VOCs) produced by *Muscodor albus* have been successfully tested for their use as mycofumigants against various soil borne plant pathogens (124). Other roles for VOCs produced by fungi include the attraction of insects responsible for spore dissemination (70) and a requirement for conidiation in some species of *Trichoderma* (91). Analysis of the VOCs produced from *T. atroviride* by headspace solid phase micro-extraction gas chromatography-mass spectrometry (HS-SPME-GCMS) demonstrated the production of 25 different volatile compounds represented by alcohols, ketones, alkanes, furanes, pyrones, monoterpenes, and sesquiterpenes (122). Analyses of volatile compounds in other species of Trichoderma have not been reported, and their genetic basis is poorly

understood. In Chapter II, I describe the analysis of VOC production, and the deletion of a terpene cyclase responsible for the production of sesquiterpene volatiles in *T. virens*.

Often the genes responsible for the biosynthesis of individual secondary metabolites in fungi are encoded within a contiguous gene cluster on a chromosome (59, 94). Examples of such clusters identified in *T. virens* include two clusters, each coding for the production of peptaibols: one containing the nonribosomal peptide synthetase (NRPS) *tex2*, a gene responsible for the production of two classes of peptaibols, 11 and 14-residue (89), and another containing the NRPS *tex1* encoding for the enzyme that biosynthesizes an 18-residue peptaibol (141). An analysis of the *T. virens* genome identified 18 polyketide synthases (PKSs), 28 NRPS, and 4 PKS/NRPS hybrid genes (63), which are all commonly associated with gene clusters (59). Biosynthetic gene clusters are regulated by pathway specific transcription factors usually located within the cluster and global regulatory factors such as *laeA* (151, 152). *LaeA* encodes for a protein methyltransferase with a high similarity to histone methyltransferases, which have important roles in regulation of gene expression through chromatin remodeling (11). LaeA and another protein, VELVET, form a complex in *Aspergilllus nidulans* (17). This interaction is responsible for the epigenetic regulation through chromosome remodeling mediated by LaeA (6). The VELVET gene (*vel1*), a homolog of *veA* in *A. nidulans*, is an important global regulator in secondary metabolism, mycoparastism, biocontrol efficiency, and spore development in *T. virens* (88). The gene encoding LaeA and its effect on regulation of secondary metabolism has not been studied in *T. virens*, but this

gene is highly conserved in filamentous fungi indicating it may play an important role in gene regulation in many other fungal species (6, 11).

The fungal hosts of *T. virens* are broadly represented among fungal and fungal-like organisms including *R. solani*, *P. ultimum*, and *Sclerotinia sclerotiorum* (20). The process of mycoparasitism by *Trichoderma* spp., including *T. virens*, follows several defined steps. Recognition of the competing fungus, followed by directional growth, occurs first (46). Constitutively expressed extracellular chitinases are produced in low levels and the bind the cell wall of the host resulting in release of cell wall oligomers from the target fungus, which are recognized by *Trichoderma* (21). Binding of these small molecules to G-protein coupled receptors allow for detection of cell wall fragments released by the competing fungus (31). The increased gene expression that results from this detection initiates the production and secretion of biologically active endochitinases (14). When contact and binding between the host and *Trichoderma* occurs, the hyphae of *Trichoderma* coil around the host, produce appressoria, and begin secreting cell wall degrading enzymes and antibiotic compounds (107, 110). These appressoria enable *Trichoderma* to enter the lumen of the host for nutrient acquisition.

In addition to the secretion of secondary metabolites, *Trichoderma* is known to protect plants through colonization of roots and stimulation of local and systemic resistance to pathogens (30, 147). Root colonization is a complex process that involves recognition mechanisms by both partners. Light and electron microscopy have shown that root colonization involves invasion of the root surface, but is limited to the first or second layer of cells (107, 147, 148). These observations are supported by the

examination of green fluorescent protein (GFP) labeled strains of *T. virens* during contact with maize roots (30). During this interaction, the fungus secretes cellulases allowing for penetration into the root (148). In response, the plant produces dense material at the sites of penetration in order to restrict fungal invasion and proliferation. The plant additionally produces chitinases and other hydrolases to aid in suppression of pathogenesis of the avirulent symbiont. Other proteins such as swollenin (12), hydrophobins (133), and endopolygalacturonase (responsible for the breakdown of pectins) (86) have been found to be involved in root colonization and deletion of genes encoding for these proteins resulted in significantly reduced root colonization.

Colonization of roots by *Trichoderma* generally results in positive impacts on plant growth, photosynthesis, and plant metabolism (24, 46, 75, 107, 131). Plants colonized by *Trichoderma* show increased shoot growth and depth of roots. The increase in root growth enhances drought tolerance and possibly resistance to compacted soils (45). Uptake of nutrients such as nitrogen is improved in colonized roots (150), which may increase the efficacy of fertilizers (45). Stimulation of *Arabidopsis thaliana* root growth colonized by *T. virens* has been linked with the production of an auxin related compound (24). Mutants of *A. thaliana* with a deletion of different auxin receptors were insensitive to the growth promoting effects of *T. virens*. In addition to the ability to stimulate root growth, association with *T. virens* increases photosynthesis and carbon production in the leaves (116, 131). Sucrose exuded from the plant roots and taken up by *T. virens* is an important part of this process. Strains with a deletion in *tvinv* were shown

to have a significant decrease in photosynthetic rates similar to those measured in the untreated control when compared with the wildtype strain.

Pathogens, physical damage from insects, some chemical treatments, and the presence of biocontrol agents may induce both localized and systemic resistance to pathogens (46, 93). This resistance can manifest as a hypersensitive response (HR), synthesis of antimicrobial secondary metabolites (phytoalexins), fortification of cell walls, and activation of defense genes (117). There are two pathways for this resistance: systemic acquired resistance (SAR) and induced systemic resistance (ISR). SAR is triggered by local infection which confers long term resistance systemically to subsequent infection from a large spectrum of pathogens including oomycetes, fungi, bacteria, and viruses (32). SAR can be characterized by the production of a large number of pathogenesis related (PR) proteins both locally and systemically. This accumulation is the result of the presence of salicylic acid (SA) and is required for resistance signaling. However, SA is not the signal responsible for systemic resistance. This signal has yet to be identified, but it is suspected that a lipid molecule may act as a mobile signal (79).

ISR results from root colonization by several species of avirulent rhizosphere bacteria (23, 117) and species of *Trichoderma* (30, 147, 149). Signal transduction during ISR is dependent on ethylene (ET) and jasmonic acid (JA) which is distinct from SAR signaling (117). This signaling pathway results in resistance to foliar bacteria, biotrophic, and necrotrophic fungi, priming of JA responsive genes, and increased formation of callose (114). Both the SAR regulatory element, NPR1, and the root specific transcription factor MYB72 are involved in ISR signaling. ISR induced by

Trichoderma spp. is a well studied phenomenon in the *T. asperellum*-cucumber system. When cucumber is inoculated with *T. asperellum* there is increased resistance to the bacterial pathogen *Pseudomonas syringae* pv. *lachrymans*, and during this process the concentration of SA is unaltered (118). Genes responsive to SA such as PR proteins (29, 30, 118) were not induced by *T. asperellum* indicating the SAR is not involved in this resistance. However, when a pathogen is introduced, the expression of genes for PR proteins is much higher than if the biocontrol agent or pathogen was used alone, indicating that *T. asperellum* primes the plant defense responses for a rapid response to pathogen ingress (118). When the JA inhibitor diethyldithiocarbamic acid and ET inhibitor silver thiosulfate were added, the resistance response was reduced indicating that both JA and ET are required for the biocontrol activity of *T. asperellum*. A gene involved in the production of JA, *lox1*, was also found to be induced in the roots as early as 1 hour after inoculation of the plant with *T. asperellum* (116, 118). Another gene found to be upregulated during the interaction between plants and *Trichoderma* spp. is phenylalanine ammonia lyase (*pal1)*. Examples of this have been demonstrated in cucumber (116), sunflower (67), and maize (30). This enzyme is the first step in the phenylpropanoid pathway, leading to the production of phytoalexins and is activated by JA/ET signaling. In maize, both *lox1* and *pal* are highly expressed when inoculated with *T. virens* (30). Increased expression is also observed when maize is treated with a protein produced by *T. virens*, SM1 (29). In both cases, increased expression of these genes coincided with increased resistance to *C. graminicola* (30, 130).

Resistance to pathogen attack is usually a response to a signaling molecule produced by an invading microorganism, called an elicitor, which can take the form of small metabolites, oligosaccharides, glycolipids, or peptides (126). This resistance response can occur in both host and non-host plants (92). Peptaibols, small peptides with antimicrobial activity, in some cases can elicit plant defense responses (19, 34, 135). Oligosaccharides and low molecular weight compounds released from both fungal and plant cell walls by the activity of *Trichoderma* enzymes may induce resistance (46, 144). Pathogen-associated molecular patterns (PAMPs) are pathogen surface derived molecules that bind to pattern recognition receptors (PRRs) which in turn trigger the expression of immune response genes and production of antimicrobial compounds (153). A microbe-associated molecular pattern (MAMP) is essentially the same as a PAMP, but is not restricted to pathogens. PAMPs and MAMPs are components of the plant immune system known as PAMP-triggered immunity (PTI). A second system of recognition and response to potential pathogens is effector triggered immunity (ETI). This system involves the R gene specific recognition of pathogen avirulence (Avr) genes, and often cultivar specific. MAMPs, PAMPs, and avirulence determinants are all considered to be elicitors due to their ability to induce resistance in the host plant. SM1, a proteinaceous elicitor from *T. virens* has been shown to prime host defenses in maize that result in increased resistance to the foliar pathogen, *C. gramincola*. Further research with SM1 has recently identified the protein as a MAMP due to its ability to induce a callose defense response in *A. thaliana* (Djonovic, unpublished). The identification of new MAMPs is an important goal in the field of biocontrol, and three paralogs to SM1 have

been detected within the genome sequence. Chapter III explores the possibility that these three proteins may have a role in fungus-plant interactions by acting as elicitors of ISR.

A MAMP is initially recognized by a PRR, which in turn triggers a mitogen-activated protein (MAP) kinase cascade resulting in the transcription of defense genes (15). In this cascade, a ras or rac-like GTPase is activated by binding of the MAMP to the receptor. This binding causes the phosphorylation of a MAPKKK, which phosporylates a MAPKK, which then phosphorylates a MAPK. The MAPK phosporylates a transcription factor within the nucleus, which allows for the transcription factor to bind to the promoter region of defense related genes. The *T. reesei* MAMP ethylene inducing xylanase (EIX) and its receptor in tomato, LeEIX2, is an example of a MAMP in fungal induced ISR (104). EIX binds to plant membranes (43, 104), which was eliminated in *LeEIX2* mutants (104). The binding of these two proteins signals the endocytosis of the protein complex, resulting in a defense response (5).

With the increasing world population and the decrease in the Food and Drug Association approved pesticides, biocontrol is becoming an increasingly important component of integrated pest management for its ability to decrease diseases in the field while promoting sustainable farming practices. *T. virens* represents a model system for the study of biocontrol mechanisms due to its ability to control plant pathogens by both direct and indirect methods. The annotation of the *T. virens* genome and the development of molecular biology tools for functional analysis and gene discovery presents an opportunity to study and improve biocontrol activity in *Trichoderma*.

My dissertation explores both direct and indirect methods of biocontrol by *T. virens* by investigating both secondary metabolism and ISR elicitor proteins. Chapter II focuses on a secondary metabolite gene cluster suspected to be involved in the production of terpenoid compounds through the deletion of a terpene synthase. The work presented in Chapter III demonstrates the ability of the SM1 paralog, SM3, to act as an elicitor and investigates the effect of deletion and over-expression of this gene in plant-microbe interactions. Chapter IV characterizes the role of a putative glycosylation site on the dimerization and subsequent elicitor activity of SM1.

CHAPTER II

A TERPENE CYCLASE, VIR4, IS RESPONSIBLE FOR SESQUITERPENE VOLATILE BIOSYNTHESIS IN THE BIOCONTROL FUNGUS *Trichoderma virens*

INTRODUCTION

Secondary metabolites produced by filamentous fungi are extremely diverse in structure and function, providing a source of novel compounds for pharmaceutical, agricultural, and medical markets (59, 94, 102). Compounds such as antibiotics (penicillin) and hormones (gibberellins) have yielded positive benefits in the areas of medicine and food production for many decades. However, mycotoxins, including fumonisins and aflatoxin, have substantial negative impacts on food production each year, and have the potential to negatively affect both humans and livestock. Other metabolites are important virulence factors for disease such as gliotoxin in mammals (*Aspergillus fumigatus*) and the metabolite produced by ACE1 in plants (*Magnaporthe oryzae*) (37, 94, 102).

Trichoderma spp. are considered to be an abundant source of secondary metabolites, producing more than 100 different compounds with some shown to have medicinal or agronomic importance (102, 119). As a member of this group, *T. virens* produces several secondary metabolites that are suggested to play a role in its ecological development (51). Examples of these compounds are gliotoxin and dimethyl gliotoxin (produced by "Q" strains), gliovirin and heptelidic acid (produced by "P" strains), and the steroid viridiol and its precursor viridin produced by both "P" and "Q" strains (51).

Gliotoxin and gliovirin are effective as an antimicrobial agents against a wide array of fungi including the primary pathogens of seedling diseases in cotton, *R. solani* and *P. ultimum* (49, 51). Viridin, another metabolite with antimicrobial activity, also possesses anticancer activity (55, 143). The derivative of viridin, viridiol, is produced by a reduction of viridin at carbon 3 in the steroid ring (58). Both viridin and viridiol belong to the furanosteroid class of compounds similar to steroids synthesized in mammals (87). Research indicates that viridin is secreted, transported back into the cell where it is reduced to viridiol, and finally released into the surrounding environment. The secretion of viridiol in the presence of seedling roots results in necrosis at the root tip, and has the potential to be developed as a bioherbicide (50, 58).

Volatile organic compounds (VOCs) represented by several chemical classes (eg. alcohols, aldehydes, esters and terpenes) are produced by many species of fungi including *Trichoderma* (13, 132). VOCs are involved in biological processes such as plant defense against predators, parasites and pathogens during biocontrol interactions, competition with other microorganisms, and production of reproductive structures in species of *Trichoderma* (13, 52, 119). *Trichoderma* spp. are commonly associated with rotting wood, and production of VOCs has been shown to inhibit the growth of competing basidiomycete wood decay fungi in this environment (13, 53). An analysis of volatile compounds produced by *T. atroviride* included alcohols, ketones, alkanes, furanes, pyrones, mono- and sesquiterpenes for a total of 25 fungal metabolites (122).

Often the genes responsible for secondary metabolite production are found in clusters. Examples of this arrangement include the aflatoxin gene cluster which contains

25 coregulated genes in *Aspergillus flavus*, the 11 genes required for trichothecene biosynthesis clustered in *Fusarium graminearum*, and a 7 gene cluster in *Gibberella fujikuroi* necessary for the production of gibberellin (152). The release of the *T. virens* genome (http://genome.jgi-psf.org) has allowed an exploratory analysis of the number and location of putative gene clusters in this biocontrol agent. The use of Secondary Metabolite Unique Regions Finder (SMURF) software (61), a tool for identifying regions of secondary metabolite gene clustering within a genome, revealed 39 gene clusters in *T. virens* that include PKS and NRPS genes (Kenerley, unpublished).

Previously, a gene cluster (vir cluster) was identified in the "P" strain IMI 304061 of *T. virens* by suppression subtractive hybridization with wild type strain against a non-conidiating mutant M7 deficient in secondary metabolite biosynthesis (87). The subtractive library created was sequenced and several full-length genes were identified as members of the cluster. These genes included three cytochrome P450s and a terpene cyclase. Sequencing of a cosmid containing the four genes demonstrated the presence of a glyceraldehyde phosphate dehydrogenase (GAPDH) at the 3' end of the cluster, but genes on the 5' end remained to be identified. The genes and organization of this cluster closely resembled that of an unannotated gene cluster in *A. oryzae*, the *G. fujikuroi* gibberellin cluster, and the *F. graminearum* trichothecene cluster. To elucidate the function of this gene cluster and determine the compounds produced, the putative terpene cyclase (*vir4*) was mutated by targeted gene disruption. Transformants positive for the deletion cassette were compared with the wild-type (WT) for production of secondary metabolites, biocontrol activity, growth, and conidiation.

MATERIALS AND METHODS

Fungal, bacteria, and plant materials. Two strains of *T. virens* were used in this study: Gv29-8 (wild-type) and Tv10.4 (an arginine auxotrophic strain) (4). Strains and transformants were maintained on potato dextrose agar (PDA) at 27ºC. Vogel's minimal medium (VM) (136) supplemented with 1.5% sucrose (VMS) was used to screen for deletion transformants and PDA with 100 mg/mL hygromycin (PDA-H)was used to screen *vir4* complemented strains.

Maize (*Zea mays* Silver Queen hybrid) seedlings were used as a host to determine gene expression of *vir4* in roots colonized by *T. virens*. Briefly, seeds were sterilized by treating with 70% ethanol for 5 minutes and 10% hydrogen peroxide for 2 hours, and then rinsed with distilled water. Surface disinfected seeds were planted in a 18X150 mm culture tube containing a 3:2 mixture (by weight) of a Lufkin fine sandy loam and fine sand (approximately 10g/tube). The sand soil mix was previously sterilized and 100 grams were mixed with 10 mL of water containing $1X10^7$ conidia per mL. Negative controls were treated with water only.

E.coli XL1-Blue Supercompetent Cells (Stratagene) were grown on LBA at 37ºC. Liquid cultures were grown at 250rpm and ampicillin (Research Products, Inc.) was used as a selective agent.

DNA manipulation. Genomic DNA from *T. virens* was extracted as previously described (145). Sequencing reactions were completed at the Texas A&M University Gene Technologies Lab. Southern blot analysis was performed according to a common protocol (108). Probes were labeled using Random Primer DNA Labeling Kit (Takara)

and Southerns were hybridized using Ultrahyb (Ambion) at 42ºC overnight. DNA amplified by PCR was purified using the Wizard® SV Gel and PCR Clean-up System (Promega). Plasmids were purified using the Wizard® *Plus* SV Miniprep kit (Promega).

Extraction of RNA and evaluation of *vir4* expression. At 36, 48, 72, 84, 108, and 120 hours post-planting, roots of maize seedlings were harvested, rinsed and tissue was ground in liquid nitrogen at each time point. Three biological replicates consisting of three plants each were assayed at each time point. Expression of *vir4* was examined when Gv29-8 was grown in the following media: (potato extract broth (PDB, Difco), molasses (MOL, 30g molasses and 5g yeast extract per L water), malt extract broth (MEB, Difco), Weindling's (WEI) (137), VMS, VM plus cellulose (VMC), *P. ultimum* cell walls (VMP), *R. solani* cell walls (VMR), VM glycerol (VMY), VM starch (VMSt), fructose (VMF), glucose (VMG), or galactose (VMGal). Cultures were grown in 100mL of each media inoculated with $2X10^6$ conidia/mL for three days at 27ºC and 135 rpm on a rotary shaker.

RNA from experiments was extracted using TRIZOL® reagent (Gibco-BRL), and DNA was removed from samples using the DNA-*free* kit (Ambion). The synthesis of cDNA was performed using the High Capacity cDNA Reverse Transcription Kit (Applied Biosystems). cDNA was subjected to PCR using the primers Vir4F (5'-CAACACTGCCTGTCATCGCTA-3') and Vir4R (5'CAGCCATCTTGGAGTGAGTCA-3') with 30 cycles (30 seconds at 95ºC, 30 seconds at 55ºC, and 1 minute at 72ºC). An exception was the root expression analysis in which 35 cycles was used. Histone (*h3*) was amplified as a control for even loading. The

primers for histone, H3F (5'-CCGTAAGTCACTGGTGGC-3') and H3R (5'-AGCTGGATGTCCTTGCTCTG-3') were used for a PCR reaction with 35 cycles (30 seconds at 95º, 30 seconds at 55ºC, and 1 minute at 72ºC).

Real-time quantitative PCR was performed to examine expression of genes within the vir cluster and to observe putative changes in a cyclase deletion mutant. Gv29-8 and Δvir4-137 were grown in PDB for three days. Tissue was washed, ground in liquid nitrogen, and RNA extracted using TRIZOL® reagent (Gibco-BRL). The DNA-freeTM DNase Treatment and Removal kit (Ambion) was used to removal any residual DNA. This RNA was used for quantitative real-time rtPCR of the gene cluster using actin (130) as a control reference. All primers used for real-time PCR in this study are presented in Table 2.1. The difference in expression of the cluster was examined using the Thermo Scientific Verso SYBR 1-Step QRT + Rox Kit. The real-time reactions was performed in a 25 uL reaction containing 1X Verso SYBR mix and 200 nM primers. Each reaction contained 100 ng total RNA and was loaded on the 7500 Fast real time PCR system (Applied Biosystems). Data were analyzed using three biological replicates, and the absence of primer dimers was confirmed by creation of a dissociation curve. The expression of each gene was normalized using the formula $2^{-\Delta\Delta_{C_T}}$ per manufacturers instructions (97).

Table 2.1 Primers used for qPCR analysis of the vir cluster.

Primer	Sequence (5' to 3')	Size
qVir1F	CCGCAAAGCTGACCAAGGT	54 bp
qVir1R	GCCATTGGCCTCGGTATG	
qVir2F	TTCAACGCCAAGAGCAATTG	61 bp
qVir2R	CCCCGGTCCAACGTTCA	
qVir3F	CCCAAAGCTGGCGACACT	58 bp
qVir3R	TGTTTGCAGAAGGGAGTTGCT	
qVir4F	TCGCAGCCGCAGATCTTC	57 bp
qVir4R	CCTCGACCCACTCTGATTCC	
qVir5F	CGTGCCGAGGTGAAACAAG	56 bp
qVir5R	CGGCGTTTCTCCAGAATAGG	
qVir6F	TCTTGGCGCTGGATTTCC	56 bp
qVir6R	CAACGCCCAGGCGATTATA	
qVir7F	ATCCTGTGCATGTCAAGCTTGT	60 bp
qVir7R	CCGGTCGCGCAAACA	
qGapdhF	TGGCATGTCTGTCCGAGTTC	57 bp
qGapdhR	CGGACCGTGAAGTCAACGA	

Construction of a gene phylogeny for *vir4* homologs. A protein BLAST was performed at the National Center for Biotechnology Information (NCBI) website (http://www.ncbi.nlm.nih.gov/) using the predicted amino acid sequence of *vir4*. The tree was constructed with PhyML 3.0 (42) after a sequence alignment using ClustalX (68). A sh-like aLRT statistical test for computing branch support was used for the tree construction (2). A maximum likely-hood phylogeny was constructed using PhyML software (http://www.atgc-montpellier.fr/phyml/) with a Blosum62 substitution model and a bootstrap of 100 (42).

Generation of *vir4* disruption and complementation vectors. The sequence of the *vir4* gene DQ456846 (87) from the *T. virens* strain IMI 304061 was used to BLAST against the *T. virens* Gv29-8 genome (http://genome.jgi-psf.org). One gene showed high nucleotide homology and was designated as *vir4*.

The *vir4* disruption vector (pFKC1) was constructed by cloning the upstream and downstream flanking regions of *vir4* into pJMB4 (4), which contains the *arg2* gene as a selectable marker for complementation of strain Tv10.4. The upstream region was inserted into the EcoRV site and the downstream region inserted into the SmaI site using blunt end cloning. Thymine tags were added to the blunt digestion sites by the addition of 0.1mM dTTPs, 2 units of Taq polymerase, and 1X pcr buffer to the digestion and incubated for twenty minutes at 72ºC. The pFKC1 vector was linearized at the *Apa*I restriction digest site for transformation into Tv10.4 strain (4).

To construct the *vir4* complementation vector (pFKC14), the *vir4* coding region along with the promoter and terminator regions were amplified using Phusion High

Fidelity Taq Polymerase (Finnzymes). Adenine overhangs were added to the amplified product by the following reaction. Four micrograms of purified DNA were combined with 0.2mM dATP, DNA taq polymerase (Promega), and 1X Taq polymerase buffer and incubated for twenty minutes at 72ºC. The reaction was used directly to clone into pGEM-T easy vector (Promega). To obtain complementation strains, pFKC14 and pCSN43, a vector containing the *hygB* gene as a selection marker, were co-transformed into the deletion mutant Δ*vir4-137*.

Transformation and screening of transformants. *T. virens* protoplasts were produced and transform using linearized DNA by the method of Baek and Kenerley (1998). Stable transformants were selected by sequential transfer of conidia to agar slants of VMS, PDA, and VMS. Viable transformants on the last round of VMS were screened by PCR using a primer upstream of the *vir4* region cloned into pJMB4, Vir4-11 (5'-CAACACGGCTTAGATTGAGTCA-3') and a primer within the *arg2* gene, Vir4-12 (5'-GGTGAGTCACGGTAACACC-3'). These primers were used to amplify a product specific for a homologous recombination event. PCR amplification was performed for 35 cycles with each cycle framed as 30 seconds at 95ºC, 30 seconds at 52ºC, and 2 minutes 30 seconds at 72ºC. Once positive transformants were identified from this screening, they were further analyzed with primers specific for *vir4* (Vir4F and Vir4R) to verify the deletion of the gene. Strains containing the correct insert, but without the 300 bp fragment of *vir4* were further analyzed by Southern blotting as shown in the figure on page 30.

To identify stable complementation mutants, conidia of isolated colonies were transferred sequentially from PDA-H, PDA, to PDA-H. Resulting stable transformants were initially screened by PCR using the primers Vir4F and Vir4R at conditions previously described.

Northern analysis of transformants. Northern analyses was performed to determine if gene transcripts in the vir4 deletion strains were absent and normalized in the complement strain. Strains were inoculated into PDB at 2.0X10^6 spores conidia/mL and grown for two days at 27ºC shaking at 135 rpm on an orbital shaker. Total RNA was extracted from harvested fungal tissue using TRIZOL® reagent (Gibco-BRL). RNA samples (10ug) were denatured and resolved in 1.5% agarose formaldehyde gel. The agarose gel was transferred to Hydrobond-N+ nylon membrane (Amersham Biosciences, UK) and hybridized overnight using Ultrahyb (Ambion) at 42ºC. The 300 bp probe amplified from genomic DNA using Vir4F and Vir4R primers was labeled using the Random Primer DNA Labeling Kit Ver. 2 (Takara) and added during the hybridization. A 400 bp amplicon of the constitutive gene *h3* (used for even loading) was amplified from genomic DNA using the primers H3F and H3R.

Measurement of secondary metabolite production in *vir4* transformants. The arginine deficient mutant Tv10.4 and Δvir4-137 were grown in malt extract broth (MEB) for 4 days, and culture filtrate was extracted using ethylacetate. Samples were air dried, resuspended in methanol, and 20 uL was spotted on a TLC Silica gel 60 F_{254} plate (EMD). A mobile phase of 70:30:0.5 chloroform:acetone:formic acid was used to separate samples on the TLC plate. The plate was allowed to dry, viewed at a UV of 254

nm, and photographed. In addition, Gv29-8, three *vir4* deletion mutants (Δvir4-61, Δvir4-87, Δvir4-137) were grown in PDB for three days, and culture filtrate was extracted as above. Resuspensions in methanol were provided to Drs. Robert Stipanovic and Lorraine Puckhaber (USDA-ARS-Southern Plains Agricultural Research Center) for analysis by high pressure liquid chromatography (HPLC).

Analysis of volatile production in *vir4* transformants by HS-SPME-GCMS. To investigate volatile production in Gv29-8 and mutants deficient in *vir4* expression, strains (Gv29-8, Tv10.4, Δvir4-87, Δvir4-137, vir4c12, and vir4c32) were sent to the laboratory of Dr. Rainer Stoppacher (Center for Analytical Chemistry, University of Natural Resources and Life Sciences, Vienna). Strains were grown for four days on PDA slants within HS vials and subjected to headspace solid phase microextraction (HS-SPME) coupled with gas chromatography-mass spectrometry (GC-MS) analysis as previously described (122). A SPME headspace autosampler extracted volatiles which were transferred to the GC-MS system for measurement and identification.

Growth assays of transformants. Growth of transformants was determined on MEA, PDA, VMS, VMG, and VML. Wild-type and transformant strains were grown on PDA and 3mm plugs were removed from the actively growing edge of the colony and placed in the center of the test media. Measurements of the colony diameter were recorded at 24, 48, and 72 hours. Diameters recorded at the 48 hour time point were recorded. The mean and standard deviation were calculated for all conditions using Microsoft Excel.

Effect of volatiles from *T. virens* on the growth and germination of *Arabidopsis thaliana*. To determine if the sesquiterpene volatiles produced by *T. virens* have an effect on root/shoot growth or germination of *Arabidopsis* seedlings, conidia of wild-type (Gv29-8) and two *vir4* mutants (Δvir4-87 and Δvir4-137) were spread on a PDA plate. After 24 hours of incubation at 27ºC, the fungal plates were placed in plastic bags with *Arabidopsis* seedlings growing on Murashige and Skoog (MS) basal medium plus Gamborg's vitamins (Sigma) and 0.75% agar. The plated seeds were incubated in the presence of the fungus (a uninoculated PDA plate served as a negative control) for three days. Seedlings were evaluated for germination and shoot and root growth.

Swarming by *Pseudomonas syringae* pv. *syringae* B728A in the presence of *T. virens* during volatile production. Swarming of *P. syringae* (kindly provided by Dr. Gross, Texas A&M University) was evaluated using a motility assay (100). A colony of *P. syringae* was grown overnight at 25ºC with shaking at 250 rpm in 2 mL of nutrient broth yeast extract (NBY). The culture was then pelletted by centrifugation at 9000 rpm for 30 seconds and resuspended in NBY. Six microliters was used to inoculate 2 mL NBY, and the culture was grown until an OD600=0.3 (equivalent to 5X10^8 colony forming units) was obtained. After 5 to 10 hours, cells were pelletted and resuspended in 10 uL sterile water. The resulting solution was dropped on a sterile filter disk in the center of a semi-solid PDA plate (0.4% agar). Cultures were incubated in a sealed bag with a 24-hour-old spread plate PDA of *T. virens*. An uninoculated PDA plate was used as a negative control. At 16 hours the swarming of *P. syringae* was observed and photographed.

Confrontation between a *vir4* deletion mutant and soil dwelling fungi. Strains of Gv29-8, Δvir4-137, *R. solani*, *Sclerotinia minor*, *P. ultimum*, *T.virens* GVP, *Sclerotinia sclerotiorum*, and *A. nidulans* were grown on PDA. A 3mm plug was removed from the perimeter of an actively growing colony and placed near the edge of a fresh PDA plate. Plugs from the wild-type and mutant were allowed to grow 24 hours prior to inoculation with the test fungi. Gv29-8 and Δvir4-137 were paired with all test fungi and cultures were allowed to grow for 72 hours. Experiments were completed in triplicate and observations of growth characteristics and inhibition were made every 24 hours.

RESULTS

The identification of the terpene cyclase *vir4* in *T. virens* Gv29-8. A BLAST search of the JGI annotated *T. virens* genome sequence revealed the presence of the *vir4* coding region (protein ID 56195) in Gv29-8. The three putative cytochrome P450s (*vir1*, *vir2*, and *vir3*) and the glyceraldehyde phosphate dehydrogenase (GAPDH) identified previously (87) were also present (Figure 2.1). Located within the cluster region were an additional putative CP450 (*vir5*), a major facilitator superfamily (MFS) transporter (*vir6*), and an oxidoreductase (*vir7*).

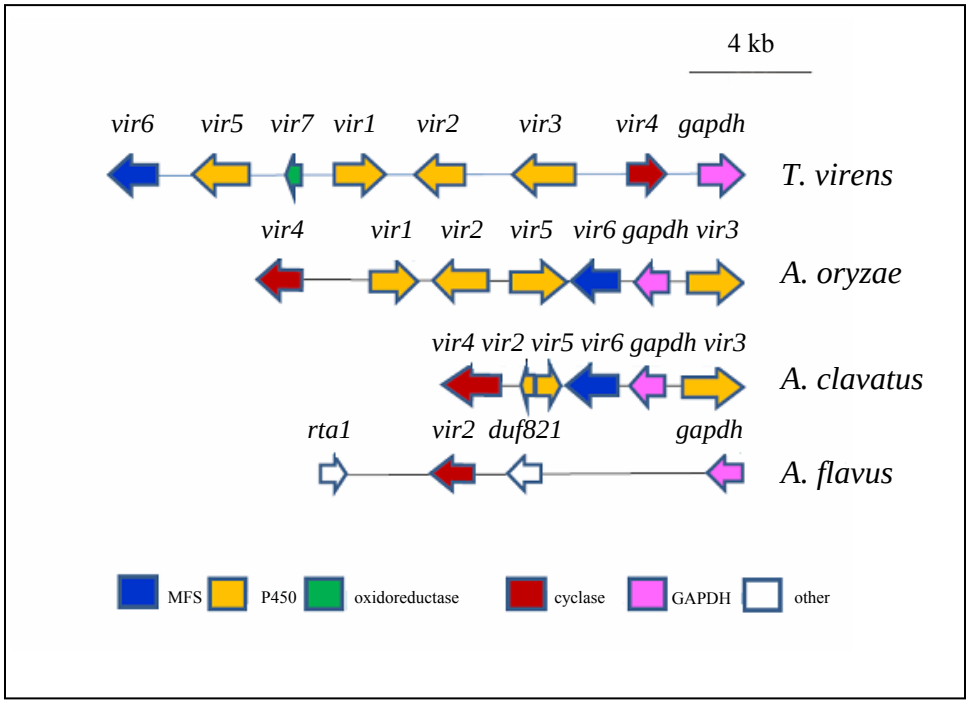

FIG. 2.1. Scheme representing vir gene cluster homology. A representation of the *T. virens* vir cluster aligned with clusters of homologous genes in *A. oryzae*, *A. clavatus*, and *A. flavus*. The color of the arrow denotes predicted function. Arrow direction indicates 5' to 3' coding orientation. Color of arrow corresponds to predicted function listed in colored boxes.

A BLAST analysis of the NCBI database (http://www.ncbi.nlm.nih.gov) demonstrated several homologous sequences of the *vir4* gene in different fungi. The predicted protein sequences were used to construct a gene phylogeny (Figure 2.2) along with class I terpenes from *T. virens* and other species of *Trichoderma*. Protein sequences were aligned in ClustalX2 and the gene phylogeny was generated in PhyML (http://www.atgc-montpellier.fr/phyml/) with a bootstrap of 100 (42). The phylogeny indicated that *vir4* from *T. virens* clustered together with *A. oryzae*, *A. clavatus*, and *A. flavus* instead of cyclases from other species of *Trichoderma*, including other homologs found in *T. virens*. Clustering of protein sequences from species of *Aspergillus* was also

observed in gene phylogenies for the CP405s in the cluster including VIR1, VIR2, VIR3, VIR5 (data not shown) as well as the GAPDH protein sequence. The MFS (VIR6), however, showed considerable variability across all species examined.

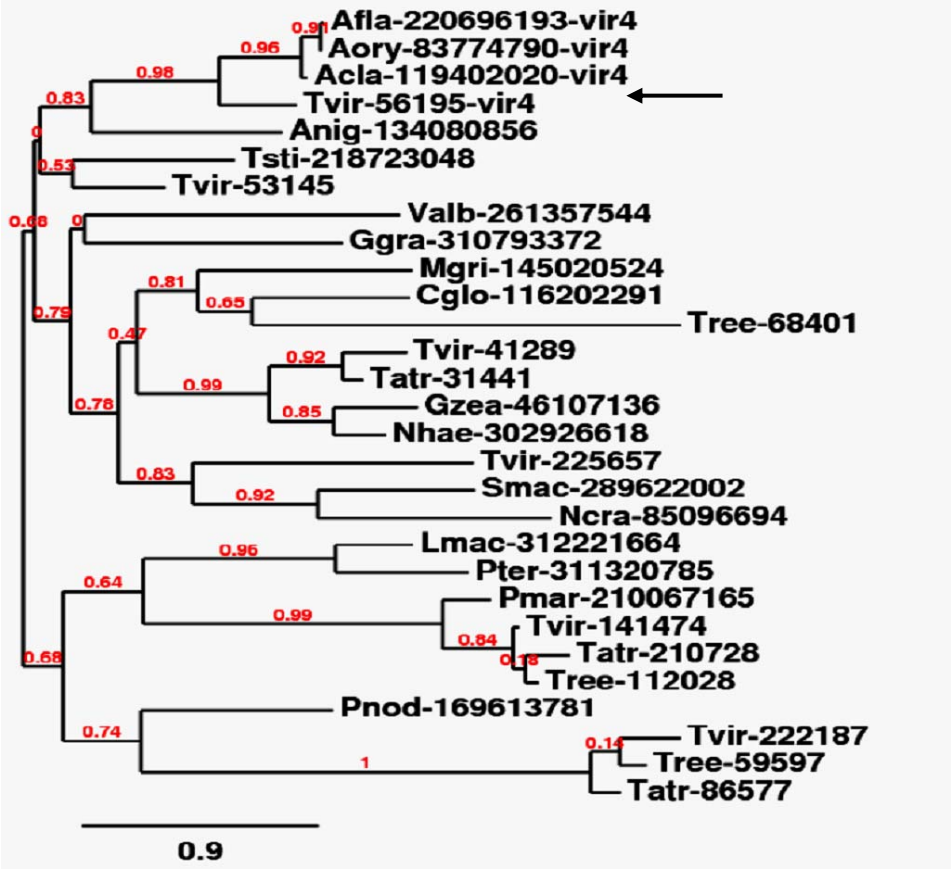

FIG. 2.2. Gene phylogeny of *vir4* cyclase homologs. Protein sequences obtained from an NCBI BLASTP search along with the class I cyclase protein sequences from *T. virens*, *T. atroviride*, and *T. reesei* were entered into a PhyML maximum-likelihood software with a bootstrap of 100 (corresponding numbers in red). Fungal species used for the tree construction were *Aspergillus flavus* (Afla), *Aspergillus oryzae* (Aory), *Aspergillus clavatus* (Acla), *Trichoderma virens* (Tvir), *Aspergillus niger* (Anig), *Talaromyces stipitatus* (Tsti), *Verticillium albo-atrum* (Valb), *Glomerella graminicola* (Ggra) , *Magnaporthe grisea* (Mgri), *Chaetomium globosum* (Cglo), *Trichoderma atroviride* (Tatr), *Gibberella zeae* (Gzea), *Nectria haematicocca* (Nhae), *Sordaria macrospora* (Smac), *Neurospora crassa* (Ncra), *Leptosphaeria* (Lmac) , *Pyrenophora teres* (Pter), *Trichoderma reesei* (Tree), and *Phaeosphaeria nodorum* (Pnod). Numbers following abbreviated names correspond to protein ID numbers.

A survey of the filamentous fungal genomes available (approximately 50) on Joint Genome Institute (http://genome.jgi-psf.org) , Broad Institute (http://www.broadinstitute.org/) , JCVI/TIGR (http://www.jcvi.org/), and the Sanger Center (http://www.sanger.ac.uk/) websites, and found that only a few species of *Aspergillus* (*A. oryzae*, *A. clavatus*, and *A. flavus*) contained homologs of more than one member of the vir cluster located together on the genome (Figure 2.1). However, this cluster was absent in other members of *Aspergillus* (*A. nidulans*, *A. fumigatus*, *A. terreus*, and *A. niger*) queried. Surprisingly, no genes with strong homology to *vir4* or other members of the gene cluster were found in *T. atroviride* or *T. reesei* (http://genome.jgi-psf.org). Almost the entire cluster was present in *A. oryzae* with the exception of *vir7*, while the number of genes varied in *A. clavatus* and *A. flavus*. The individual genes in this case appear to have undergone rearrangement so that members of the cluster are not present in the same order (Figure 2.1).

Expression analysis of *vir4*. A time course analysis of *vir4* gene expression during root colonization by *T. virens* at 36, 48, 72, 84, 108, and 120 hours was completed to determine the likelihood that *vir4* was involved in plant microbe interactions. Expression of *vir4* was not observed at any time point (rt-pcr, 30 cycles, data not shown). The results were similar when the cycle number was increased to 35 for the PCR reaction (Figure 2.3). This indicates that *vir4* is not expressed during root colonization of maize seedlings by Gv29-8 during the time points collected. These data are similar to that found by RNA-Seq (Illumina®) for expression of genes in fungal

tissue associated with plant roots in hydroponic growth conditions (Kenerley, unpublished). Under these conditions, *vir4* showed very low normalized counts indicating little to no expression in planta.

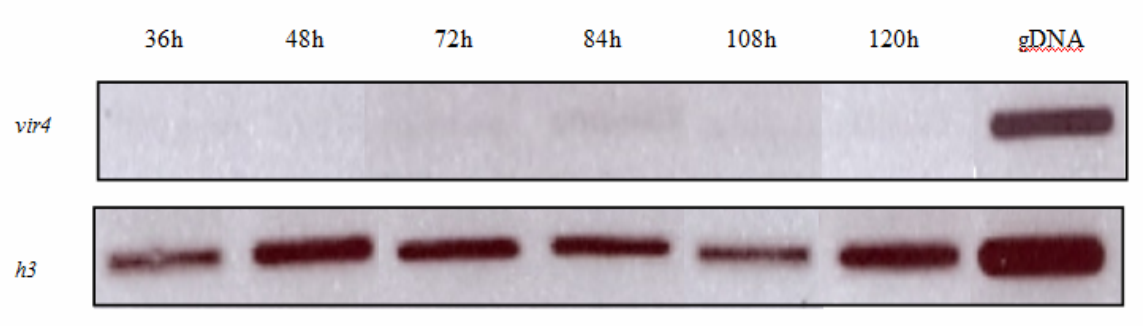

FIG. 2.3. Time course evaluation of *vir4* expression by rtPCR. Maize root tissue for RNA extraction was collected at 36, 48, 72, 84, 108, and 120 hours after planting maize seeds in soil infested with *T. virens* conidia. The histone gene from *T. virens*, *h3*, was used as a loading control.

When Gv29-8 is grown in different media, *vir4* was expressed but the intensity was medium dependent. The greatest level of expression was observed in PDB and MOL while the lowest expression was noted in VMC, VMP, and VMR. MEB, WEI, VMY, and VMSt each had low levels of expression (Figure 2.4). Under other sole carbohydrate conditions such as sucrose, fructose, glucose, and galactose no expression was observed (data not shown).

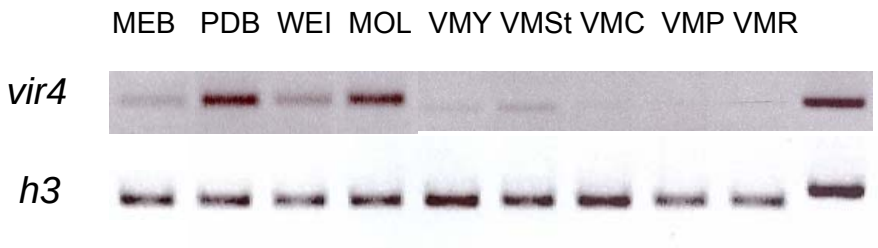

FIG. 2.4. Expression analysis of *vir4* when grown with different media. Gv29-8 was grown for 3 days in MEB, PDB, WEI, MOL, VMY, VMst, VMC, VMP, or VMR. RNA was extracted for rtPCR analysis. Histone (*h3*) was used as a loading control.

Identification and screening of *vir4* deletion and complementation transformants. The *vir4* deletion vector pFKC1 was used to replace the *vir4* open-reading frame with the arginine-specific carbamoyl-phosphate synthetase coding region (Figure 2.5A). One hundred and fourteen stable transformants were screened for insertion of the *arg2* cassette in place of the *vir4* coding region by PCR (data not shown). Transformants with loss of the *vir4* coding region were further evaluated by Southern blot (Figure 2.5B). The three transformants (61, 87, and 137) were all negative for the 1.3 kb band associated with the *vir4* coding region. All three did contain the 4.2 kb band from the deletion cassette. The transformant Δvir4-87 contained three extra bands on the blot (5000 bp, 2500 bp, and 650 bp). Only the *vir4* complements vir4c12 and vir4c32 contained both bands. An extra band at 575 bp was observed in vir4c32.

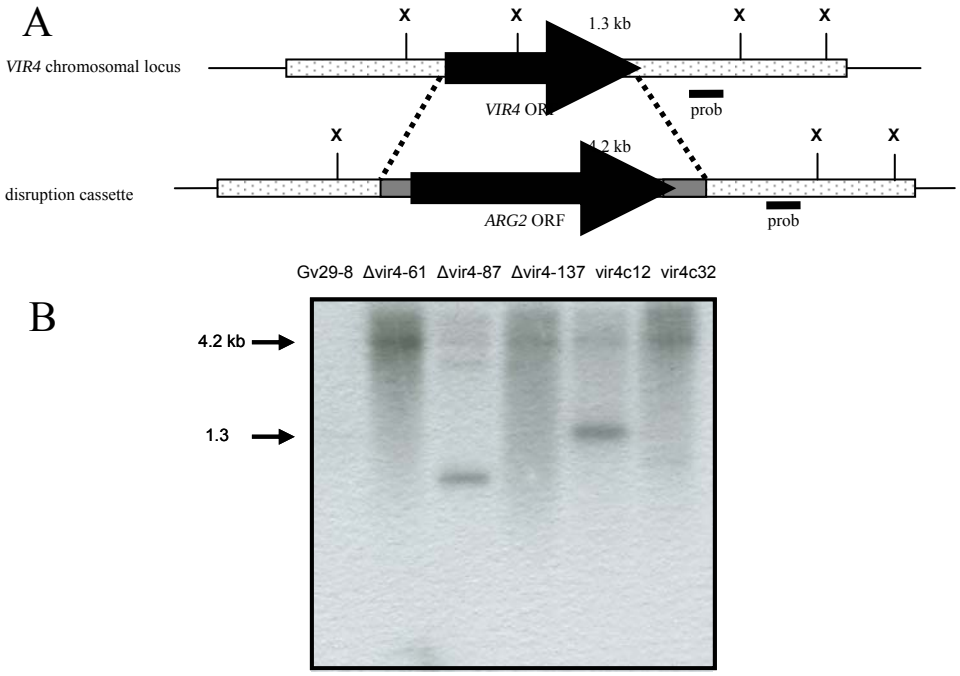

FIG. 2.5. Southern analysis and confirmation of *vir4* transformants. (A) Scheme of the gene deletion strategy. The *vir4* open reading frame is replaced by a homologous integration event with a 3.0 fragment of the *ARG2* gene from *T. virens* (4). A 1.3 kb band would result in *T. virens* wild-type strain and a 4.2 kb fragment in the deletion strains when digested with *Xba*I (X). (B) Southern analysis of *T. virens* wild-type and *vir4* deletion strains (Δvir4-61, Δvir4-87, and Δvir4-137) and *vir4* complementation strains (vir4comp-12 and vir4comp-32). DNA was hybridized using a *vir4* probe (327bp) indicated in figure A. Numbers on the right indicated expected size in native and deletion events.

Transformants for *vir4* complementation were screened by PCR for both the presence of the deletion cassette and the complementation cassette (Figure 2.6A). These transformants were then grown in PDB for 3 days, RNA was extracted and analyzed for expression of *vir4* by rtPCR (Figure 2.6B). Two transformants, vir4c12 and vir4c32, were positive for expression of the cyclase gene and were further analyzed by Southern blot (Figure 2.5B). The vir4c12 complement showed reintegration of the *vir4* gene and the vir4c32 complement was negative for proper insertion.

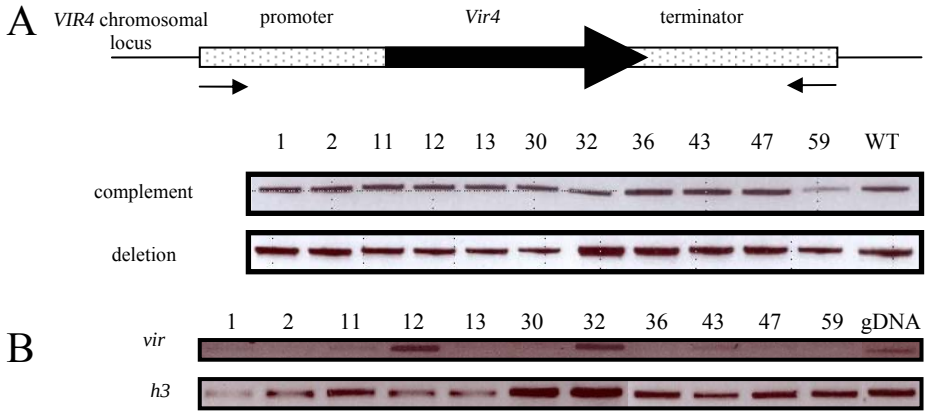

FIG. 2.6. Screening and expression of *vir4* complementation transformants. (A) Top panel: Schematic representing the region transformed into Δvir4-137. Arrows indicate location of primers used to amplify for cloning into pGEM-T Easy vector. Bottom panel: PCR of transformants for both the insertion of the complement cassette and deletion insert from Δvir4-137. (B) Expression of *vir4* in transformants evaluated by rtPCR. Histone (*h3*) was amplified a control for even loading of cDNA. Genomic DNA was used a positive control for PCR amplification.

Vir4 expression and secondary metabolite production in transformants.

Deletion transformants and background Tv10.4 were grown in PDB for 2 days and RNA was extracted as previously described. No transcripts from *vir4* were detected in any of the deletion mutants, confirming disruption of the gene (Figure 2.7).

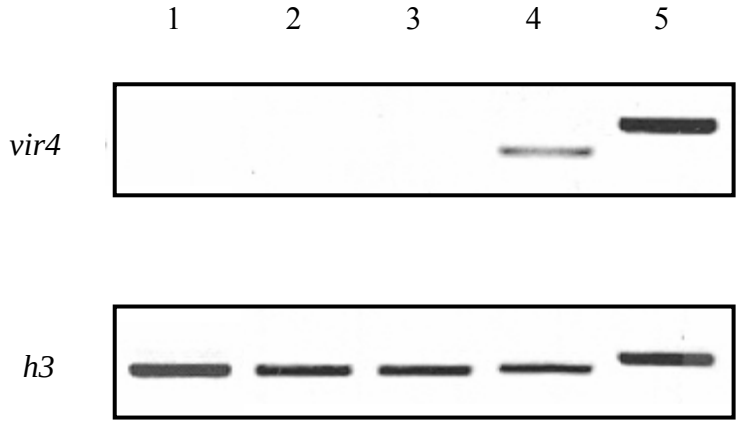

FIG. 2.7. Reverse transcriptase PCR of putative deletion mutants. Lane 1: Δvir4-61; Lane 2: Δvir4-87; Lane 3: Δvir4-137; Lane 4: Tv10.4; Lane 5: Tv10.4 genomic DNA. Histone (*h3*) was used as a control for equal loading.

Observation of secondary metabolite production in the *vir4* deletion mutants revealed that the compounds viridin, gliotoxin, and dimethylgliotoxin were still produced in quantities similar to Gv29-8 and Tv10.4 (Figure 2.8). TLC analysis showed that the metabolite spectrum was identical in the arginine deficient background (Tv10.4) and mutant (Δvir4-137), and the spot associated with viridin was present in both strains.

B

	Gliotoxin	Dimethylgliotoxin
Gv29-8	2.214	0.291
Δvir4-61	2.31	0.108
Δvir4-87	2.102	0.127
Δvir4-	2.082	0.202

FIG. 2.8. Secondary metabolite production in strains of *T. virens.* (A) Thin-layer chromotography (TLC) of strains Tv10.4 and Δvir4-137. Arrow indicates location of band associated with viridin. (B) Concentration of gliotoxin and dimethylgliotoxin in mg/mL measured by high-performance liquid chromotography (HPLC).

The concentration of gliotoxin and dimethylgliotoxin measured by HPLC indicate that levels in all three mutants (Δvir4-61, Δvir4-87, Δvir4-137) was similar to wild-type. Gliotoxin and dimethylgliotoxin production in all transformants was maintained. Variation in concentrations of metabolites was observed, but additional replicates need to be performed to determine if this is natural variation among the strains.

In the laboratory of Dr. Rainer Schuhmacher, volatiles were measured by HS-SPME-GCMS in Gv29-8 and two of the deletion strains when grown on PDA. The analysis of VOCs demonstrated the production of 35 different sesquiterpene in Gv29-8 (Figure 2.9). In the two cyclase mutants, Δvir4-87 and Δvir4-137 (Figure 2.9), 32 of these volatiles were absent. These measurements were repeated with Tv10.4 and the conclusions were similar (data not shown). Also, Tv10.4 and Gv29-8 were found to produce similar quantities of the volatiles measured. In addition, these experiments were repeated with the *vir4* complement, vir4c12 (Figure 2.10). Analysis illustrated that the production of all volatiles deficient in the cyclase mutants is reestablished in the complements. However, the concentrations of the volatiles were observed to be less than those measured in Gv29-8.

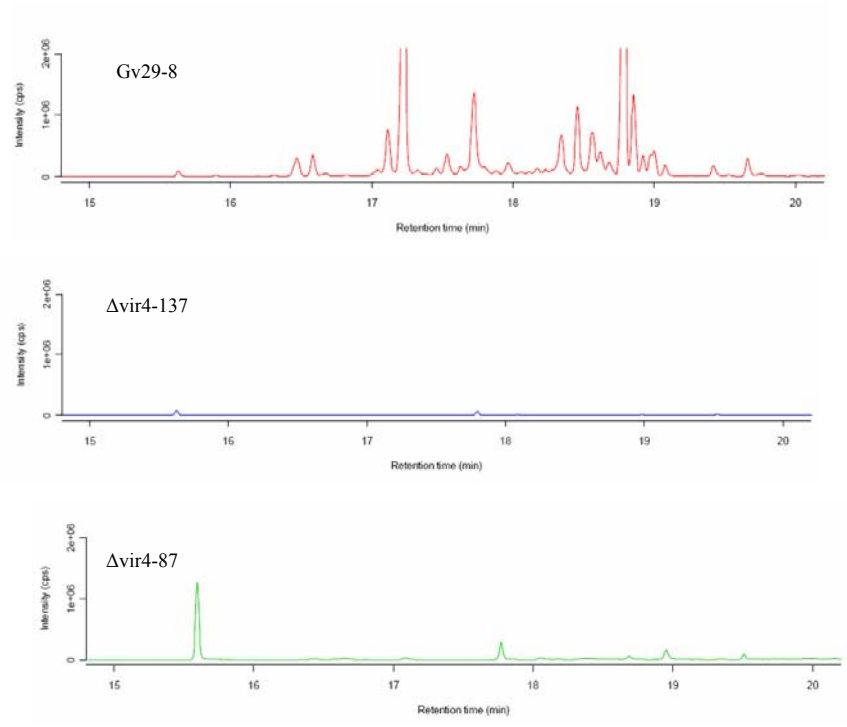

FIG. 2.9. Volatile analysis of *T. virens* strains by HS-SPME-GCMS. Wild-type (Tv29-8) is represented in red, Δvir4-137 in blue, and Δvir4-87 in green. Strains were cultivated in HS vials containing PDA for 52 hours before measurements were taken.

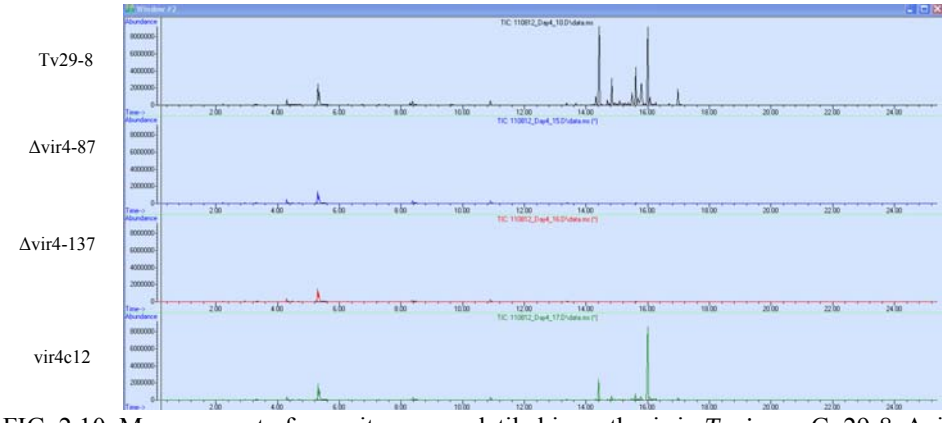

FIG. 2.10. Measurement of sesquiterpene volatile biosynthesis in *T. virens*. Gv29-8, Δvir4-87, Δvir4-137, and vir4c12 were grown for 4 days in HS vials containing PDA and volatiles were measured by HS-SPME-GCMS. Volatile concentrations are indicated by peak height.

Growth measurements of transformants. To determine if growth among the deletion transformants (Δvir4-87, Δvir4-137) and wild-type are different, strains were grown on MEA, PDA, VMS, VMG, and VML. Both deletion mutants grew at a significantly slower rate than the wildtype (Figure 2.11). Complements were also tested for changes in growth rate (Figure 2.12). Both complements were intermediate between the growth of WT and Δvir4-137 on PDA. On VMS, no difference was observed between the complements and the deletion mutant. Vir4c12 had the growth rate closest to that observed for Gv29-8 making it an ideal candidate for the volatile measurements (see Figure 2.10).

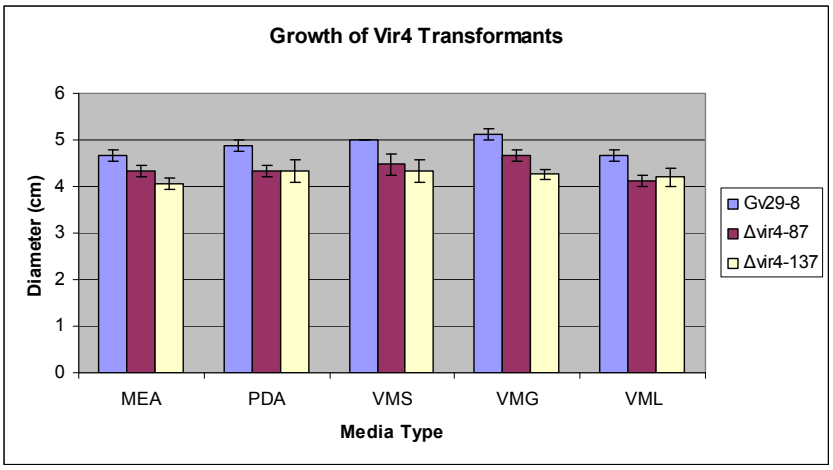

FIG. 2.11. Growth of cyclase deletion mutants. Gv29-8, Δvir4-87, and Δvir4-137 were each cultivated on MEA, PDA, VMS, VMG, and VML. Cultures were grown for two days and colony diameter was measured.

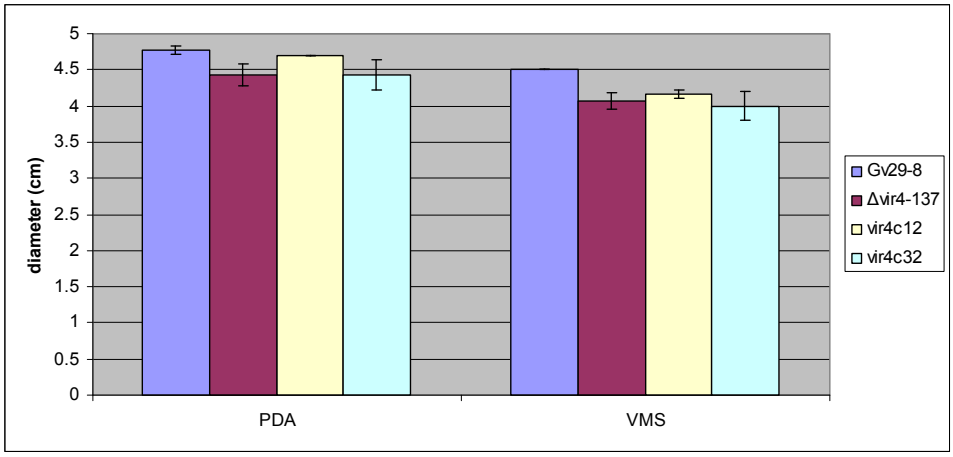

FIG. 2.12. Comparison of growth of *vir4* complements to Gv29-8. Gv29-8, Δvir4-137, vir4c12, and vir4c32 were grown for 2 days on PDA or VMS agar and colony diameter was measured.

Cluster expression of v*ir4* transformants. Expression of the genes located in the vir cluster was evaluated for Gv29-8 and Δvir4-137 using quantitive real time PCR (qPCR). Only three genes were found to be regulated significantly different in the mutant as compared to the wild-type (Figure 2.13). Two putative cytochrome P450s (*vir1* and *vir5*) and a putative oxidoreductase (*vir7*) had higher expression in the wild-type as compared to Δvir4-137. The greatest change in expression was observed with *vir7*.

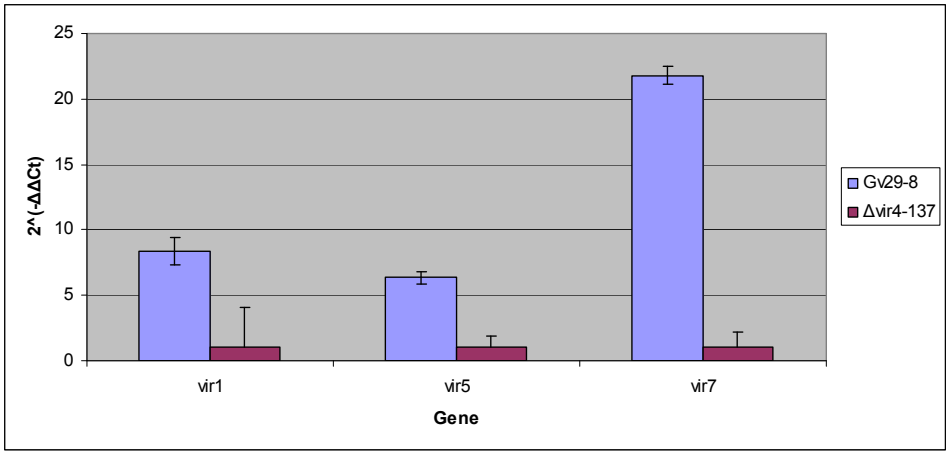

FIG. 2.13. Results of qPCR analysis of vir cluster genes. Quantitative real time PCR was performed in the wild-type (Gv29-8) and the *vir4* deletion mutant (Δvir4-137) for all cluster genes. The 2^(-ddCT) was statistically different for three genes (*vir1*, *vir5*, and *vir7*) in Δvir4-137 compared to Gv29-8.

Phenotypic analyses. To test for phenotypic differences between Gv29-8 and the *vir4* deletion mutants, a series of experiments were performed. *Arabidopsis thaliana* germinating seedlings were exposed to volatiles produced by Gv29-8, Δvir4-87, Δvir4-137, and a negative control. Standard deviations of germination percentage, root length, and shoot length were found to overlap among all the strains tested (Table 2.2).

TABLE 2.2. Analysis of volatile effects of *T. virens* on germination and growth of *Arabidopsis*.

	Neg	**Δvir4-87**	**Δvir4-137**	**Gv29-8**
% Germination	41.67%	40%	57%	43.33%
SD	12.60%	5%	16%	5.80%
Ave Root Growth	0.888889	1.733333	1.606944	1.002381
SD	0.342612	0.583895	0.123907	0.177329
Ave Leaf Growth	0.31667	0.455556	0.433333	0.355556
SD	0.05	0.072648	0.070711	0.072648

[a] Untreated control

The presence of *T. virens* had a measurable effect on the ability of *P. syringae* pv. *syringae* to swarm (Figure 2.14). This enhanced effect on swarming, however, was similar to what was observed in the presence of the *vir4* knockout Δvir4-137. This was comparable to observations made with *Serratia marcescens* (data not shown). No difference in colony growth was noted and the production of pigment associated with the production of a secondary metabolite, prodigiosin was present in *S. marcescens*.

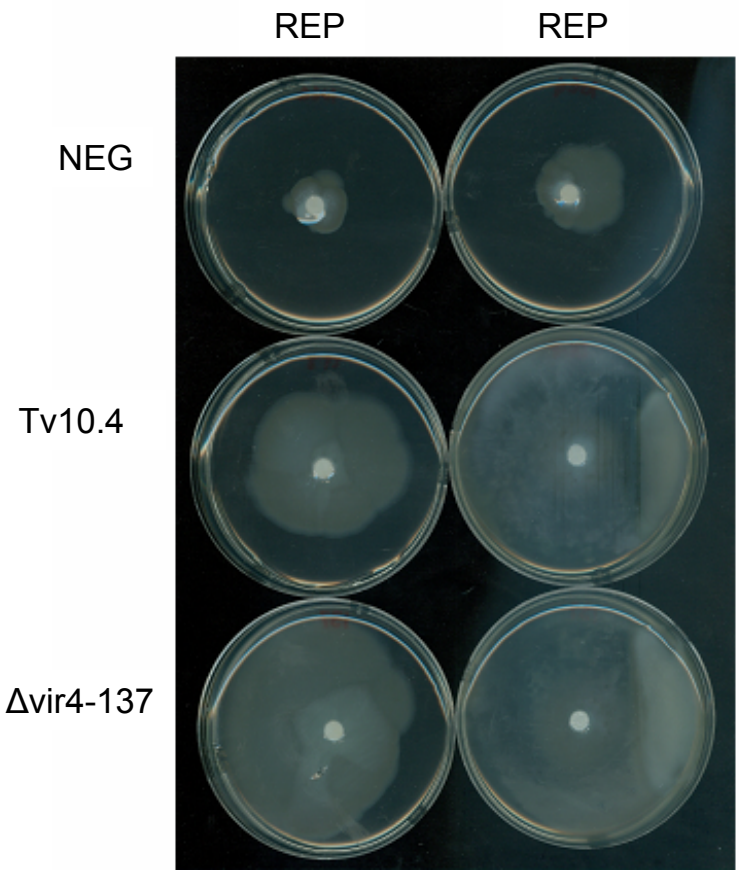

FIG. 2.14. Effect of volatiles from strains of *T. virens* on swarming ability of *Pseudomonas syringae*. Two experimental repetitions (REP1 and REP2) were performed with no *T. virens* (NEG), Tv10.4, and Δvir4-137.

The ability of the deletion strain Δvir4-137 to inhibit growth of other fungal species was measured by confrontation assay. The wild-type (Gv29-8) and the mutant were confronted with 6 different fungi (*R. solani*, *S. minor*, *P. ultimum*, the *T. virens* 'P' strain GVP, *S. sclerotiorum*, and *A. nidulans*) (Figure 2.15). There were no differences observed for growth, sensitivity to secondary metabolites, conidiation, and/or arial hyphae production in any of the rival fungal strains. The ability of *T. virens* Δvir4-137 to parasitize the competing fungi was uncompromised.

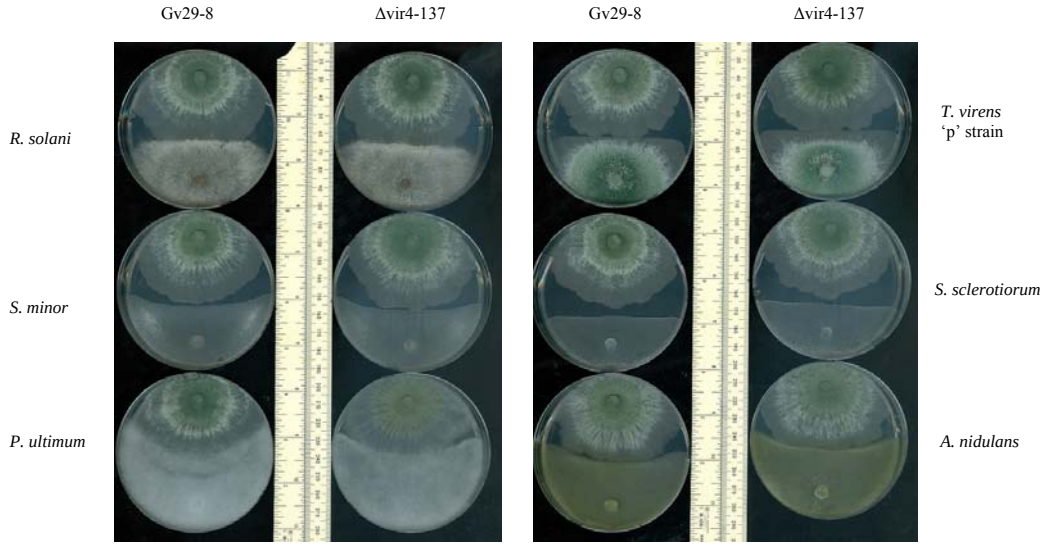

FIG. 2.15. Confrontation of *T. virens* strains with soil borne fungi. Gv29-8 or Δvir4-137 were confronted with *Rhizoctonia solani*, *Sclerotinia minor*, *Pythium ultimum*, the *T. virens* 'p' strain GVP, *Sclerotinia sclerotiorum*, or *Aspergillus nidulans*.

DISCUSSION

The putative cyclase *vir4* is a member of a gene cluster from *T. virens* with homologs in other fungal species. Previously, a subtraction library created using a strain of *T. virens* and a secondary metabolite deficient mutant identified a gene cluster containing a putative terpene cyclase (*vir4*) (87). This gene was identified in the *T. virens* Gv29-8 genome sequence (http://genome.jgi-psf.org) as a member of a gene cluster. This cluster also contains four putative cytochrome P450s (CP450), a oxidoreductase, a MFS, and is associated with a GAPDH (Figure 2.2). CP450s, oxidoreductases, and MFS genes have been found to be members of other gene clusters in *T. virens*. The *tex13/14* gene cluster, containing a NRPS/PKS hybrid, contains two CP450s and one oxidoreductase (Mukherjee, et al., In Press). Another cluster responsible

for the production of gliotoxin in *T. virens*, contains 2 CP450s and one MFS transporter (Kenerley, unpublished). The *gapdh* gene, however, appears to be unique to this gene cluster. The association of this gene with the vir cluster in all homologous cluster sequences suggests that the function of this gene is related to sesquiterpene volatile synthesis, but further experiments would need to be performed to establish this beyond a correlation.

A BLAST search of the NCBI website revealed that homologs to *vir4* are present in other fungal species. The predicted protein sequences were used to construct a gene phylogeny of the *vir4* homologs revealing that *vir4* was not closely related to any known putative cyclase genes from other *Trichoderma* species. Instead, the closest in homology to *vir4* were cyclases from *A. oryzae*, *A. flavus*, and *A. clavatus* (Figure 2.1). As well, the homologs of the vir cluster were also associated with the putative cyclases in these *Aspergillus* species (Figure 2.2) with *A. oryzae* containing all of the genes of the putative cluster except for the oxidoreductase. The presence of homologous gene clusters within the genomes of distantly related fungi has been observed previously with other secondary metabolite clusters. The gene cluster responsible for the production of gliotoxin in *T. virens* (Kenerley, unpublished) is also found in *A. fumigatus* (39, 66). Similar to the vir cluster in *T. virens* and *A. oryzae*, the genes in gliotoxin cluster are in different locations on the chromosome and some of the genes code in opposite directions. The observations of homologous gene clusters in distantly related species of fungi have been predicted to be the effect of horizontal gene transfer into fungi from

either plants or bacteria (106, 111). Whether this is the case in the vir cluster has yet to be studied.

The gene *vir4* is induced in complex nutrient conditions. Expression of the *vir4* gene was measured under several conditions to aid in predicting the function of the final products of the gene cluster. Expression of *vir4* was absent when associated with plant roots. Gene expression was observed over several time points (Figure 2.3) when maize was inoculated with Gv29-8 and was consistant with Illumina® data previously taken from maize tissue inoculated with Gv29-8 in a hydroponic system (data not shown). The lack of expression suggests that *vir4* may not be involved in *T. virens*-plant interactions, at least during root colonization. Alternatively, expression was not observed during the initial phases of sensing, contact, penetration and colonization of plant roots (the earliest time point measurement being 36 hours) or when in contact with more mature plant roots (the last time point measurement is 120 hours). To address this, future work will include measurements of root colonization and protection from *C. graminicola* in maize.

Conditions in which the highest level of expression was observed was *T. virens* was grown on a complex liquid media, such as PDB and MOL, inoculated with conidial suspension (Figure 2.4). VM containing various sole carbohydrate sources showed little to no expression regardless of the carbohydrate used. Even preparations of *R. solani* or *P. ultimum* cell walls within the medium did not increase the expression. The detection of volatile production of *T. virens* on PDA also served to indicate that a complex growth medium is required for *vir4* gene expression and subsequent sesquiterpene volatile

production in *T. virens* (Figure 2.9 and Figure 2.10). The production of volatiles on complex carbohydrate sources is not unique, as *Aspergillus oryzae*, which contains the vir cluster, is known for the production of many volatiles important in the aroma of fermented soy based products such as miso and soy sauce (69). However, the biological function of these volatiles and their production on minimal media has not been well documented in *A. oryzae*.

A putative cyclase (*vir4*) is responsible for production of sesquiterpene volatiles in *T. virens*. My original hypothesis was that the vir cluster was responsible for the production of the steroidal compounds viridin and viridiol (87). Deletion mutants of the putative terpene cyclase *vir4* were generated (Figure 2.5), and tested for their ability to make viridin and viridiol. Extraction of culture filtrate and subsequent TLC analysis determined that viridin was still being produced by the Δvir4-137 strain (Figure 2.8A). Viridin is the precursor for viridiol and a cyclase would be an unlikely candidate for conversion of viridin to viridiol (58). HPLC analysis confirmed the presence of both gliotoxin and dimethylgliotoxin, suggesting that *vir4* is not responsible for the synthesis of these common secondary metabolites from *T. virens.*

Volatile detection by Dr. Rainer Schuhmacher (Vienna, Austria) determined that Gv29-8 produced atleast 35 sesquiterpene volatiles that were largely absent in the deletion mutants Δvir4-87 and Δvir4-137 (Figure 2.9). To confirm that deletion of the *vir4* gene was responsible for the lack of volatile production in the mutants, a complementation strain was created. All 35 volatiles measured in the wild-type were present in the complement, proving that *vir4* is responsible for biosynthesis of atleast 32

sesquiterpene volatiles in *T. virens* Gv29-8. In the production of terpene compounds (monoterpenes, diterpenes, sesquiterpenes, and steroids), cyclases have been determined to be enzymes responsible for a very early step in the biochemical pathway (60). Sesquiterpenes are synthesized from farnesyl diphosphate by the cyclization activity of the enzyme. Disruption of a cyclase, therefore, can account for the majority of the compounds produced. The other genes within the vir cluster may be responsible for the extreme diversity of the sesquiterpene volatiles produced by different alterations to the terpene ring, but further gene deletions need to be constructed to determine their role.

The deletion in *vir4* down-regulates the expression of three genes in the vir secondary metabolite cluster. To understand the effect of the deletion of *vir4* on the other members of the vir cluster, quantitative real time PCR was performed comparing the expression of all the putative cluster genes between Gv29-8 and Δvir4-137. This analysis demonstrated that the expression of three genes (*vir1*, *vir5*, and *vir7*) was higher in Gv29-8 as compared to the deletion mutant (Figure 2.13). These genes are located adjacent to each other along the chromosome (Figure 2.2) and may be co-regulated. The insertion of *arg2* into the gene cluster is unlikely to have caused a disruption of gene expression, due to the unaltered expression of *vir2* and *vir3* which lie between *vir4* and *vir1, vir5,* vir7. However, metabolic feedback has been found to occur in secondary metabolite gene clusters (26). In this case, the presence of the metabolite will activate transcription of the genes responsible for this biosynthesis. This is a possible explanation for the disruption of gene expression in the Δvir4-137 transformant, but further study will be required to demonstrate that metabolic feed back is responsible.

Determining the role of sesquiterpene volatiles in *T. virens* biology. VOCs are small, vaporized compounds that have the important role of intra- and interspecies recognition within the soil environment (138). In fungi, this recognition is involved in defense processes, fungistasis, and interactions with plants (54, 83, 121, 123). Antagonism of other fungi influenced by volatiles occurs during interactions of *F. oxysporum formae speciales* and *F. oxysporum* wild-type in which virulence of the plant pathogenic strain is suppressed (85). As well, many fungi are suppressed by volatiles produced by *Muscodor albus* (123, 124). Other species of *Trichoderma* have demonstrated measurable fungistasis of wood rot fungi (140) and sesquiterpenes produced by *T. virens* (such as heptelidic acid) have antimicrobial activity (40). When the sesquiterpene volatiles produced by *T. virens* were evaluated using the *vir* deletion mutants, however, confrontation assays with several different fungi did not illustrate significant differences between mutants and wild-type (Figure 2.15). Only one basidiomycete was evaluated during this confrontation assay (*R. solani*). The other fungi confronted were Ascomycetes. The volatiles from *T. virens* may be inhibitory to a specific group of fungi that our evaluation did not include. To evaluate the possibility that these volatiles are inhibitory against bacteria instead of fungi, the effect of *T. virens* volatiles were tested against *P. syringae* and *S. marcescens*. No measurable affect was observed in swarming of *P. syringae* (Figure 2.14) or growth of *S. marcescens* (data not shown).

Volatiles produced by fungi have also been documented to have an involvement in plant interactions (83, 121). In these cases, volatiles were implicated in establishment

of root colonization by mycorrizal fungi (83) and altering root formation and structure (121). Volatiles produced by *T. virens* Gv29-8, however, did not have an observable effect on the growth and germination of *Arabidopsis*. The germination percentage, root growth, and shoot growth were unaffected in both wild-type and mutant strains as compared to the negative control (Table 2.2). The measurement of root colonization by the *vir4* mutants as compared to wild-type, has yet to be completed. It is possible that any effect of sesquiterpene volatiles produced by *T. virens* is not measurable by the method used, which may be revealed by root colonization analysis.

The only difference measurable between Gv29-8 and the *vir4* deletion mutants was a decreased growth rate for the mutant on various solid media (Figure 2.11). This difference in growth was somewhat recovered in the complementation strain indicating that it is an affect from the deletion of *vir4* coding region (Figure 2.12). The results of these assays correspond to expression data previously discussed, in which expression was not observed from tissue in plant roots or grown in the presence of *R. solani* and *P. ultimum* cell walls.

To date, the role of sesquiterpene volatiles has yet to be determined. Individual sesquiterpene volatiles are being identified using gas chromatograph standards and data banks at the Center for Analytical Chemistry, University of Natural Resources and Life Sciences, Vienna. The function of many volatile compounds have been determined to be involved within the soil community interactions of plants, fungi, bacteria, and insects (82). Once the 35 volatiles have been identified the role for the individual compounds may be established and purified compounds can be tested for their activity.

CHAPTER III

THE DISCOVERY AND INVESTIGATION OF A PARALOG OF THE PROTEINACEOUS ELICITOR, SM1

INTRODUCTION

Plants have evolved mechanisms that enable plant tissues to recognize invading microbes and activate responses to both beneficial and pathogenic microorganisms. Signaling molecules (elicitors) have an important role in the process of recognition providing for the detection of microbes and the initiation of an appropriate response by the plant host (46, 117). Among the elicitors known to initiate this process are cysteine rich proteins such as hydrophobins, elicitins, and fungal avr products. Resistance to plant pathogens induced by elicitors, also known as induced systemic resistance (ISR), is a critical process that is not fully understood (117). ISR initiated by *T. virens* in planta has been studied through use of the proteinaceous elicitor SM1 (29, 30). Native purified SM1 on cotton triggers hydrogen peroxide production and induces the expression of defense genes (29). The application of SM1 increased resistance to the foliar pathogen *Colletotrichum* sp. on cotton. Treatment of both leaves and roots of maize with SM1 also increased resistance of maize to *C. graminicola* (29, 130). Colonization of maize roots with *T. virens* primes maize for resistance to foliar pathogens and this resistance is lost when treated with SM1 deficient strains (30).

SM1 is a small secreted cysteine rich secreted protein produced by *T. virens* and is a member of the cerato-platanin (cp) protein family (95). Characteristics of this protein family include extracellular location and cleavage of a secretion tag, four

cysteine residues experimentally proven to form two disulfide bridges, and moderate hydrophobicity (35, 95). The first identified cerato-platanin (CP) is a pathogen-associated molecular pattern (PAMP) produced by the plant pathogen *Ceratocystis fimbriata*, the cause of canker stain disease in *Platanus acerifolia* (77). Application of this protein directly to plant leaves causes cell necrosis, autofluorescence, and phytoalexin production (95, 109). The closely related MgSM1 from *Magnaporthe oryzae* initiates a hypersensitive response, increases expression of defense related genes, and is required for virulence in rice (57, 146). BcSpl1, a cerato-platanin protein from *Botrytis cinerea* contributes to virulence on a variety of host plants and is an elicitor of the hypersensitive response in *Arabidopsis* (36).

Unlike cerato-platanins from plant pathogenic fungi, SM1 is not a virulence factor nor phytotoxic when applied directly to leaves (29). When leaves of rice or cotton were infiltrated with SM1, both plants experienced the production of hydrogen peroxide and the induction of autofluorescence. As well, cotton cotyledons infiltrated with the protein had increased resistance to the foliar pathogen *Colletotrichum* sp. Maize seeds treated with strains deleted in *sm1* showed a decreased level of resistance to *C. graminicola*, whereas overexpression strains had an increased level of resistance to the same pathogen (30). Gene expression using rtPCR suggested that the appearance of ISR primed by *T. virens* is controlled through the jasmonic acid defense pathway, and priming is lost in *sm1* deletion strains.

Our analysis of the sequenced genome for *T. virens* using a basic local alignment search tool (BLAST) (1) revealed the presence of three paralogs of *sm1*. Gene

expression in the presence of maize roots and the phylogenic relationship among the paralogs suggested that one paralog (*sm3*) warranted further study as a putative elicitor. The ability of *sm3* to elicit expression of defense related genes in maize was analyzed using recombinant protein from *Pichia pastoris*. Upregulation of *pal* and *aos* genes in maize upon treatment with the recombinant SM3 further indicated a role for this protein in ISR.

MATERIALS AND METHODS

Growth conditions of fungi and bacteria. Two strains of *T. virens* were used in this study, wild type strain, Gv29-8, and *sm1* deletion strain Δ*sm1-25* (30). For selection of *sm3* deletion and over-expressing strains, transformants were grown on potato dextrose agar (PDA, Difco) or PDA supplemented with 100 mg/mL of the hygromycin (PDA-H). Still-cultures of *T. virens* were inoculated with $2X10^6$ conidia/mL in 100 mL Vogel's minimal media (VM) (136) plus 1.5% sucrose (VMS) for 7 days with no shaking.

Pichia pastoris was routinely maintained on yeast extract peptone dextrose medium (YPD) or a minimal medium consisting of yeast nitrogen base (YNB) and biotin (Invitrogen). Liquid media used included a buffered complex medium supplemented with either glycerol (BMGY) or methanol (BMMY). Geneticin® (A.G. Scientific) was incorporated into media as a selection agent used to screen for multiple gene copy insertion.

E.coli XL1-Blue Supercompetent Cells (Stratagene) were sustained on Luria-Bertani (84) agar (LBA). All cultures were grown at 37ºC and liquid cultures were

grown at 250 rpm. Ampicillin (Research Products, Inc.) was used as a selective agent for all bacterial transformants.

DNA Manipulation. Genomic DNA from *T. virens* was extracted as previously described (145). Sequencing reactions were completed at the Texas A&M University Gene Technologies Lab. DNA amplified by PCR was purified using the Wizard® SV Gel and PCR Clean-up System (Promega). Plasmids were purified using the Wizard® *Plus* SV Miniprep kit (Promega).

Identification and analysis of 3 s*m1* paralogs in *T. virens*. The protein sequence of *sm1* was used for a BLAST analysis of the *T. virens* genome sequence (http://genome.jgi-psf.org). This search revealed the presence of three genes with homology to *sm1*. The protein sequences were examined further by analysis of the predicted protein sequences and post-translational modification predictions using proteomic tools (SignalP, NetNGlyc, and NetPhos) available from Expasy tools (http://expasy.org/tools/).

Gene expression analysis of *sm3* in maize and liquid media. For expression in planta, maize seeds were surface disinfected by a five minute treatment with 70% ethanol followed by two hours in 10% hydrogen peroxide. Surface disinfested seeds were incubated in a moist chamber for 72 hours to induce germination. Hydroponic chambers containing 0.5X Murashige and Skoog with Gamborg's vitamins (MS) plus 0.05% sucrose were used to grow the maize seedlings for an additional 3 days. Fungal tissue was prepared by inoculating 100mL VMS with $3X10^7$ conidia/mL and incubating at 27ºC shaking at 135 rpm for 16 hours. Germlings were harvested and washed with

sterile water using miracloth (Calbiochem). One gram of fungal tissue was used to inoculate each hydroponic chamber containing maize seedlings. Hydroponic chambers were incubated for an additional two days with slow shaking (25 rpm) to allow maize roots to grow in the presence of *T. virens*. Maize root tissues and any fungal hyphae associated with the roots were washed and ground in liquid nitrogen for RNA extraction.

The *sm1* paralogs were also evaluated for expression after growth in liquid media. Conditions evaluated were PDA, malt extract broth (MEB, Difco), glucose yeast extract broth plus casamino acids (GYEC) (141), Weindling's medium (WEI) (137), molasses (MOL, 30g molasses and 5g yeast extract/L), VMS, VM plus lactose (VML), VM plus glycerol (VMY), VM plus glucose (VMG), or VM plus fructose (VMF). All cultures consisted of 100 mL of each medium inoculated with $2X10^6$ conidia/mL. Cultures were incubated for three days at 27ºC shaking at 135rpm. In addition, VMS inoculated with *T. virens* was allowed to stand without shaking (still-culture) for seven days before tissue collection. Expression in the presence of plant pathogen cell walls was examined by the addition of 1.5% cell walls of *Rhizoctonia solani* (VMR) or *Pythium ultimum* (VMP).

For all expression analysis, RNA was extracted using TRIZOL® reagent (Gibco-BRL). The DNA-freeTM DNase Treatment and Removal kit (Ambion) was used to remove any residual DNA. The synthesis of cDNA was performed using the High Capacity cDNA Reverse Transcription Kit (Applied Biosystems). Primers used for rtPCR analysis in both *T. virens* and maize are shown in Table 3.1.

Table 3.1. Primers used for rtPCR analysis.

Primer	Sequence (5' to 3')	Reference
SM1F	ACTGTCCAACATCTTCACTCT	This study
SM1R	CAATGTTGAAGCCAGAAGCA	
SM2F	TTCCAAATAGCTGCCATTGTC	This study
SM2R	TGGGCTCGTCCATCTGTGAGA	
SM3F	GGTGTCAATGGCCTCATCACC	This study
SM3R	AAACCTGTGTAGCCACAGCA	
SM4F	GCCCTTTAAGCGAAGTCGCA	This study
SM4R	CATCCACCTCAGTGGCATTTG	
H3F	CCGTAAGTCCACTGGTGGC	This study
H3R	AGCTGGATGTCCTTGCTCTG	
GAPc-F	GCTAGCTGCACCACAAACTG	Vargas et. al
GAPc-R	TAGCCCCACTCGTTGTCGTAC	
ZmPAL	CGAGGTCAACTCCGTGAACG	Djonovic et. al
ZmPAL	GCTCTGCACGTGGTTGGTGA	

Construction of a cerato-platanin gene phylogeny. A gene phylogeny of cerato-platanin proteins from both Basidiomycete and Ascomycete fungi using maximum likelihood analysis was constructed. A protein BLAST was performed at the National Center for Biotechnology Information (NCBI) website (http://www.ncbi.nlm.nih.gov/), Joint Genome Institute (JGI), EMBL, and the Broad Institute using the amino acid sequence of SM1. The tree was constructed with PhyML 3.0 (42) after a sequence alignment using ClustalX (68). A sh-like aLRT branch support was used for the tree construction (2). A maximum likely-hood phylogeny was

constructed using PhyML software (http://www.atgc-montpellier.fr/phyml/) with a Blosum62 substitution model and a bootstrap of 100 (42).

Transformation of *Pichia pastoris* for production of SM3 (picSM3). The vector for *P. pastoris* transformation was constructed to add a FLAG tag (33, 48) to the 5' end of the coding region of *sm3*. The FLAG tag sequence was introduced into the N-terminus of *sm3* after removing the native putative signal peptide sequence using the primers SM3-EcoRI-F (5'-ATTAGAATTCGATTACAAGGATGACGACGATAAGGGAGCTGGTGCAGGCGCTGGAGCCGGTGCCACTTACGTATCCTTTGACACTGGCT-3') and SM3-NotI-R (5'-TATAGCGGCCGCGTAAACGGTGAACAATCCACATTCATTTACAG-3'). Between the FLAG sequence and *sm3*, a GA5 linker was inserted. The cDNA fragment of the recombinant *sm3* was digested with EcoRI and NotI, and cloned into the pGEM-T easy vector (Promega) with sequencing confirmation. The expression construct was made by subcloning the recombinant *sm3* cDNA into the EcoRI/Not I site in pPIC9K (Invitrogen).

Approximately 10 μg of the plasmid expression construct was digested by SalI and purified by phenol/chloroform extraction as previously described (29). After ethanol precipitation, the pellet was dissolved in 10 μl of TE buffer (pH 7.5). Electroporation of the methanol utilization slow strain (Mut^S) of *P. pastoris* (KM71, an auxotrophic mutant negative for histidine production and utilization of methanol) was performed following the manufacturer's instructions (Invitrogen). The electroporation parameters used were: 1.5K, 25μF, and 200 Ω. The cells were spread onto regeneration dextrose (RD) agar.

Selection was performed on a YPD plus Geneticin® plate followed by PCR screening of the *P. pastoris* clones. Concentrations of Geneticin® used were 0.5, 1.0, and 1.75 mg/mL. Ten transformants positive for Geneticin® resistance were screened for protein production by Western blotting. A single colony from each transformant was used to inoculate 100 mL of BMGY in a 500 mL baffled flask. The cultures were grown for 18 hours at 25º shaking at 150 rpm. Cells were harvested at 3,000 X g for 5 minutes at room temperature. The supernatant was decanted and the cells were washed twice with 10 mL BMMY and recentrifuged. The cells were resuspended in 20 mL of BMMY for protein induction. Cultures were incubated for 48 hours with the addition of 1% methanol after 24 hours. From the ten transformants assayed, one (KM1) was selected for a time course study based on results of Western blotting of the culture filtrate.

A standard Western blotting protocol was used for detection of picSM3 and native SM3 (108). Protein extracts were run on SDS-PAGE gels and electroblotted onto a nitrocellulose membrane (GE Water & Process Technologies). Flag tagged picSM3 was detected using the anti-Flag antibody and an anti-SM3 antibody. Native SM3 was detected using the anti-SM3 antibody. Antibodies for SM3 were produced by GenScript using the 15 amino acid synthetic peptide (FDTGYDDPSRSMTQC) unique to SM3 when compared to SM1. Antibodies were purified using affinity chromatography and subjected to HPLC and ELISA to determine purity and activity. The pre-immune serum was included as a positive control. Both antibodies were used at a ratio of 1:2000 antibody to blocking buffer. The anti-Flag antibody was used to detect flag tagged protein by an anti-rabbit antibody conjugated to alkaline phosphatase and visualized

using5-bromo-4-chloro-3-indolyl phosphate p-toluidine salt and nitrotetrasolium blue. The anti-SM3 antibody was visualized by fluorescence using an anti-rabbit antibody conjugated to horse radish peroxidase (HRP) (Pierce) and the SuperSignal® West Pico Chemiluminescent Substrate Kit (Thermo Scientific).

Temporal optimization of picSM3 production. KM1 was grown as described above for methanol induction. Every 24 hours for six days 1 mL of total yeast culture was collected and 1% methanol was added to the remaining culture to induce protein expression. Each 1 mL sample was centrifuged at 13,000 RPM in a bench top centrifuge for 2 minutes. The supernatant was collected and frozen at -80ºC until evaluated by Western blotting. At the end of the timecourse, 10 µL of culture filtrate from each timepoint was analyzed by SDS-Page and Western blotting. Immunodetection was performed with anti-FLAG antibodies (Rockland, Inc.).

Purification of SM3 from *P. pastoris*, mass spectrometry, and SM3 antibody synthesis. KM1 was grown on YPD and a single colony was used to inoculate a 10 mL starter culture of BMGY. The culture was incubated at 27ºC and 150 rpm for 18 hours. One liter of BMGY was inoculated with the starter culture and grown under the same conditions until growth reached log phase (OD_{600} = 2-6). The cells were harvested by centrifugation at 3,000 x g for 5 minutes at room temperature using a Sorvall RCSC centrifuge with a GSA rotor. The cells were washed twice with BMMY and pelletted by centrifugation. Cells were resuspended in 600 mL of BMMY in a 1 liter flask covered with cheese cloth and incubated at 25ºC and 150 RPM for six days. Every 24 hours 1% methanol was added to ensure induction of picSM3.

After six days of incubation, cells were removed by centrifugation at 3,000 x g for 5 minutes and the supernatant was collected. Protein was precipitated using 80% ammonium sulfate at 4ºC with slow stirring. Crude protein was collected by centrifugation at 10,000 RPM for 10 minutes using a GSA rotor. Protein was resuspended in 10mM ammonium bicarbonate and dialyzed against 20mM ammonium bicarbonate for 40 hours with a change of dialysis buffer every 4 hours.

Dialyzed protein extracts were applied to a Macro-Prep® High Q Support (Biorad) anion exchange (AEX) column pre-equilibrated with 20mM Tris-HCl (pH 7.5). Proteins were eluted using a 0-0.5 M NaCl gradient in the equilibration buffer. The elution fractions were analyzed by SDS-Page and Western blot using the FLAG antibody. Fractions positive for the FLAG tag were pooled and applied to a Bio-Gel® (Biorad) P-30 gel filtration chromatography (GFC) column equilibrated with 50 mM Tris-HCl (pH 7.5) and 150 mM NaCl. Fractions were analyzed by SDS-Page and Western blotting. The purified protein (picSM3) was then subjected to tandem mass spectrometry (MS/MS) spectral analysis for peptide fragment matching (Technion Israel Institute of Technology).

Testing of picSM3 for glycosylation. To enzymatically cleave n-glycosylation of picSM3, 10 μg of purified protein was treated with Peptide: N-Glycosidase F (PNGase F) per manufactures instructions (New England Biolabs). Treated protein was assessed by SDS-PAGE and Coomassie staining or transferred to a membrane and evaluated by glycostaining.

To stain picSM3 for glycosylation, a periodic acid/Schiff (PAS) staining method was used (105). Protein were immobilized on a nitrocellulose membrane by electrotransfer from an SDS-PAGE gel and incubated in 10ml periodic acid solution (1% periodic acid and 3% acetic acid) for 15 minutes. The blot was washed with water three times for five minutes each. Ten milliliters of Schiff's reagent (ten grams of basic fuchsin dissolved in 900mL of boiling distilled water, cooled and added 25mL concentrated HCl and 5 grams of sodium metabisulfite) was added to the membrane and incubated for 15 minutes in a container covered in aluminum foil (to avoid light). After staining, the blot was washed for 5 minutes in 10mL of 0.5% w/v sodium metabisulfate solution and then washed with water to visualize the bands.

Elicitation of maize defense genes when treated with picSM3. Maize seedlings were inoculated with picSM3 using a protocol previously described (16). Three replicates containing four plants were inoculated and RNA was extracted from total seedling tissue. Reverse transcription PCR was performed with primers for glyceraldehyde-3-phosphate dehydrogenase (*gapc*) and phenylalanine ammonia lyase (*pal*) (see Table 3.1) for 25 cycles of 30s at 94ºC, 30s at 58ºC, and 30s at 72ºC.

Construction of vectors for disruption and over-expression of *sm3* in *T. virens.* The construct for deletion of *sm3* in the Gv29-8 or Δsm1-25 background was created by double joint nested PCR using the *hygB* selection marker as previously described (129, 131). The upstream region of *sm3* was amplified using the primers sm3-7 (5'-CACAGGAGCTGCGGCTAC-3') and sm3-8 (5'-ATTGATGTGTTGACCTCCACGGAGGCGAGTTAC-3') and the downstream was

amplified with sm3-9 (5'-TCTGGATATAAGATCGTTGGTGTCACTGGAGAA=3') and sm3-10 (5'-ATGAGAAACCTGTCTAGCTC-3'). Both fragments were amplified with 35 PCR cycles of 30s at 95ºC, 30s at 54ºC, and 90s at 72ºC and purified using the Wizard® SV Gel and PCR Clean-Up System (Promega). Fifty nanograms of the upstream and downstream fragments were mixed with 150ng of the amplified *hygB* cassette, and a double joint reaction of 15 cycles with 30s at 95ºC, 20m at 52ºC, and 5m at 72ºC was performed. This was followed by a nested reaction with the primers sm3-11 (5'-CCGTGGTTTGAGAGGTCTCAAT-3') and sm3-12 (5'-AAGCAAGGCCAATATAAAGAAGC-3') and 33 cycles of 30ºs at 95C, 30s at 52ºC, and 3m at 72ºC. The resulting fragment was purified and 10 µg was used to transform Gv29-8 for single deletion mutants or Δsm1-25 for deletion mutants in *sm1* and *sm3* (double deletion).

The over-expression vector (pFKC7) was constructed by cloning the *sm3* coding region between the promoter and terminator regions of the *T. virens gpd* (glyceraldehyde-3-phosphate dehydrogenase) gene contained within pJMB1 (145). The *sm3* coding region was amplified using the sm3-13 (5'-ATGCAGCTCGGCAGCCTCTT-3') and sm3-14 (5'-CGCGGATCCTCAGTAAACGGTGAACAATC-3') in a PCR reaction consisting of 35 cycles of 30s at 95ºC, 30s at 58ºC, and 60s at 72ºC. This fragment and pJMB1 were digested with *EcoR*V and *BamH*I and ligated.

Transformation and identification of disruption, over-expression and double mutations in *T. virens* for *sm3*. Protoplasts of *T. virens* were produced and transformed

using linearized DNA by the method of Baek and Kenerley (1998). Stable deletion transformants were selected by sequential transfer of conidia to agar slants of PDA-H, PDA, and PDA-H. Viable transformants on the last round of selection on PDA-H were screened by polymerase chain reactions (PCR) using a primer upstream of the deletion construct (sm3-7) and within hygromycin (HygR). These primers were used to amplify a product specific to a homologous recombination event. PCR amplification was performed for 35 cycles with each cycle framed as 30 seconds at 95ºC, 30 seconds at 53ºC, and 3 minutes 30 seconds at 72ºC. Once positive transformants were identified from this screening, they were further analyzed with primers specific for *sm3* to verify the deletion of the gene. The primers Sm3F and Sm3R were used as previous for PCR amplification.

To identify stable over-expression mutants, conidia of isolated colonies were transferred sequentially from PDA-H, PDA, to PDA-H. Resulting stable transformants were initially screened by PCR using the primers Sm3F and GPDFwd2 (5'-TAATGTCGCTCATCCGATGCC-3') for 35 cycles of 30s at 95ºC, 30s at 58ºC, and 60s at 72ºC.

Expression and protein production in transformants. A northern analysis *sm3* over-expression of transformants and rtPCR for deletion strains was performed using RNA from cultures grown in still-culture (deletion strains) or VMS shaking at 135rpm for 3 days (over-expression strains) with a inoculation concentration of $2X10^6$ conidia/mL. Ten micrograms of RNA extracted from the tissue using TriReagent (Molecular Research Center, Inc.) was denatured, run on a 1.5% agarose formaldehyde

gel, and transferred to a Hydrobond-N+ nylon membrane (GE Healthcare). Blots were hybridized overnight at 42ºC using Ultrahyb (Ambion) using the probes amplified with sm3F and sm3R primers (350bp). A *histone* fragment (H3F and H3R) was used as a control for even loading.

Transformants were grown for 7 days in still-culture (deletion strains) or 5 days in 100mL PDB (over-expression strains). Thirty milliliters of culture filtrate was frozen and lyophilized. The pellet was resuspended in 1 mL of water and 300uL samples were precipitated with 30% tricholoroacetic acid (TCA) and washed four times with 70% ethanol. Pellets were resuspended in buffer containing 50mM Tris pH 7.5, 5M Urea, 50mM NaCl, and 5mM EDTA. Samples were run on SDS-PAGE and Western blotting analysis as described for picSM3.

Confrontation of mutants with plant pathogenic fungi. Strains Gv29-8, Δsm3-4 (mutant), *R. solani*, *S. minor*, and *P. ultimum* were grown on PDA and 3mm plugs were removed from the actively growing colony edge for confrontation experiments. Plugs from Gv29-8 and Δsm3-4 were placed on one edge of a fresh PDA plate, and the colonies permitted to grow for 24 hours. Each strain was confronted with a plug from a competing fungus and cultures were allowed to grow for an additional 72 hours. Experiments were completed in triplicate and observations of growth characteristics and inhibition were made every 24 hours.

Analysis of the ability of transformants to induce resistance in maize against the foliar pathogen *C. graminicola.* To analyze the ability of *sm3* deletion mutants to induce ISR in maize, plants were inoculated with Gv29-8, Δsm3-4, Δsm3-6, and Δsm3-

40 as previously described (30) except *Zea mays* Silver Queen hybrid was used instead of *Zea mays* B73 inbred line.

RESULTS

Clustal alignment and promoter analysis of *sm1* paralogs. An alignment of the amino acid sequences of all four paralogs revealed several potential conserved motifs among them (Figure 3.1). At the n-terminus of all four proteins was a predicted secretion signal peptide 18 amino acids long. As well, four cysteine residues were common between all protein sequences and have been found to be conserved in several cerato-platanin proteins (130) These cysteine residues are important in the formation of disulfide bridge essential for maintaining protein structure (95). Other conserved amino acids in the *sm1* paralogs were a putative phosphorylation site at amino acid number 29, and a potential oxidation site at amino acid 54. The protein sequences also suggested that *sm1*, *sm3*, and *sm4* had the potential to be glycosylated at an asparagine residue, however these sites were different for each protein (amino acid 31, 75, and 130, respectively) (Figure 3.1).

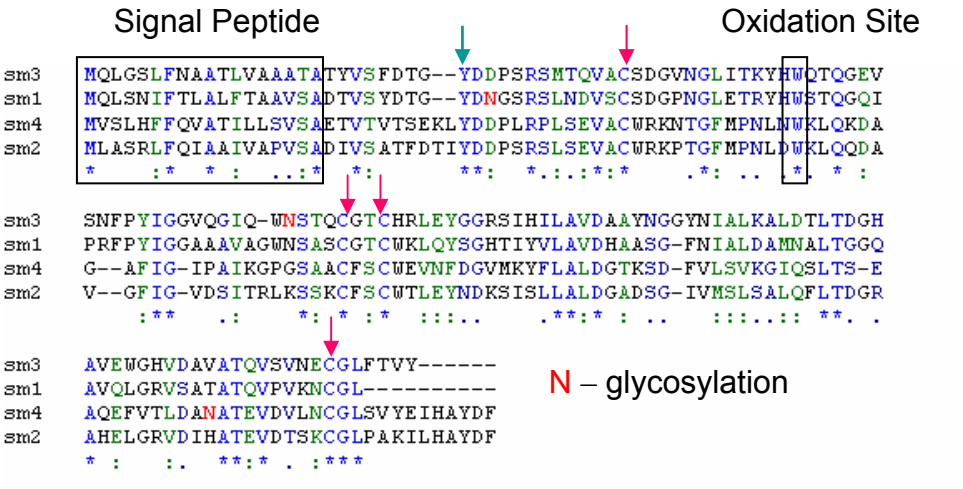

Fig. 3.1. Clustal alignment of *sm1* paralogs from *T. virens*. Protein sequences of 4 cerato-platanin proteins were aligned using ClustalX2. The box at the n-terminus of the protein sequences indicates a signal peptide for secretion and the box at the tryptophan is a putative oxidation site. Blue arrows are phosphorylation sites and pink arrows indicate conserved cysteine residues. Putative asparagine glycosylation sites are shown in red.

The promoter region, arbitrarily framed as 2kb upstream of the start codon (similar for the evaluation of SM1 in Djonovic et al. 2006) for each of the *sm1* paralogs, was examined for the presence of transcription factor binding sites. Putative TATA and CAAT box binding sites were identified upstream of the start codon for all genes with the exception of *sm4*, which was missing a TATA box. Ten putative transcription factor (TF) binding sites were identified within the 3' region of the four genes (Table 3.2). In addition to putative TF binding sites for *sm1* previously documented (29) the promoter sequence for *sm1* was assessed for the presence of the following sites: phosphate repression (139), *ste12p* MAPK control binding (103), the ccctga repressor binding (7),

and the AbaA condiophore development (125) (Table 3.2). The only putative transcription factor binding site additionally identified in *sm1* was AbaA with three potential sites located in the sequence. The promoter for *sm2* contained two putative Ste12p sites, one repressor site, and one AbaA site. *Sm3* contained potential sequences for Ste12p (two), phosphate repression (one), repressor binding (one), and AbaA (one). The carbon repression binding site for the transcription factor CreA (65) was identified in all three paralogs with two potential sites in *sm2*, one site in *sm3*, and 1 site in *sm4*. The motif for AreA, a transcription factor responsible for nitrogen repression (101) was detected in *sm2* and *sm3* with two potential sites in each. One potential site for the pH response motif that binds PacC (127) was found in both *sm3* and *sm4*. The stress responsive element STRE (80) binding sequence was identified in all three paralogs with six copies in *sm2*, two copies in *sm3*, and two copies in *sm4*. The Myc1 binding motif, associated with mycoparasitism (25), was identified in *sm3*, but not in the other paralogs. The Myc2 domain with similar function was missing in all three promoters.

TABLE 3.2 Putative transcription factor binding sites in the promoters of cpf genes.

Promoter Elements	Sm1	Sm2	Sm3	Sm4
CreA - Carbon Repression	6[a]	2	1	1
AreA - Nitrogen Repression	1	2	2	0
PacC - pH Response	3	0	1	1
STRE - Stress Response	2	6	2	2
Myc1 - mycoparasitism	3	-0	1	0
Myc3 - mycoparasitism	2	0	0	0
Ste12p - MAPK control	0	2	2	2
phosphate repression	0	0	1	0
ccctga - Repressor Binding	0	1	1	0
AbaA - conidiophore development	3	1	1	0

[a] Numbers correspond to number of putative transcription factor sites identified in the promoter.

Phylogenetic analysis of *sm1* paralogs. To determine the relationships between the four paralogs and other members of the CP family, a gene phylogeny was produced (Figure 3.2). Cerato-platanin (cp) protein homologs have been found in both Basidiomycetes and Ascomycetes. The tree was rooted with three Basidomycete fungi (*Antrodia camphorate*, *Laccaria bicolor*, and *Postia placenta*) and two major clades emerged. The first clade contains proteins from the remaining Basidiomycetes, the *Aspergillus* proteins, and the plant pathogen *C. fimbrata*. The second clade contains

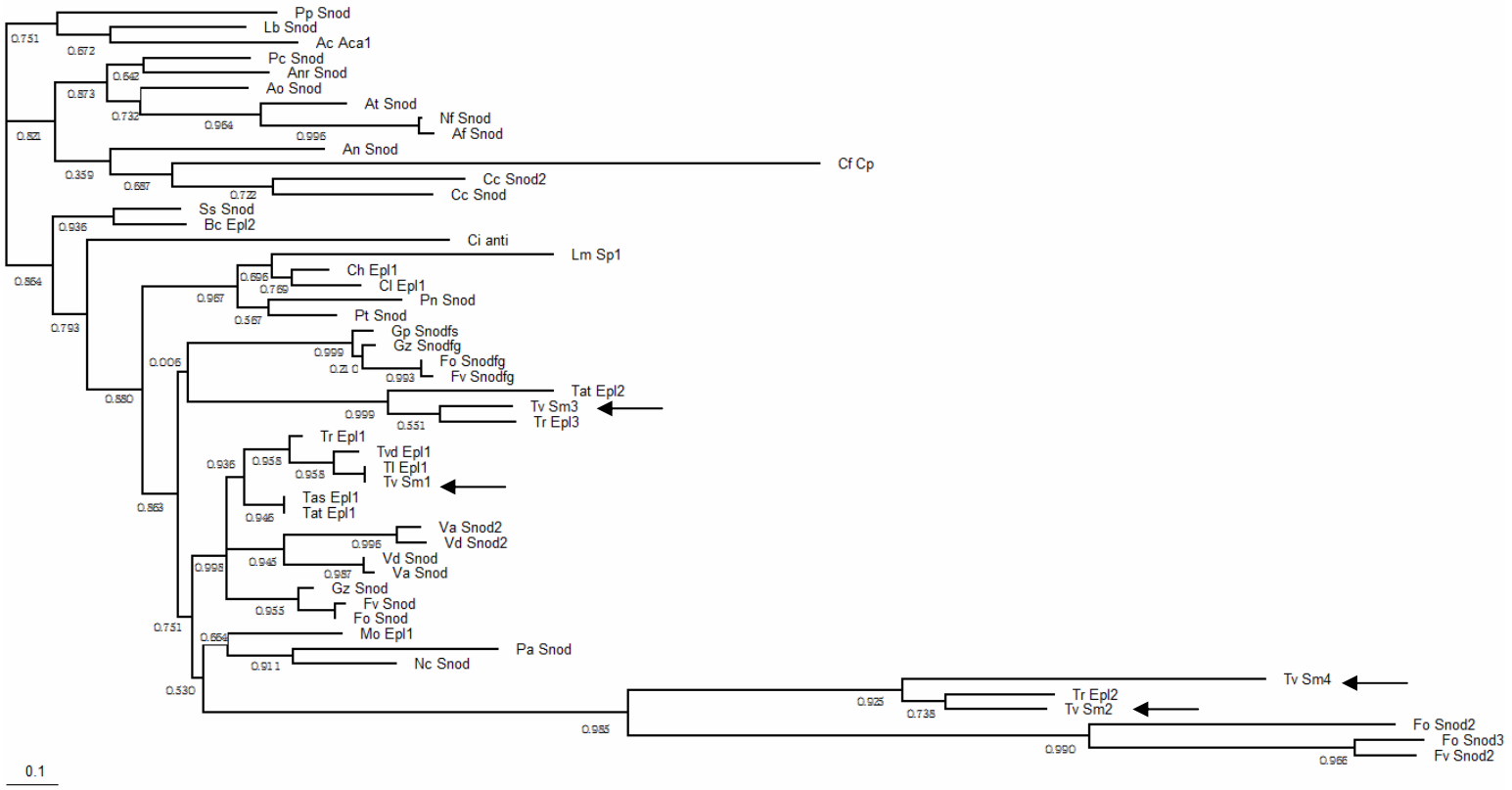

FIG. 3.2. A gene phylogeny of the cerato-platanin family of proteins. Protein sequences were entered into a PhyML maximum-likelihood software with a bootstrap of 100 (corresponding numbers on individual branches). The abbreviations designate the following fungal species: *Antrodia camphorate* (Ac), *Aspergillus nidulans* (An), *Aspergillus oryzae* (Ao), *Aspergillus terreus* (At), *Botrytis cinerea* (Bc), *Coprinopsis cinerea* (Cc), *Ceratocystis fimbriata* (Cf), *Cochliobolus heterostrophus* (Ch), *Coccidiodes immitis* (Cc), *Cochliobolus lunatus* (Cl), *Fusarium oxysporum* (Fo), *Fusarium verticillioides* (Fv), *Gibberella pulicaris* (Gp), *Gibberella zeae* (Gz), *Laccaria bicolor* (Lb), *Leptosphaeria maculans* (Lm), *Magnaporthe oryzea* (Mo), *Neurospora crassa* (Nc), *Neosartorya fischeri* (Nf), *Potentilla anserine* (Pa), *Penicillium chrysgenum* (Pc), *Phaeosphaeria nodorum* (Pn), *Postia placenta* (Pp), *Pyrenosphora tritici-repentis* (Pt), *Sclerotinia sclerotiorum* (Ss), *Trichoderma asperellum* (Tas), *Trichoderma atroviride* (Tat), *Trichoderma longbrachiatum* (Tl), *Trichoderma reesei* (Tr), *Trichoderma virens* (Tv), *Trichoderma viride* (Tvd), *Verticillium albo-atrum* (Va), and *Verticillium dahliae* (Vd). Arrows indicate the presence of *T. virens* cerato-platanin proteins.

several distinct branches, containing great species diversity as compared with the other clade. All four *T.virens* paralogs except for *sm2* and *sm4*, assemble on separate branches of the clade. Both *sm2* and *sm4* reside on a branch separated distantly from both *sm1* and *sm3*.

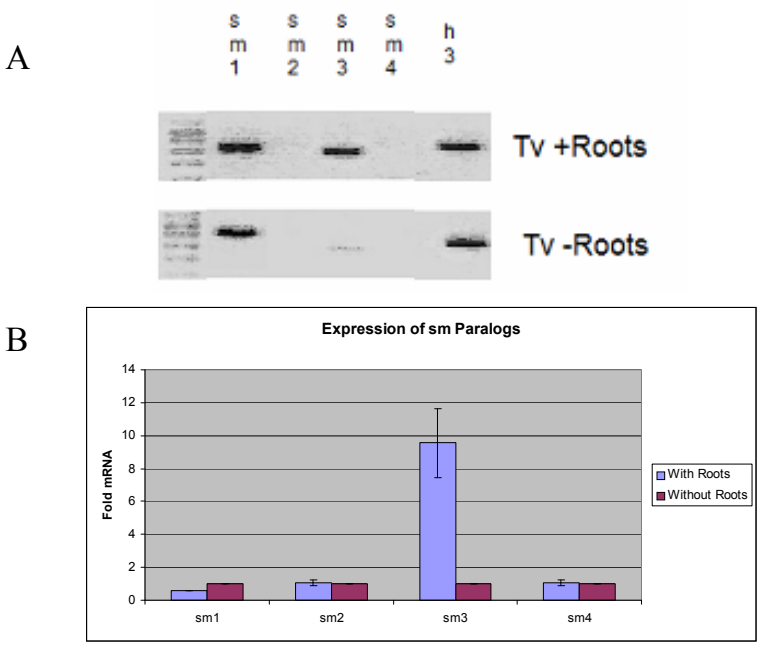

FIG. 3.3. Expression analysis of paralogs of *sm1*. A) rtPCR analysis of the four *T. virens* cerato-platanin paralogs in cultivated with maize roots in a hydroponic system. The control (Tv-roots) for this experiment was Murashige and Skoog (MS) medium without the presence of maize roots. Expression of the histone 3 housekeeping gene was used to indicate the total amount of cDNA. B) Quantative real-time PCR of the *T.virens* cultivated with maize roots for the cerato-platanin paralogs. Controls were the same as those used for rtPCR. This experiment verifies the upregulation of *sm3*. An eight fold increase in *sm3* was demonstrated in mycelia grown in the presence of maize roots compared to mycelia grown in MS medium without roots.

Expression analysis of *sm1* paralogs. Expression of the *sm1* paralogs was determined under several different conditions including different carbon sources, complex media, in the presence of plant roots, during confrontation with *Rhizoctonia*

solani, and in still-culture. The two genes, *sm2* and *sm4*, were not expressed under any of the conditions tested. *Sm3*, however, was expressed under two of the conditions examined. In the presence of plant roots in a maize hydroponic system, *sm3* was expressed in roots, but no expression was observed in MS only (Figure 3.3A,B). *Sm1* had expression under both conditions with an upregulation in the presence of roots. This increase in expression in the presence of roots is consistant with previous observations (30). The other condition in which *sm3* expression was observed was during growth in still culture (Figure 3.4). This expression was similar in both Gv29-8 and the *sm1* deletion strain (Δsm1-25).

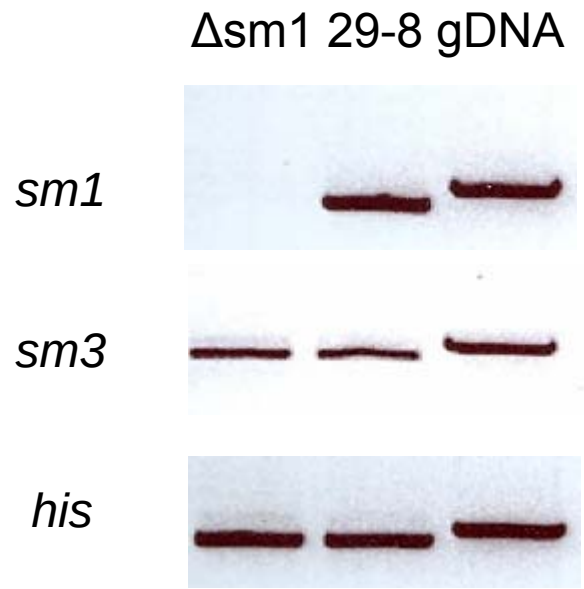

FIG. 3.4. Expression of *sm1* and *sm3* in still-culture. Reverse transcription PCR was performed on RNA extracted from fungal tissue of the *sm1* deletion mutant (Δsm1) and Gv29-8 after growth in still-culture (VMS) for 7 days. The histone gene (*h3*) was used as the loading control and genomic DNA was used as the PCR positive control.

Production of recombinant SM3 in the *Pichia pastoris* protein expression system. To evaluate SM3 for the ability to induce resistance to pathogens in plants, protein was produced in *P. pastoris* (picSM3). A time course analysis of protein production in one of the positive clones (KM1) revealed an increase of synthesis over six days (Figure 3.5). PicSM3 protein was detected at all time points by anti-FLAG antibody with the most protein appearing at 144 hours. No degradation due to proteases was detected on the SDS-PAGE gel.

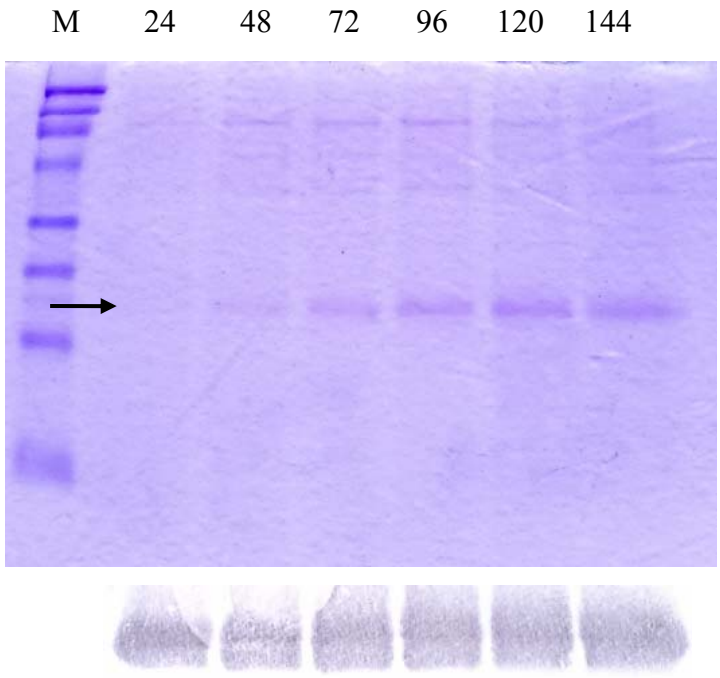

FIG. 3.5. Time course of picSM3 protein production in *P. pastoris*. Cultures were grown as described in Materials and Methods and samples were taken every 24 hours for 144 hours. These samples were analyzed by SDS-PAGE gel and picSM3 was immunodetected using an antibody against the FLAG tag. Location of picSM3 is indicated by arrow

Purification of recombinant SM3 by protein chromatography and MS/MS spectral matching. Purification of picSM3 was conducted in a strain of *P. pastoris* grown under methanol inducing conditions. The bulk protein was subjected to anion

exchange chromatography, and the recombinant SM3 protein was found to elute in fractions 25-32 (Figure 3.6A). These fractions were pooled and further subjected to gel filtration chromatography (Figure 3.6B). Pure picSM3 was eluted in fractions 42-52 with homogeneity of the sample determined by SDS-PAGE and Western blotting (Figure not shown).

Purified picSM3 was subjected to tandem mass spectrometry (MS/MS) spectral analysis. The peptide fragment spectrum was matched to that of the predicted SM3 protein sequence (data not shown). Based on these results, the mass of the protein was calculated to be 16 kD with a pI of 4.58.

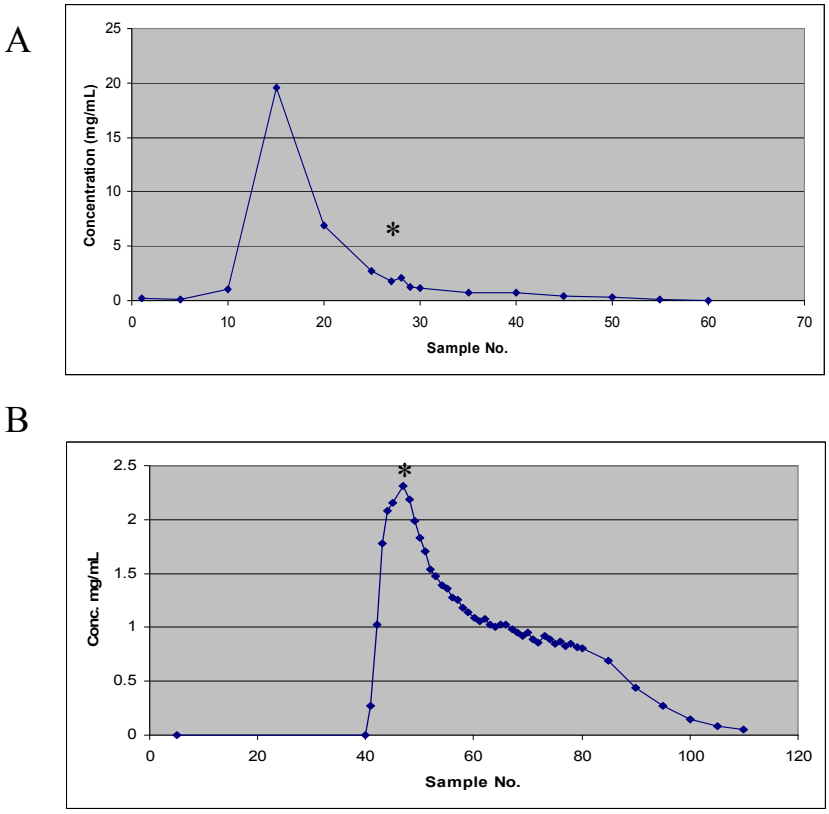

FIG. 3.6. Purification of picSM3. Protein was purified by anion exchange (A) and gel filtration chromatography (B). Asterix indicates elution of picSM3.

Antibodies produced by GenScript were tested using picSM3 and native SM1. As a control the anti-sera provided was used against both proteins (Figure 3.7). The anti-sera detected no signal for either SM1 or picSM3. The anti-SM3 antibody only detected picSM3. There was no detection of SM1 indicating that there is no redundancy in the antibody binding.

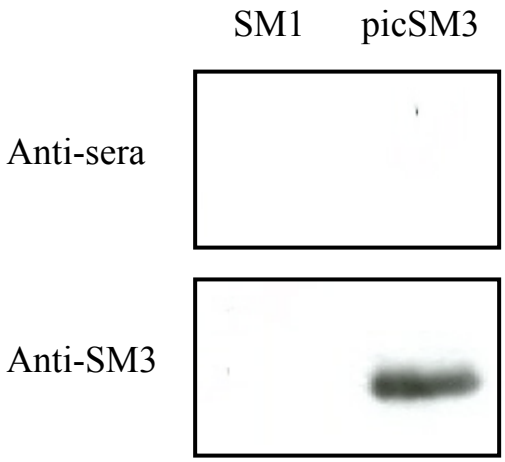

FIG. 3.7. Assessment of SM3 antibodies against purified SM1 or picSM3. Rabbit preimmune anti-seria was also used for Western blotting as a control.

Glycosylation analysis of SM3 from *Pichia pastoris.* SignalP 4.0 (http://www.cbs.dtu.dk/services/SignalP/) predicts the glycosylation of an asparagine located at amino acid 75 in SM3. To determine if picSM3 has been glycosylated, purified protein was treated with PNGase F and separated on an SDS-PAGE gel. PNGase F treated protein ran faster than the untreated control on the gel indicating that a sugar moiety had been cleaved from the deglycosylated protein (Figure 3.8A). PAS staining confirmed the deglycosylation of picSM3 (Figure 3.8B). Untreated picSM3

stained similar to that of the positive control, horse radish peroxidase, whereas the PNGase treated protein did not stain. The lack of staining of the enzymatically treated protein was similar to that of the negative control, lysozyme.

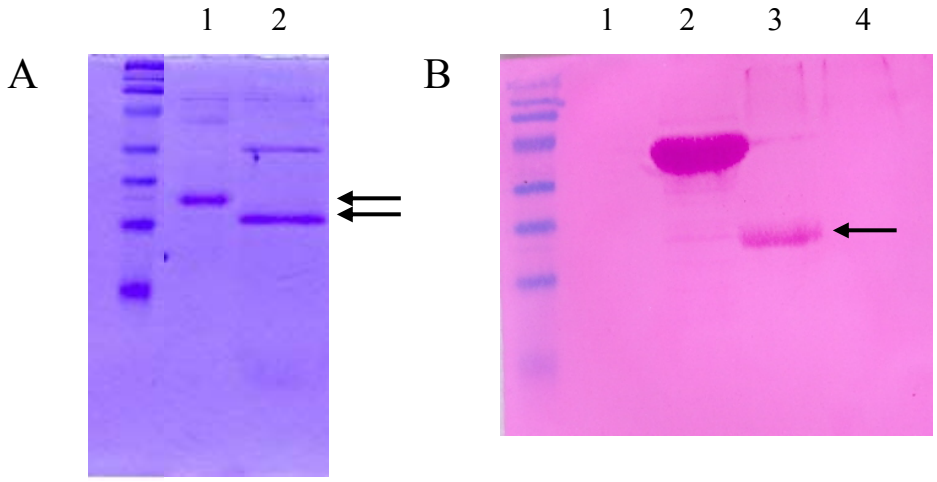

FIG. 3.8. Glycosylation analysis of picSM3. (A) SDS-Page. Lane 1: picSM3, Lane 2: picSM3 treated with PNGase F. (B) Periodic Acid Schiff stain for glycosylated proteins. Lane 1: Lyzozyme (negative control); Lane 2: Horseradish Peroxidase (positive control); Lane 3: picSM3; Lane 4: picSM3 treated with PNGase F. Arrows indicate protein of interest on gel.

Elicitation of maize defense genes with treatment of roots with recombinant SM3. Roots of seedlings were treated with purified picSM3 to determine if the recombinant protein has the ability to induce transcription of defense related genes in maize (Figure 3.9). Reverse transcription PCR indicates that much like SM1, picSM3 upregulates the expression of *pal* as compared to the water control.

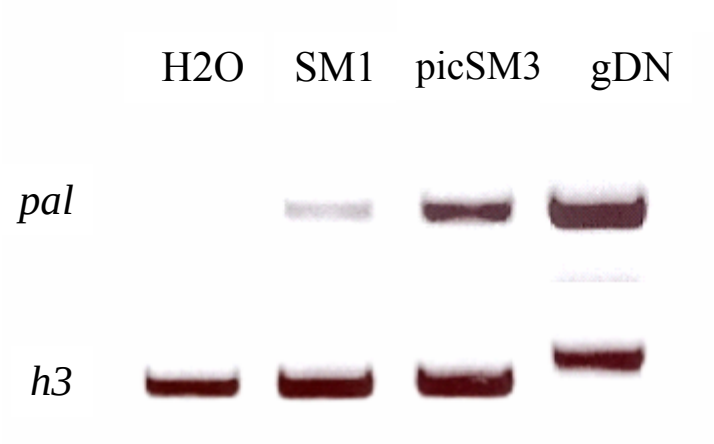

FIG 3.9. Reverse transcriptase PCR analysis of defense genes in maize. Maize seedlings treated with water, SM1, or picSM3 by application to the root tip. Histone *(h3)* was used as a positive control for expression and genomic DNA (gDNA) was used as a positive control for PCR.

Identification of *sm3* disruption, over-expression, and *sm1:sm3* double mutants. Deletion, over-expression mutants for *sm3,* as well as *sm3* deletion mutants in a *sm1* deletion background (Δsm1-25) were generated to further study the role of *sm3* in plant-microbe interactions. The *sm3* deletion construct was used to transform Gv29-8 and Δsm1-25, replacing the *sm3* open reading frame with the *hygB* coding region (Figure 3.10A). Thirty-five and 27 stable transformants were screened by PCR for the single disruption mutant and the double mutant, respectively (data not shown). Transformants with a loss of the *sm3* coding region were evaluated further by PCR (Figure 3.10B). Three single deletion transformants (Δsm3-4, Δsm3-6, and Δsm3-40) and the Δsm1:Δsm3 transformant (Δsm1:Δsm3-65) were identified.

Transformants for *sm3* over-expression were screened by PCR analysis (Figure 3.11) and all five were positive for insertion of *sm3* between the promoter and terminator of *gpd*.

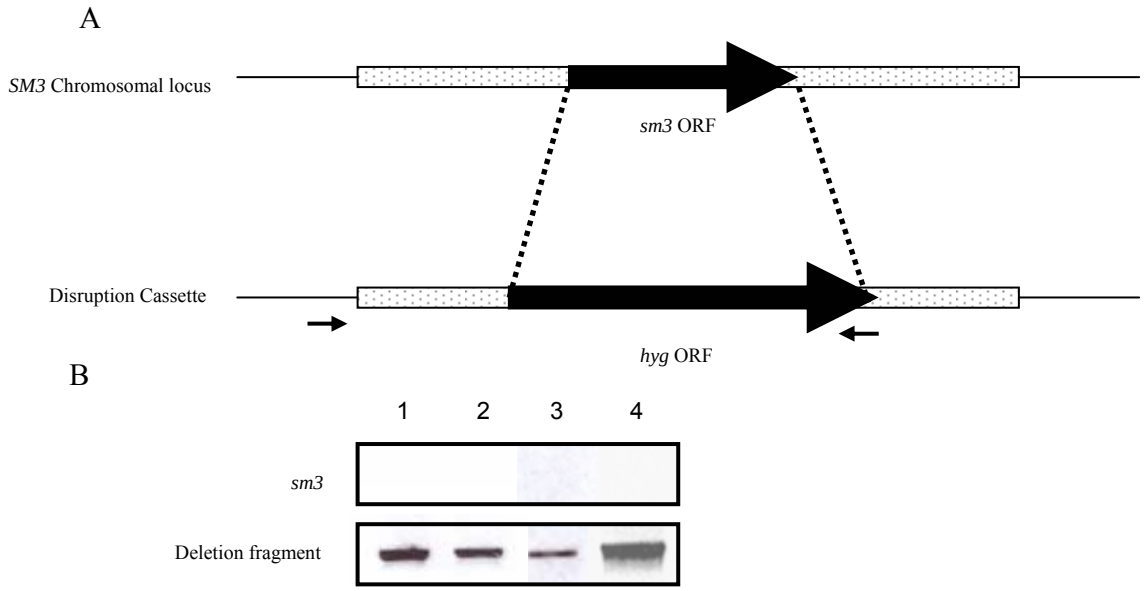

FIG. 3.10. Confirmation of *sm3* disruptants. (A) Scheme of strategy for gene deletion. The native *sm3* is replaced with a 1.5 kb fragment of the hygromycin resistance cassette (*hyg*). This yielded a band of 1.9 kb when evaluated by PCR using the primers sm3-11 and HygR. The arrows indicate location of primers. (B) PCR analysis of the *sm3* deletion strains. Lane 1: Δsm3-4, lane 2:Δsm3-6, lane 3: Δsm3-40 and lane 4: the *sm1:sm3* double mutant (Δsm1:Δsm3-65).

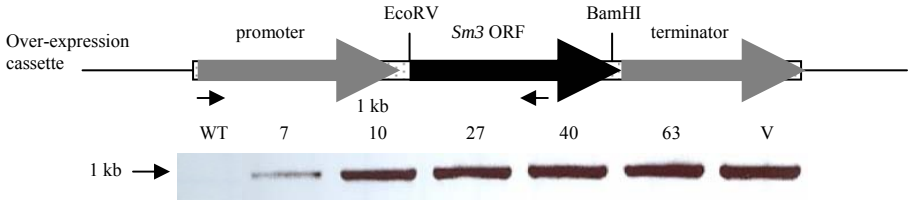

FIG. 3.11. Gene over-expression strategy and selection of transformants by PCR. Top panel, a schematic representing the construction of the *sm3* over-expression construct. A 480 bp fragment containing *sm3* was cloned between a glyceraldehyde phosphate dehydrogenase (gpd) promoter and terminator using *EcoRV* and *BamHI* restriction digest sites. Small arrows indicate the primers used for screening transformants. Bottom panel: Screening of transformants using PCR. WT indicates wild-type and V designates the vector used for transformation (positive control). Gene over-expression transformants screened were sm3oe-7, sm3oe-10, sm3oe-27, sm3oe-40, and sm3oe-63.

***Sm3* expression and protein production in transformants.** All deletion mutants were grown in still-culture conditions for examination of *sm3* expression. Strains positive for the presence of the *sm3* over-expression cassette were grown for 3 days in VMS. RNA extracted from these cultures was evaluated by Northern blot (Figure 3.12). No transcripts for *sm3* were observed in any deletion strains, confirming disruption of the gene (Figure3.12A). The over-expression strains showed greatly increased expression of *sm3* compared to Gv29-8 under the same conditions (Figure 3.12B).

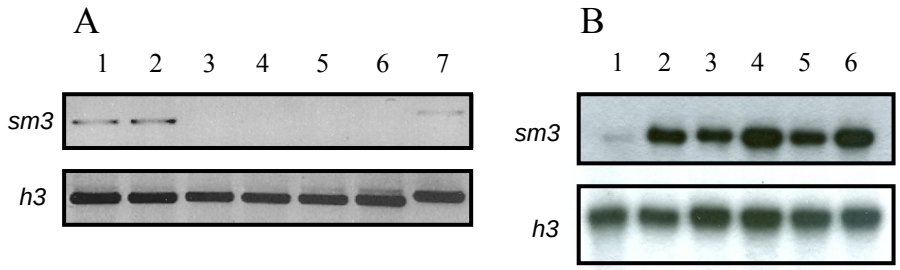

FIG. 3.12. Analysis of *sm3* expression in transformants. (A) Reverse transcription PCR of *sm3* deletion strains. Lane 1: Gv29-8; Lane 2: Δsm1-25; Lane 3: Δsm3-4; Lane 4: Δsm3-6; Lane 5: Δsm3-40; Lane 6: Δsm1:Δsm3-65; Lane 7: Gv29-8 genomic DNA. Histone *(h3)* gene was used as a control for even loading. (B) Northern blot of *sm3* over-expression strains. Lane 1: Gv29-8; Lane 2: sm3oe-7; Lane 3: sm3oe-10; Lane 4: sm3oe-27; Lane 5: sm3oe-40; Lane 6: sm3oe-65. The histone (*h3*) gene was used as a control for even loading.

Production of SM3 by the deletion strains was evaluated by SDS-PAGE and Western blot analysis. Protein was extracted from still-culture conditions and detected using anti-SM3 (Figure 3.13). All mutant strains were negative for the production of SM3. In Gv29-8, SM3 was identified as a band that separated similar to SM1

(approximately 16 kDa) under these conditions. Interestingly, SM3 was not observed in the protein fraction extracted from Δsm1-25.

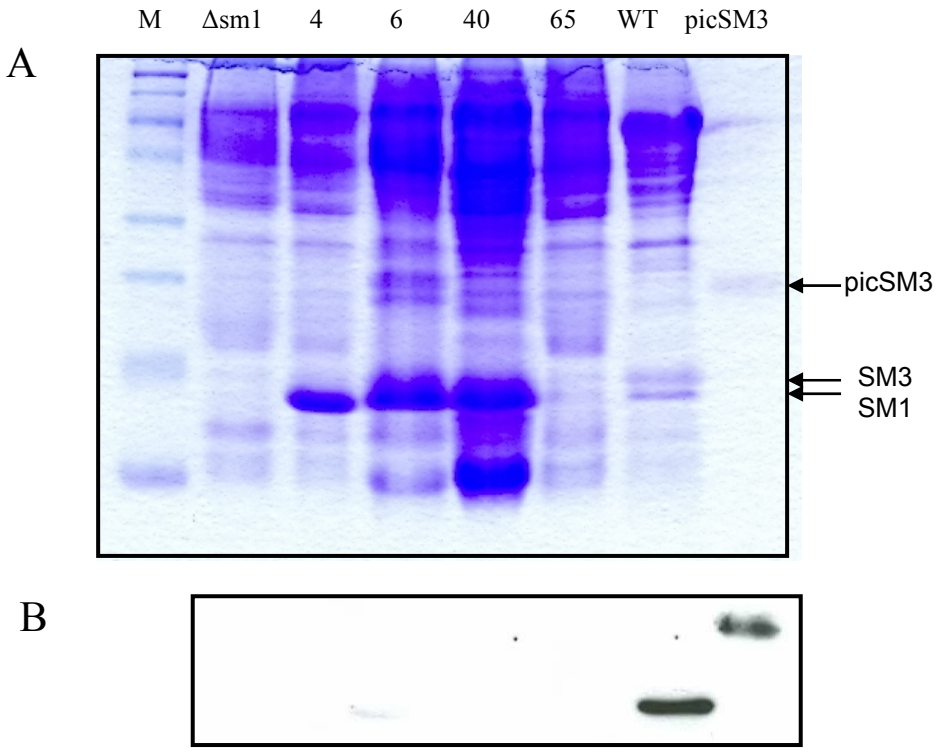

FIG. 3.13. SDS-PAGE and Western blotting analysis of *sm3* deletion mutants. The *sm1* deletion mutant, the *sm3* deletion mutants (Δsm3-4, Δsm3-6, and Δsm3-40), the *sm1:sm3* deletion mutant (Δsm1:Δsm3-65), and Gv29-8(WT) were grown in still culture and total protein from culture filtrate was examined for presence of SM3 by SDS-PAGE (A) and Western blotting (B). The blot was probed with anti-SM3 antibody and picSM3 was used as a positive control for the Western blotting.

SDS-PAGE and Western analysis of protein produced in over-expression strains revealed the presence of SM3 in all transformants, though sm3oe-40 was detected faintly (Figure 3.14). Protein detected under these conditions was observed as two distinct bands. Protein extraction and Western analysis was performed twice to confirm these

results. In protein extracted from Δsm1-25 (the genetic background for the over-expression strains), SM3 was not detected.

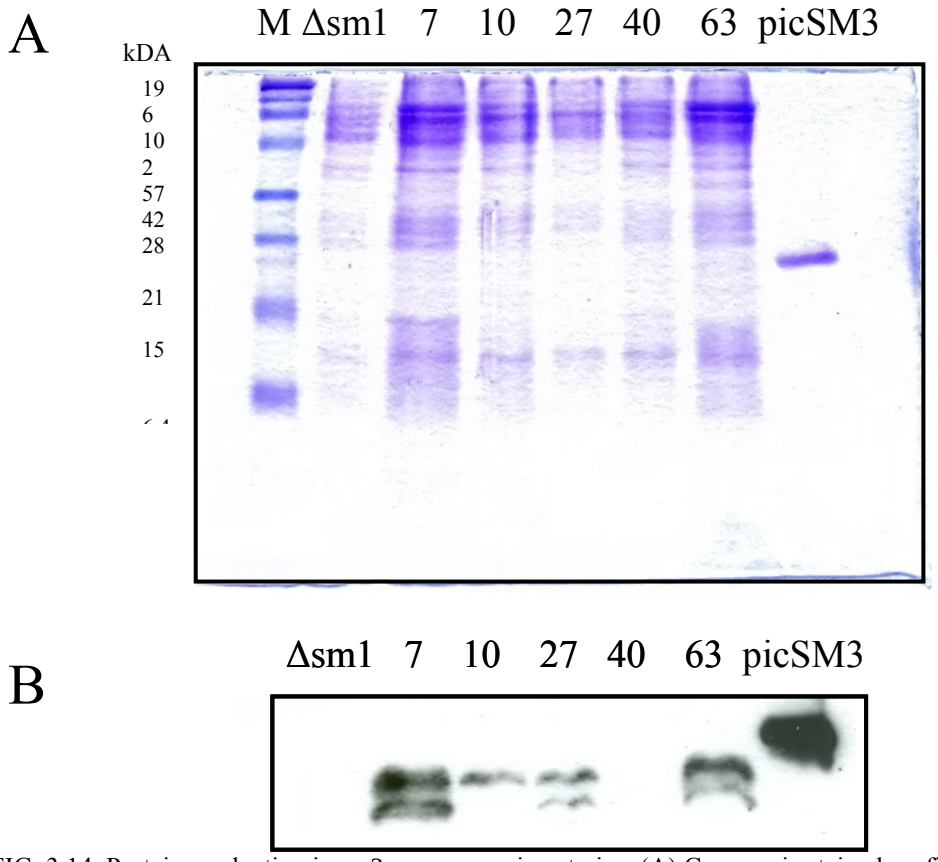

FIG. 3.14. Protein production in *sm3* over-expession strains. (A) Coomassie stained profile of the SDS-PAGE analysis of protein extracted from culture filtrate. Equal volumes of concentrated samples were loaded into each lane for all samples except 3µg of *sm3* purified from *P. pastoris.* Treatments from left to right: protein marker, *sm1* deletion mutant (background of transformants), *sm3* over-expression transformants (7, 10, 27, 40, and 63), and picSM3. (B) Western blot analysis of culture filtrate from over-expression mutants. Blot corresponds to SDS-PAGE gel shown above.

***Sm3* deletion mutants show no change in fungistatic activity against plant pathogenic fungi.** The deletion mutant Δsm3-4 and Gv29-8 were confronted against *R. solani*, *P. ultimum*, and *S. minor* to examine the role of *sm3* in mycoparasitism (Figure

3.15). For each of the competing fungi, there was no difference observed for growth, sensitivity, and/or arial hyphae production. The ability of *T. virens* to compete with these plant pathogens was uncompromised in Δsm3-4.

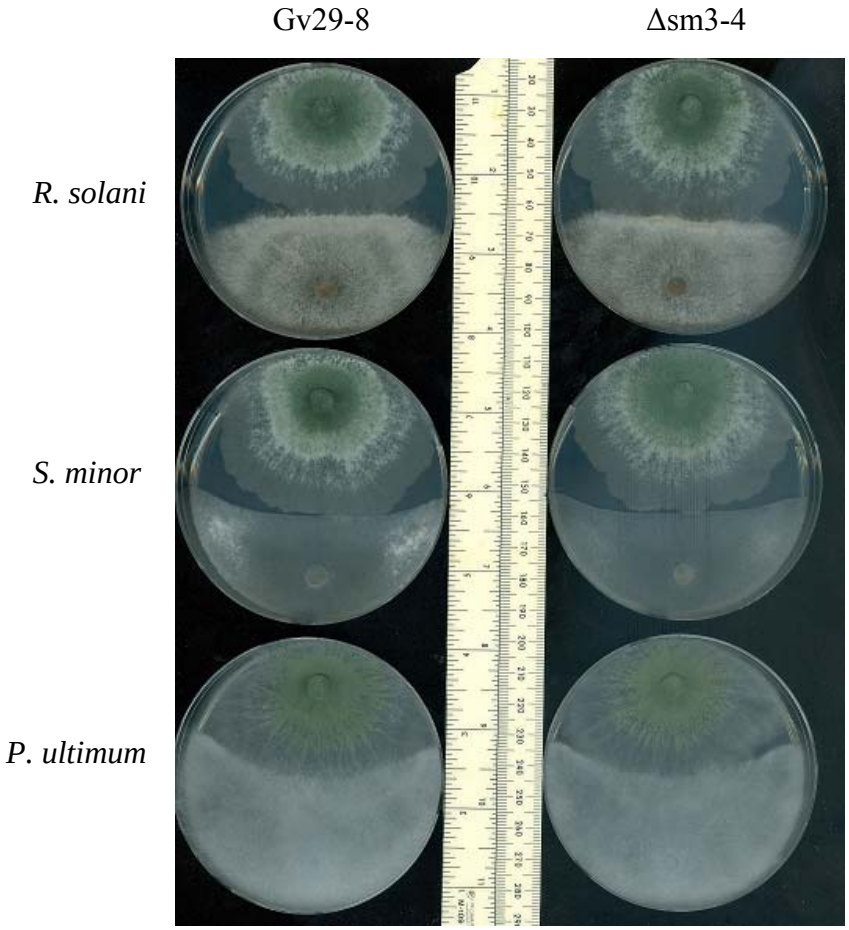

FIG. 3.15. Fungistatic activity of *sm3* mutant. The ability of Δsm3-4 to inhibit fungal growth in *R. solani*, *S. minor* or *P. ultimum* by confrontation assay on PDA. *T. virens* is at the top of the petridish and the competing plant pathogen is pictured at the bottom of the petridish.

***Sm3* deletion mutants show no change in ability to protect maize from *Colletotrichum graminicola*.** To assess the relevance of the expression of *sm3* in plant

roots, three *sm3* deletion mutants (4, 6, and 40) and Gv29-8 were tested in a maize-*C. graminicola* ISR induction assay (30). Plants treated with Gv29-8 had significantly smaller lesions than the untreated control (Figure 3.16). Lesion size in maize seedlings treated with *sm3* deletion mutants were significantly smaller than the untreated control, but comparable to plants treated with Gv29-8.

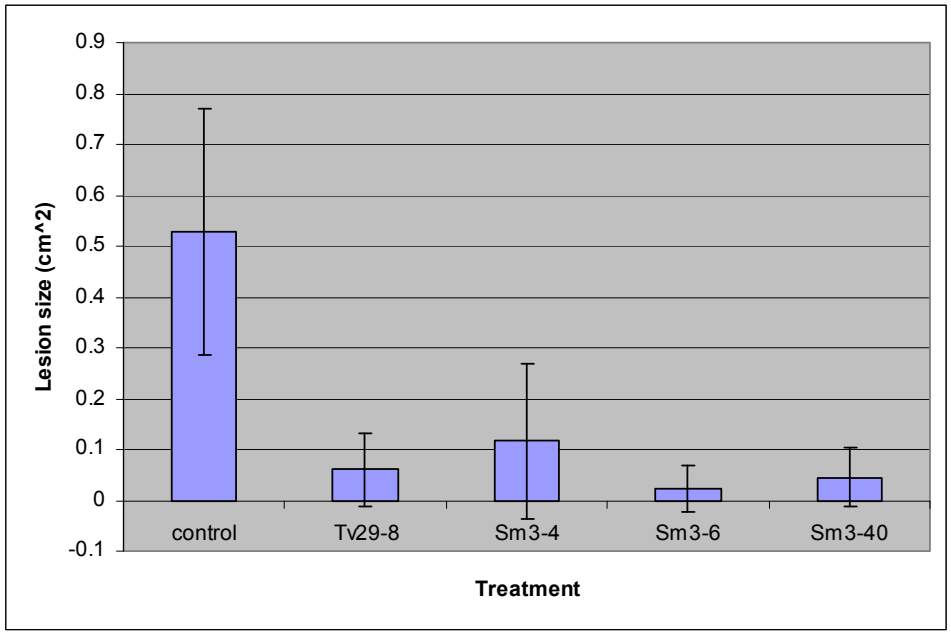

FIG. 3.16. Ability of deletion mutants to elicit defense responses in maize. Two week old maize plants previously treated with WT (Gv29-8) or deletion mutant (Δsm3-4, Δsm3-6, and Δsm3-40) were inoculated with 650 *C. gramincola* spores and incubated with four days. On day four, lesions were measured and bars indicate mean lesion size of six replicates with four plants with standard deviation bars.

DISCUSSION

In *T. virens* there are three paralogs of the proteinaceous elicitor SM1. SM1 is a member of the cerato-platanin family of proteins (cpf). This family consists of proteins that are small, cysteine rich, and secreted (95). Several members of this family

have been found to display elicitor activity and may function as virulence factors for the development of plant diseases (36, 57, 77). The cpf protein, SM1, from *T. virens* has been previously identified as a proteinaceous elicitor of ISR in maize and cotton (29, 30). However, there are some cpf proteins that do not have a role in plant disease development, and their function remains unknown (115, 130, 142).

Three paralogs of SM1 were identified in *T. virens.* The amino acid sequences of these proteins provided for the prediction of a secretion signal, a phosphorylation site, four cysteine residues, and glycosylation sites in *sm3* and *sm4* (Figure 3.1). All four proteins contain features that characterize cpf proteins: size, hydrophobicity, signal peptide, and a conserved cysteine residue pattern (29, 36, 95, 130). A gene phylogeny with other cpf proteins, also provided evidence that all three proteins are paralogs of SM1 and members of the cp family of proteins.

To determine the relationships between the four cerato-platanin proteins, a gene phylogeny was produced (Figure 3.2). Genome searches and previous research has revealed that cpf protein homologs are found in both Basidiomycetes and Ascomycetes in indicating that cpf protein existed in the common ancestory of these phyla (36, 142, 146). After the tree was rooted with three Basidomycete fungi (*Antrodia camphorate*, *Laccaria bicolor*, and *Postia placenta*), two major clades emerged. The first contains the proteins from the remaining Basidiomycetes, the *Aspergillus* species, and *C. fimbrata*, a plant pathogen. The grouping together of both Basidiomycetes and Ascomycetes indicates that the functions of these proteins may be the same between both phyla. The second clade contains several distinct branches. The largest number of

species and species diversity is found in this clade indicating that the homologs found here may represent the ancestral function of this protein family. Two *T.virens* paralogs (*sm1* and *sm3*) assemble on separate branches of the clade, allowing for the possibility of a gene duplication and functional divergence within these proteins.

The promoter regions of all four paralogs contain large of diversity for number and presence of putative transcription factor binding sites. *Sm1* contained the largest number and greatest variation of motifs in the upstream coding sequence (Table 3.1). The diversity of transcription factor binding motifs is consistent with previous work of *sm1* that showed this gene to be expressed under many conditions. The other genes (*sm2*, *sm3*, and *sm4*) showed fewer motifs with the promoter of *sm4* having the least with only six of the examined putative transcription factor binding sites. *Sm2* has six putative sites for STRE stress response elements. Although *sm2* and *sm4* were not expressed under any of the conditions examined, they may be responsive under specific stress conditions that were not assessed in this study.

***Sm3* is expressed in plant roots and in still-culture conditions.** The only *sm1* paralog to show expression in any of the conditions tested was *sm3*. This gene was expressed in plant roots and during growth in still-culture (Figure 3.3 and Figure 3.4). Another protein family, hydrophobins, has been found to be expressed under similar conditions (133). During growth of *Trichoderma* within plant roots hydrophobins have been found to be essential for root colonization and involved in aerial growth of hyphae and structure of conidia and conidiophores. Aerial hyphal growth and production of conidia both occur during growth of *T. virens* in still culture, but are not present in

submerged tissue. Cpf proteins have been shown to have close homology to hydrophobins (95) and to aggregate in similar manner (96). This suggests that *sm3* may have a similar function to hydrophobins in *T. virens.*

SM3 produced in *P. pastoris* upregulates *pal* in maize seedlings. Native SM3 was not readily identified because the lack of an antibody (only available at end of most experiments) and the discovery that SM3 was difficult to solubilize. Therefore, to study the function of SM3 in plant-*T. virens* interactions, protein was produced in the *Pichia* protein expression system. Recombinant SM3 with a FLAG tag was successfully produced with largest production occurring at 120 hours (Figure 3.4). Protein was purified from culture filtrate using anion exchange chromatography (AEX) and gel filtration chromatography (GFC), which has been successful for other members of this family (29, 130) (Figure 3.6). Using the same protocol, SM1 eluted in a very different place from picSM3 (30, 130) indicating that picSM3 holds a different charge than SM1 and binds to the column more tightly.

Mass spectrometry analysis and SM3 antibodies confirmed the identity of the purified protein as SM3 (Figure 3.7), allowing for the protein to be characterized. On a SDS-PAGE gel, picSM3 ran higher than expected indicating it may be post-translationally modified. Digestion with PNGase F and PAS stain was performed (Figure 3.8) to determine if the modification is involved in glycosylation. The digestion produced a smaller protein that ran faster on an SDS-PAGE gel confirming the removal of a sugar moiety from the protein (Figure 3.8A). The PAS protocol will stain any glycosylated protein pink as a reaction with the sugar group. Untreated picSM3 stained a

bright pink, similar to the positive control, whereas the protein treated with PNGase F was undetected by the strain (Figure 3.8B). Both tests confirm the glycosylation of picSM3. Previous research indicates that native SM1 is glycosylated at a putative n-glycosylation site (130). The study of this glycosylation site is the topic of Chapter IV.

Purified picSM3 was further assessed for ISR activity by inoculating maize seedlings to determine if the defense response gene, *pal*, was induced. *Pal* has been found to be responsive to treatment with elicitors of ISR (30) and during interactions with species of *Trichoderma (30, 46, 118).* Reverse transcriptase PCR (rtPCR) revealed the upregulation of *pal* with picSM3 treatment (Figure 3.9). This indicates that SM3 may have the ability to act as an elicitor.

Evaluation of genetically modified strains. The role of SM3 to in the biology of *T. virens* was examined in deletion and over-expression strains. Protein production by these strains was evaluated when the strains were grown in still-culture. The *sm3* single (wild-type background) and double deletion (Δsm1-25 background) strains were found not to produce native SM3, whereas the wild-type contained a band that responded to the SM3 antibody on Western blot (Figure 3.13). Both the *sm1* deletion strain and the double mutant failed to produce either SM1 or SM3. The single *sm3* deletion strains produced an increased amount of SM1 as compared to wild-type. In still-culture both *sm1* and *sm3* are expressed in wild-type and *sm3* is expressed in the *sm1* deletion mutant (Figure 3.3). The expression of *sm3* with undetectable SM3 production observed in Δsm1-25 still-culture filtrate was unexpected. As well, in the *sm3* deletion strains, SM1 was produced in amounts significantly greater than those observed in the wild-type

strain. In wild-type, the protein amounts appear to be similar. In still-culture, the deletion of *sm1* results in a decrease of SM3, but deletion of *sm3* increases the production of SM1. These data suggest there may be co-regulation between SM1 and SM3 at the protein level. There are future experiments that may clarify these observations. First, protein amounts of SM3 in the *sm1* over-expression strains should be observed as well as expression of *sm1* in *sm3* deletion mutants. A interesting experiment would be to determine if a similar phenomenon is observed in planta.

Another observation from the protein gels and Western blots was the size of SM3. The protein observed on SDS-Page for both over-expressers and Gv29-8 was larger than SM1 and ran higher on the gel than the protein size would predict. As well, two bands were present in extracts from the over-expression mutants (Figure 3.14). Both observations may indicate a post-translational modification. This was similar to what was seen with picSM3. Native SM3 may be glycosylated similar to picSM3. In other proteins such as flagellin and pillins, glycosylation of the protein was required for elicitor function and subsequent defense responses mounted by the host plant (8, 41). There may be a similar effect with picSM3, and future work will include treating maize seedlings with deglycosylated protein to test for elicitor effectiveness.

Phenotypic analysis of transformants. To analyze the deletion strains for both methods of biocontrol, transformants were challenged in a confrontation assay and tested for their ability to elicit defense responses in maize infected with *C. graminicola*. The *sm3* confrontation assay yielded no differences between the wild-type and *sm3* deletion strain (Figure 3.15). This is not surprising considering that previous tests performed with

SM1 demonstrated no activity toward a range of plant pathogenic organisms (29). Measurement of lesion size on maize leaves determined the *sm3* deletion strains maintained the ability to induce ISR as compared with Gv29-8 (Figure 3.14). SM1 was still present in the *sm3* deletion strains so some ISR capability was expected, however, no change in ISR was surprising considering that picSM3 can upregulate a defense gene in maize (Figure 3.7). However, the explanation for this may be found in the features of the native SM3 protein. To solubilize SM3 for analysis on SDS-PAGE gels, protein extracts required treatment with 5M urea (Materials and Methods). SDS and β-mercaptoethanol, usually are used to disrupt protein structure and linearize for electrophoresis, were insufficient to solubilize SM3. Protein extracts from the same experiment not treated with urea failed to detect SM3 on Western blot (data not shown). Protein insolubility is usually due to increased hydrophobic residues in the protein structure, similar to what is observed in hydrophobins (72, 73). The hydrophobic regions cause the individual proteins to aggregate. This aggregation has also been observed in other cpf proteins (96, 115, 130). Specifically, EPL1 from *Trichoderma atroviride* will form dimeric structures when in the presence of the plant (130). Unlike CP from *C. fimbriata* (96), previous research in *T. atroviride* has shown that when in dimer form EPL1 in unable to elicit defense responses. Therefore, in the case of SM3, the hydrophobicity of the protein may be encouraging the formation of protein complexes, rendering the protein inactive as an elicitor.

In summary, *T. virens* contains four paralogous genes potentially encoding for cpf proteins within the genome (*sm1*, *sm2*, *sm3*, and *sm4*). SM1 has been previously

studied and found to be an elicitor of ISR in maize and cotton (29, 30). Of the other three paralogs, only *sm3* was found to be expressed under any of the conditions tested (maize roots and still-culture). Protein produced in *P. pastoris* had the ability to upregulate *pal* in maize seedlings, so deletion and over-expression mutants were created. The native protein produced in these mutants suggests the possible co-regulation of these proteins in still-culture conditions. When further evaluated, these mutants revealed no change compared to wild-type in the confrontation or ISR analysis. At present, the function of SM3 in *T. virens* remains unresolved.

CHAPTER IV

ANALYSIS OF A PUTATIVE GLYCOSYLATION SITE IN THE *TRICHODERMA VIRENS* ELICITOR SM1

INTRODUCTION

The process of self-association of proteins and formation of oligomeric structures is common in biological systems (81). Independent function of proteins in cellular processes is rare and often aggregation with other proteins is required for enzymatic activity. This association can present several advantages including improved regulation by controlling accessibility to active sites, enhanced stability of the protein, and increased complexity in biological signaling systems (81). Specifically, protein dimerization or oligomerization is a regulatory element in key cellular processes controlled by enzymes, ion channels, receptors, and transcription factors. Secreted proteins from filamentous fungi have also been observed to form aggregations (96, 128). Hydrophobins are surface proteins found to be involved in aerial growth, fungal attachment, and root colonization in *Trichoderma* spp. (72, 73, 133). This class of proteins readily aggregates in the surrounding environment, in fungal cell walls, and on the surface of conidia. The ability of these proteins to lower surface tension and perform important functions for the fungus is enhanced by protein aggregation (71, 73). Cerato-plantanin (CP), a protein closely related to hydrophobins, also characteristically aggregates after secretion and during interaction with the host due to its moderate hydrophobicity (96). Aggregated CP is more effective than soluble CP at activating

defense responses including phytoalexin synthesis and localized cell death in treated plant leaves.

Cerato-platanin proteins (cp) produced by *Trichoderma* spp. have also been observed to form oligomers after secretion (29, 130). The most recent studies examined SM1 and EPL1 from *T. virens* and *T. atroviride*, respectively (115, 130). Both proteins can be detected in monomer and dimer forms however, SM1 appears primarily as a monomer and EPL1 as a dimer (115, 130). When the ability of the two forms of each protein to elicit plant defense responses was investigated, only the monomer form of both proteins was shown as an effective elicitor. Deletion of *epl1* rendered no difference in the ability of *T. atroviride* to induce ISR and demonstrate plant protection (115). However, colonization of maize plants by strains of *T. virens* with a deletion of *sm1* resulted in a decrease in resistance to the pathogen *C. graminicola*. These data suggested that SM1has an ability to maintain its monomeric form, which is necessary to induce systemic resistance in the plant. NetNGlyc 1.0 (http://www.cbs.dtu.dk/services/NetNGlyc/) predicts EPL1 and SM1 differ in the presence of a glycosylation site at position 10 within the amino acid sequence. Testing for glycosylation by staining of the two proteins implied that SM1 was glycosylated, but not EPL1 (130). The glycosylation of SM1 suggests that the addition of a sugar moiety is required to prevent aggregation and maintain monomeric form in cerato-platanin proteins (96, 130).

To test the hypothesis that glycosylation is required for SM1 to maintain a monomeric structure, a point mutation was generated within the coding region of SM1.

We reason that this mutation would effectively block any possible n-glycosylation of the protein. Transformants were generated containing the insert and sequenced for the presence of the point mutation. The recombinant protein was purified using column chromatography and compared to native SM1 for structure and glycosylation.

MATERIALS AND METHODS

Growth of fungal and bacterial strains. Two strains of *Trichoderma virens* were used in this study, wild type strain, Gv29-8, and *sm1* deletion strain Δ*sm1-25* (30). For selection of point mutation strains, transformants were grown on potato dextrose agar (PDA, Difco) or PDA plus 100mg/mL hygromycin (PDA-H). *E.coli* XL1-Blue Supercompetent Cells (Stratagene) were sustained on Luria-Bertani (84) agar (LBA). All cultures were grown at 37ºC and liquid cultures were grown at 250 rpm. Ampicillin (Research Products, Inc.) was used as a selective agent for all bacterial transformants.

DNA Manipulation. Genomic DNA from *T. virens* was extracted as previously described (145). Sequencing reactions were completed at the Texas A&M University Gene Technologies Lab. DNA amplified by PCR was purified using the Wizard® SV Gel and PCR Clean-up System (Promega). Plasmids were purified using the Wizard® *Plus* SV Miniprep kit (Promega).

Construction of a point mutation vector. The coding region along with the promoter and terminator of *sm1* were amplified by PCR reaction consisting of 35 cycles (95ºC for 30 seconds, 53ºC for 30 seconds, and 72ºC for 4.5 minutes) using the primers 5'-AAGGAAAAAAAAGAGTGAGCACCCTCCTTT-3' (PTM1) and 5'-CTAGCCGAATCTCACTTTCATCGT-3' (PTM2). The fragment was cloned into the

pGEM-T Easy vector (Promega) and transformed into *E. coli* XL1-Blue (Stratagene). Resulting clones were sequenced, and one was chosen for point mutation (pFKC3).

The Quik Change Site Directed Mutagenesis Kit (Stratagene) was used to create a point mutation in the putative glycosylation site of the coding region of *sm1* in pFKC3. The primers 5'-TCTCCTACGACACCGGCTACGACGATGGCTCC-3' (PTM3) and 5'-AGACGTCGTTCAGAGAGCGGGAGCCATCGTCG-3' were designed to amplify the complete vector with the point mutation following manufacturers instructions. Colonies were screened by blue-white selection for proper insertion into the pGEM vector using the ampicillin resistance marker and two positive clones were sequenced for the point mutation. One (pFKC10) was selected for transformation of *T. virens*.

Transformation and screening of transformants. Transformants were generated by co-transformation of pFKC10 with pCSN43, a vector containing the hygromycin selection cassette, into the *sm1* deletion mutant *T. virens* Δsm1-25 (30). Stable transformants were selected by consecutive transfer of conidia to PDA-H, PDA, and PDA-H. Resulting stable *T. virens* transformants were initially screened by PCR with the same primers for initial amplification of the insert. Three point mutation transformants (ptm5, ptm41, and ptm57) were identified, and the *sm1* coding region sequenced for the presence of the nucleotide change.

Positive transformants were next evaluated for the production of the altered protein. The mutant strains were grown in VMS for 7 days at 27ºC and 135 rpm. Tissue was removed by vacuum filtration and culture filtrate was precipitated using 80% ammonium sulfate. The saturated culture filtrate was centrifuged at 10,000 RPM for 10

minutes using a GSA rotor. The supernatant was decanted and the pellet was resuspended in 20mM ammonium bicarbonate. This solution was dialyzed against 10mM ammonium bicarbonate for 40 hours with 10 buffer changes. The concentration of the resulting protein was determined by NanoDrop (Thermo Fisher) and 40 μg of protein was analyzed by SDS-Page and Western analysis with anti-SM1.

Purification of PTM protein. The transformant ptm41 was grown in 4 liters of VMS for 7 days at room temperature shaking at 150 rpm. Protein was precipitated and dialyzed as described above. The protein was loaded onto a Macro-Prep® High Q Support (Biorad) AEX column preequilibrated with 20mM Tris-HCl (pH 7.5). Proteins were eluted using a 0-0.5 M NaCl gradient in the equilibration buffer. The elution fractions were analyzed by SDS-PAGE and Western blot using the SM1 antibody. Fractions positive for the presence of SM1 were pooled and applied to a Bio-Gel® (Biorad) P-30 gel filtration chromatography (GFC) column equilibrated with 50 mM Tris-HCl (pH 7.5) and 150 mM NaCl. Fractions were analyzed by SDS-PAGE and Western blot.

Native gel electrophoresis. Five micrograms of purified altered SM1 (PTM) or SM1 were suspended in native protein sample buffer (Tris-HCl pH 6.8, bromophenol blue, water, and glycerol) and loaded onto a 15% acrylamide gel lacking sodium dodecyl sulfate (SDS). Samples were run at 30V overnight at 4ºC. The gel was then Coomassie stained and visualized.

Evaluation of dimerization and glycosylation of PTM. To observe protein oligomerization in PTM, the protein was incubated at 4ºC for 7 days. As a control, this

protocol was also performed with SM1. At each 24 hour interval, 5 μg of protein was sampled and stored at -20ºC until use. All samples were run on SDS-PAGE and assayed by Western blot using the anti-SM1 antibody.

Glycosylation staining of PTM. Analysis of protein glycosylation for purified SM1 and PTM was performed using Glycoprotein Detection Reagent (Pierce). Protein with concentration of 1.25mg/mL was treated as per manufacturer instructions. Absorbance measurements were made using a Spectra Fluor UV spectrophotometer (Tecan) at 590nm.

RESULTS

Strains that produce recombinant SM1. A point mutation was created in the coding region of SM1 to change asparagine to aspartic acid at position 10 in the mature protein sequence. This change would effectively delete the putative glycosylation site within the protein. A vector containing a 2kb region of the promoter, the SM1 open reading frame, and a 1kb region of the terminator (Figure 4.1A top panel) was first cloned into a pGEM-T easy vector and then a point mutation was generated within the vector. This vector was used to transform a *sm1* deletion strain and stable transformants were screened using PCR analysis (Figure 4.1A bottom panel). Three transformants (5, 41, and 57) were identified using the *sm1* specific primers and sequenced for the integrity of the *sm1* coding region and the presence of the point mutation. All three transformants were positive for the replacement of an adenine with a guanine within the gene sequence.

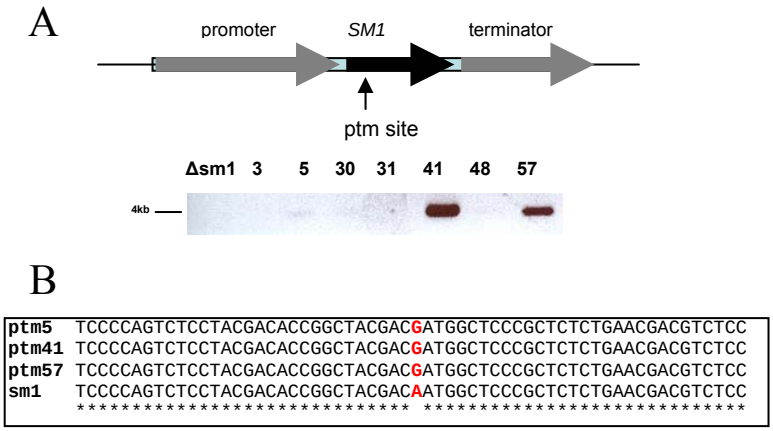

FIG. 4.1. Confirmation of *sm1* point mutation transformants. (A) Point mutation strategy and selection of transformants by PCR. Top panel, point mutation construct: PCR fragment containing a 2 kb upstream region, the open reading frame, and 1kb of the downstream region of *sm1* was cloned into a pGEM-T easy vector (Promega). Bottom panel: gel electrophoresis of a 400bp PCR product amplified from the genomic DNA of 7 putative transformants; lane 1, *sm1* deletion genomic DNA (negative control); lanes 2-8 putative transformants (3, 5, 30, 31, 41, 48, and 57). (B) Sequencing results of PCR positive transformants for presence of a point mutation. Native sequence contains an adenine, whereas the point mutated sequence contains a guanine at the same location.

PTM protein production in transformants. Transformants 5, 41, and 57 were grown for 7 days in VMS in addition to Δsm1-25 as a negative control. The total protein from each strain was dialyzed and run on a SDS-PAGE gel and Coomassie stained (Figure 4.2A). Purified native SM1 was also run on the gel as a positive control. In addition, Western blot analysis using an anti-SM1 antibody was performed (Figure 4.2B). Both the PAGE gel and the Western blot confirmed the presence of PTM and the size of this protein was similar to that of native SM1. Both the gel and the Western revealed that similar to SM1, PTM is primarily in monomer form.

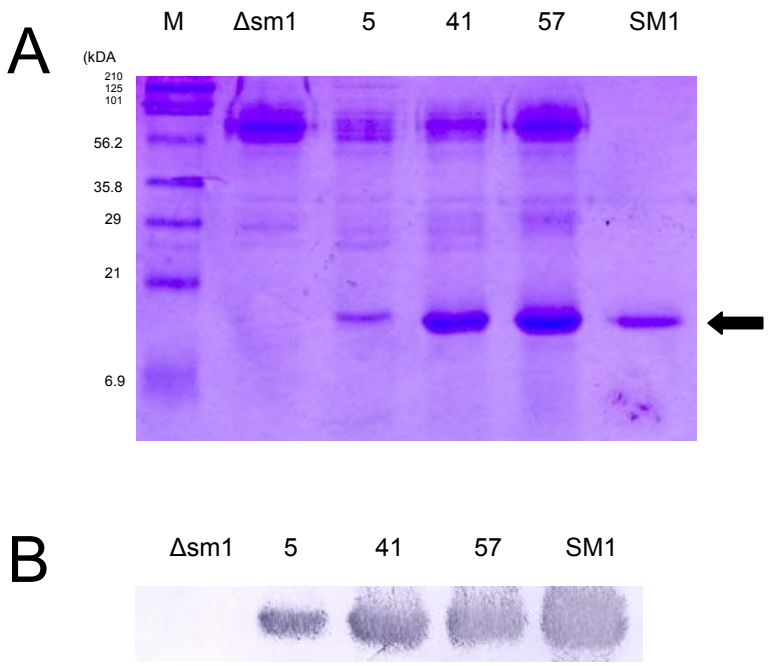

FIG. 4.2. Protein profile of transformants. The *sm1* deletion strain (Δsm1) and point mutation strains compared to purified SM1 protein from *T. virens*. (A) Coomassie stained pattern of the SDS-PAGE analysis for strains grown in VMS and incubated for 7 days at 25ºC. Note that the SM1 from the point mutated strains is the same size as native SM1 (indicated by arrow). (B) Western blotting analysis of point mutation strains using a polyclonal antibody raised against SM1.

Purification of PTM using anion exchange and gel filtration chromatography. To characterize the structure and glycosylation of PTM, we proceeded to purify PTM from transformant culture filtrate. Precipitated total protein was subject to anion exchange (AEX) chromatography. The elution profile is shown in Figure 4.3A. PTM eluted at approximately 80mM NaCl (fraction 18), which is equivalent to what is observed with native SM1. The fraction obtained from AEX was pooled and passed through a gel filtration column and PTM eluted in fractions 62-73 (Figure 4.3B), which is consistent with the properties of SM1. The consecutive chromatography steps allowed for the protein to be purified to homogeneity, and the purity of these final fractions was determined by immunodetection with anti-SM1.

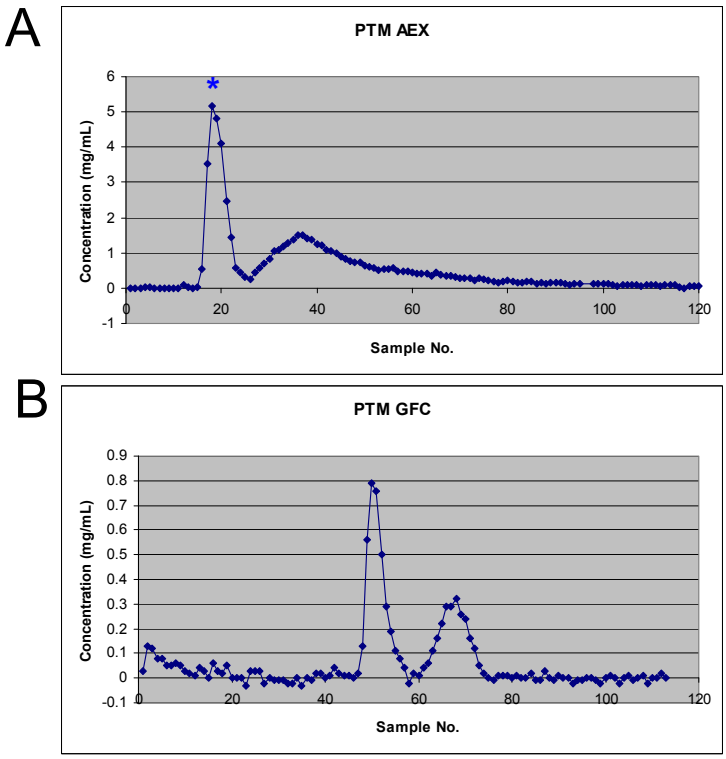

FIG. 4.3. Purification of altered SM1. (A) Anion exchange chromatography (AEX). Precipitated culture filtrate of ptm41 was dialyzed and loaded onto a High Q support column (0.5X20 cm) (Biorad) pre-equilibrated with 20mM Tris-HCl (pH7.5). Proteins were eluted with a 0-0.5 M NaCl linear gradient in the equilibration buffer. Collected fractions were immunodetected using anti-SM1 antibodies. Fractions 18-21 contained PTM (modified protein). (B) Gel filtration chromatography (GFC). Fractions containing PTM from AEX were pooled and purified by GFC through Bio-Gel P30 column (1.0X100cm) (Biorad). Fractions 62-73 were immunodetected and found to contain the PTM protein. The * symbol indicates the location of protein elution.

Analysis of PTM by gel electrophoresis. To observe the characteristics of the purified PTM protein in relation to SM1, both denaturing and native gel electrophoresis was performed. A SDS-PAGE gel (Figure 4.4A) containing both PTM and SM1 indicated no size change in the point mutated protein due to the absence of glycosylation. This was confirmed by Western blot analysis (Figure 4.4B). A non-denaturing native gel was also completed to compare the structure and charge of PTM

and SM1 (Figure 4.4C). Under these conditions PTM moved faster through the gel than purified SM1.

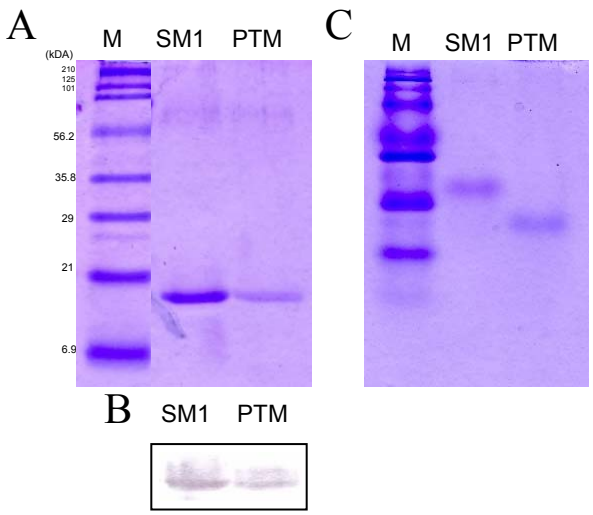

FIG. 4.4. Behavior of PTM and SM1 on protein gels. (A) Purified fractions of PTM were pooled and dialyzed. 5µg of the resulting protein along with 5µg of SM1 were run together on a SDS-Page gel and Coomassie stained. (B) Both pooled fractions and SM1 (5µg each) were run on a SDS-PAGE gel and immunodetected using anti-SM1 antibodies. (C) SM1 and PTM were run on a native protein gel and Coomassie stained.

Evaluation of point mutated protein. Aggregation of other CP proteins was shown to increase over time (96). The oligomeric state of PTM and SM1 in water at 4ºC was evaluated daily for seven days. Aliquots from each time point were evaluated by Western blot using anti-SM1. Over the 7 day time course no difference was observed in the amount of dimerization for both proteins, with their structures remaining primarily as a monomer (Figure 4.5).

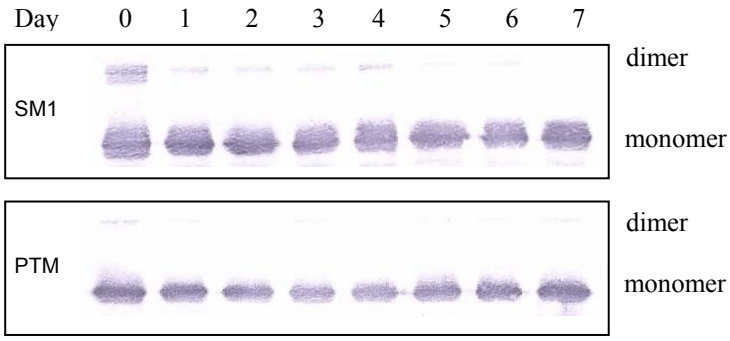

FIG. 4.5. Dimerization of PTM and SM1. Fractions of SM1 and PTM were maintained in water at 4ºC and every 24 hours for 7 days 5 µg of protein was collected. The resulting fractions were run on a SDS-PAGE gel and immunodetected with anti-SM1 antibodies.

Purified forms of SM1 and PTM were stained for glycoprotein detection and evaluated by UV spectrometry. The amount of absorbance detected directly correlated to the amount of sugar bound to the protein. SM1 and PTM had a significantly larger absorbance than the blank control (Figure 4.6). However, there was no difference in absorbance between both proteins indicating no difference in the glycosylation of the two proteins.

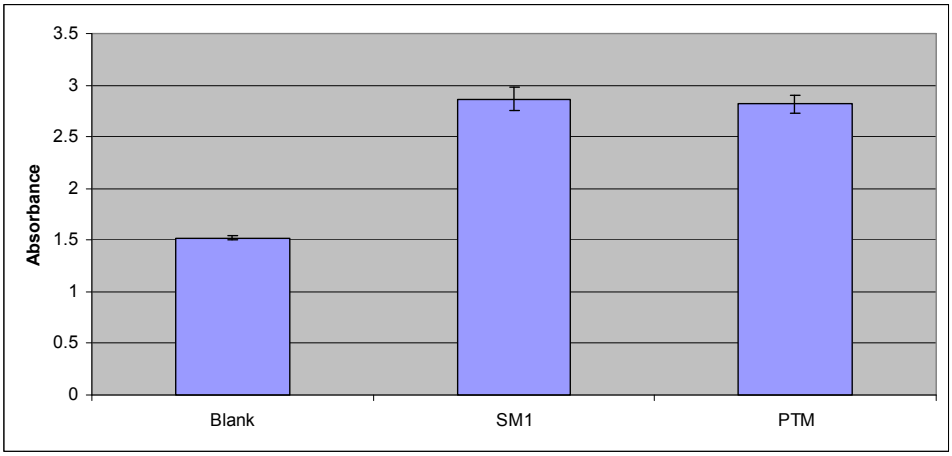

FIG. 4.6. Glycosylation staining of proteins. Recombinant protein (PTM) as compared to SM1 were stained and absorbance at 590 nm was measured.

DISCUSSION

Evaluation of recombinant strains of *T. virens* containing a point mutation in a putative glycosylation site. Protein aggregation is observed in many biological systems and is required for processes such as enzymatic regulation, transcription factor binding, and G-protein coupling (81). Recent research has demonstrated that SM1 exists in culture filtrate as both a monomer and dimer, but only the monomer form had the ability to induce resistance in maize (130). The *T. atroviride* homolog to SM1, EPL1, only naturally exists as a dimer and does not appear to induce resistance (115, 130). A comparison between SM1 and EPL1 indicated that only the monomer form of both proteins was able to elicit defense responses in the plant. These data suggest a mechanism is required for SM1 to maintain its monomeric form, which is necessary to elicit ISR in the plant. The attachment of a sugar moiety to a putative glycosylation site present in SM1 and absent in EPL1 has been hypothesized as the reason SM1 remains in monomer form after secretion (96, 130). To test this hypothesis a point mutation was created in the putative glycosylation site of SM1 and transformed into a *sm1* deletion strain.

Transformants positive for the insertion of the altered *sm1* were analyzed by gel electrophoresis. The size of the recombinant protein on the SDS-PAGE appeared to be the same as what was observed for the native protein. A secondary modification will often cause this protein to run slower on the gel and measure as a larger size due to increased mass. As well, increased amounts of the dimer form of SM1 were not observed on either the SDS-PAGE gel or the Western blot. Both results indicate the

deletion of the putative glycosylation site does not change the behavior of the protein under these conditions, and therefore the protein may not be glycosylated at this site.

Analysis of the protein structure and glycosylation of the altered protein. To study the behavior of PTM further, the protein was purified using anion exchange chromatography (AEX) and gel filtration chromatography (GFC) (Figure 4.3). PTM eluted on AEX at the salt concentration previously documented for SM1 (29, 130). Although the protein had been altered, the overall charge remained sufficiently similar to behave as SM1 under these conditions.

PTM was also evaluated by native gel electrophoresis, in which proteins move through the matrix based on structure and charge. Although the two proteins ran the same on an SDS-PAGE gel (Figure 4.4A) under native conditions, PTM ran faster on the gel than SM1 (Figure 4.4C). The difference in speed between PTM and SM1 may be for two reasons; the structure of PTM had become more globular and could move through the matrix more efficiently, or the charge of PTM may have been altered. The aspargine residue within SM1 was changed to an aspartic acid in PTM. Asparagine has a neutral charge, whereas aspartic acid is an acidic residue. Acidic proteins have a tendency to move faster through a native gel (62), therefore it is mostly likely the change in the charge of the protein facilitated the altered behavior of PTM on a native gel.

Other proteins have been shown to form higher order aggregates over time (96, 120). To understand if this is a similar phenomenon in SM1, proteins were incubated in water at 4ºC and protein fractions collected over seven days. Western blot analysis revealed that there was no change in monomer to dimer ratios observed for either SM1

or PTM during the course of incubation. These data indicate that the putative glycosylation site in SM1 is not involved in maintaining the monomer form of the protein and another mechanism must exist to either facilitate or negate dimer formation in EPL1 and SM1, respectively.

Previously SM1 had a measurable amount of glycosylation when calculated using a glycostain reagent (130). To determine whether the detection of glycosylation is lost in PTM, the glycostain was performed with SM1 and PTM. Both proteins had a statistically similar measured absorbance higher than that of the negative control, indicating glycosylation. As well, the absorbance numbers for SM1 corresponded to previous measurements (Vargas, unpublished).

In conclusion, after mutation, purification, and evaluation of the point mutated protein, the putative glycosylation site is not involved in maintenance of the monomer form of SM1. The site is also not responsible for the measurement of glycosylation of the protein. There are two putative o-glycosylation sites at amino acid 2 and 111 in the mature protein sequence. It is possible that these sites are glycosylated and detected during the glycostain. However, this seems unlikely because recent structural analysis of SM1 has not revealed the presence of any saccharide groups bound to any amino acids within the protein (Krieger and Kenerley, unpublished). The crystal structure of CP has determined that although this protein is not glycosylated, it does interact with oligosaccharides (27). This has allowed us to form the hypothesis that SM1 is not glycosylated; instead it binds with a polysaccharide or another small molecule.

Understanding the potential role these interacting molecules play during elicitation of plant defense priming may present new applications in biocontrol.

CHAPTER V

CONCLUSIONS

Trichoderma virens is a beneficial symbiotic fungus known its ability to protect plants from disease through the production of secondary metabolites and the induction of systemic responses that result in resistance to various pathogens. With the sequenced genome and the availability of molecular tools for gene discovery and manipulation, *T. virens* represents a model system for the study of biocontrol. Both the mechanisms of biocontrol, direct and indirect, are represented in the research presented in this dissertation. The direct system includes the production of volatiles, and the indirect mode of defense is the induction of plant defense responses through proteinaceous elicitors.

A gene cluster present in *T. virens* (vir cluster) contains several genes predicted to be involved in the biosynthesis of terpenoid compounds. The putative genes present in this cluster were four cytochrome P450s, one oxidoreductase, a MFS transporter, and a terpene cyclase. A putative *gapdh* gene was found to be associated with the cluster, but the function of this enzyme in the secondary metabolite production of this cluster is unknown. This cluster is present in members of *Aspergillus*, but species of *Trichoderma* examined lacked close homologs to any of the genes within the cluster sequence. The putative cyclase (*vir4*), thought to encode an enzyme involved in an early step of the terpenoid biosynthetic pathway was examined further to understand the function of the vir cluster. Expression analysis revealed that *vir4* is expressed when *T. virens* is grown

in liquid media conditions. However, when grown in plant roots or in the presence of fungal cell walls, *vir4* was not expressed in *T. virens*.

Mutants with a deletion of the *vir4* ORF were constructed as another approach to assist in resolving the function of *vir4*. Thin layer chromatography and high-pressure liquid chromatography of culture filtrates from the deletion strains confirmed the presence of commonly studied suite of secondary metabolites (e.g. gliotoxin, dimethylgliotoxin, and viridin). When wild-type and deletion strains were analyzed by HS-SPME-GCMS, 35 sesquiterpene volatiles were produced in Gv29-8, but 32 of these compounds were lacking in the *vir* deletion mutants. When *vir4* was complemented by reintegration of the promoter, terminator, and open reading frame into a deletion mutant, the production of all 32 volatile compounds was restored. Expression analysis of the cluster using real-time PCR demonstrated that three genes within the cluster had a significantly greater level of expression in the wild-type than in a deletion strain. Phenotypic measurements showed a decreased growth rate in the deletion strains as compared to wild-type. The complement strains showed partial return of the wild-type growth rate. No differences between the deletion strains and wild-type were observed in fungal confrontation, interaction with *Arabidopsis* seedlings, or effects on bacterial growth and swarming (Chapter II). At present the function of these volatiles in *T. virens* biology is unknown. This work represents the first report of a gene encoding for biosynthesis of volatile compounds in *T. virens*, and a gene cluster involved in terpenoid volatile synthesis in filamentous fungi.

To further understand the role of proteinaceous elicitors in induced systemic resistance, research to identify and characterize homologs of *sm1* with putative elicitor activity was performed. Three homologous sequences to *sm1* were discovered by a search of the *T. virens* genome. Analysis of the conserved motifs within the coding region of these genes and construction of a gene phylogeny confirmed these proteins as members of the cerato-platanin family of proteins. When the promoter regions of these genes were compared to *sm1*, the paralogs revealed less complexity in number and types of transcription factor binding sites examined. However, only *sm3* was found to be expressed in the numerous conditions examined. The *sm3* transcript was identified were in the presence of plant roots and during growth in still-culture. SM3 was produced *Pichia pastoris* to provide sufficient quantities and to promote ease of purification in order to examine the potential of SM3 as an elicitor of ISR. The recombinant protein, picSM3, is glycosylated and can upregulate the defense gene *pal* when applied to maize seedling roots.

Deletion and over-expression strains were constructed to assist in understanding the function of *sm3* in *T. virens*. Observations of SM1 and SM3 on a SDS-PAGE gel revealed different amounts of protein in the deletion mutants compared with Gv29-8 when grown in still-culture. Even though *sm3* was expressed in Δsm1-25, neither SM1 nor SM3 were produced by this mutant. However, in the *sm3* deletion strains, SM3 was not produced, but SM1 was produced in considerably larger quantities than in wild-type. These observations suggest that regulation between the two proteins in still-culture may be linked. Another observation when evaluating the proteins by electrophoresis was the

difference in size between SM1 and SM3, and the production of two bands in the over-expression strains. These two observations suggest, similar to the protein (picSM3) produced in *Pichia*, native SM3 is glycosylated. The deletion strains did not show any differences in the ability to compete with fungal plant pathogens. As well, ISR was not impaired when maize seedlings were inoculated with the deletion or wild-type strains. The inability to detect a difference during in the induction of plant defenses may be due to aggregation of SM3 during interaction with the plant and subsequent loss of elicitor activity (Chapter III).

To further understand the role of protein aggregation by SM1, a point mutation in a putative glycosylation site of the coding region was constructed, changing an asparagine to aspartic acid within the amino acid sequence. Protein size and dimerization was evaluated from strains positive for the insertion of the altered *sm1* by SDS-PAGE and Western analysis. The size and dimerization ratios of the altered protein (PTM) when *T. virens* was grown in VMS were unchanged when compared to native SM1. To evaluate the modified protein in greater detail, PTM was purified using column chromatography which demonstrated the elution of PTM was similar to SM1 during AEX. Although SM1 and PTM run at the same size on an SDS-PAGE gel, analysis by native gel electrophoresis indicated that the structure or charge of PTM was altered sufficiently such that PTM ran faster than SM1. Finally, measurement of glycosylation staining with purified SM1 and PTM indicated no difference in absorbance, as both were positive for carbohydrate staining. These data have allowed us to conclude that n-glycosylation in SM1 is not responsible for preventing dimerization, and that SM1 may

not be glycosylated. Our current hypothesis is that SM1 interacts with a carbohydrate or other small molecule that is responsive to the glycostain (Chapter IV).

REFERENCES

1. **Altschul, S. F., W. Gish, W. Miller, E. W. Myers, and D. J. Lipman.** 1990. Basic local alignment search tool. Journal of Molecular Biology **215:**403-410.

2. **Anisimova, M., and O. Gascuel.** 2006. Approximate likelihood-ratio test for branches: a fast, accurate, and powerful alternative. Systematic Biology **55:**539-552.

3. **Baek, J. M., C. R. Howell, and C. M. Kenerley.** 1999. The role of an extracellular chitinase from *Trichoderma virens* Gv29-8 in the biocontrol of *Rhizoctonia solani*. Current Genetics **35:**41-50.

4. **Baek, J. M., and C. M. Kenerley.** 1998. The arg2 gene of *Trichoderma virens*: cloning and development of a homologous transformation system. Fungal Genetics and Biology **23:**34-44.

5. **Bar, M., M. Sharfman, M. Ron, and A. Avni.** 2010. BAK1 is required for the attenuation of ethylene-inducing xylanase (Eix)-induced defense responses by the decoy receptor LeEix1. Plant Journal **63:**791-800.

6. **Bayram, O., S. Krappmann, M. Ni, J. W. Bok, K. Helmstaedt, O. Valerius, S. Braus-Stromeyer, N. J. Kwon, N. P. Keller, J. H. Yu, and G. H. Braus.** 2008. VelB/VeA/LaeA complex coordinates light signal with fungal development and secondary metabolism. Science **320:**1504-1506.

7. **Benen, L., L. Parenicova, M. K. V. Someren, H. Kester, and J. Visser.** 1996. Molecular genetic and biochemical aspects of pectin degradation in *Aspergillus*, *Progress in Biotechnology*. **14:**331-346.

8. **Benz, I., and M. A. Schmidt.** 2002. Never say never again: protein glycosylation in pathogenic bacteria. Molecular Microbiology **45:**267-276.

9. **Berg, G.** 2009. Plant-microbe interactions promoting plant growth and health: perspectives for controlled use of microorganisms in agriculture. Applied Microbiology Technology **84:**11-18.

10. **Biemelt, S., and U. Sonnewald.** 2006. Plant-microbe interactions to probe regulation of plant carbon metabolism. Journal of Plant Physiology **163:**307-318.

11. **Bok, J. W., and N. P. Keller.** 2004. LaeA, a regulator of secondary metabolism in *Aspergillus* spp. Eukaryotic Cell **3:**527-535.

12. **Brotman, Y., E. Briff, A. Viterbo, and I. Chet.** 2008. Role of swollenin, an expansin-like protein from *Trichoderma*, in plant root colonization. Plant Physiology **147:**779-789.

13. **Bruce, A., R. E. Wheatley, S. N. Humphris, C. A. Hackett, and M. E. J. Florence.** 2000. Production of volatile organic compounds by *Trichoderma* in media containing different amino acids and their effect on selected wood decay fungi. Holzforschung **54:**481-486.

14. **Brunner, K., C. K. Peterbauer, R. L. Mach, M. Lorito, S. Zeilinger, and C. P. Kubicek.** 2003. The Nag1 N-acetylglucosaminidase of *Trichoderma atroviride* is essential for chitinase induction by chitin and of major relevance to biocontrol. Current Genetics **43:**289-295.

15. **Buchanan, B., W. Gruissem, and R. Jones.** 2000. Biocemistry and Molecular Biology of Plants. American Society of Plant Physiologists, Rockville, MD.

16. **Buensanteai, N., P. K. Mukherjee, B. A. Horwitz, C. Cheng, L. J. Dangott, and C. M. Kenerley.** 2009. Expression and purification of biologically active *Trichoderma virens* proteinaceous elicitor Sm1 in *Pichia pastoris*. Protein Expression and Purification **72:**131-138.

17. **Calvo, A. M.** 2008. The VeA regulatory system and its role in morphological and chemical development in fungi. Fungal Genetics and Biology **45:**1053-1061.

18. **Campos, V., R. C. d. Pinho, and E. Freire.** 2010. Volatiles produced by interacting microorganisms potentially useful for the control of plant pathogens. Ciencia e Agrotecnologia **34:**525-535.

19. **Chen, F., J. C. D'Auria, D. Tholl, J. R. Ross, J. Gershenzon, J. P. Noel, and E. Pichersky.** 2003. An *Arabidopsis thaliana* gene for methylsalicylate biosynthesis, identified by a biochemical genomics approach, has a role in defense. Plant Journal **36:**577-588.

20. **Chernin, L., and I. Chet.** 2002. Microbial Enzymes in the Biocontrol of Plant Pathogens and Pests. Marcel Dekker, New York.

21. **Chet, I., G. E. Harman, and R. Baker.** 1981. *Trichoderma hamatum* - Its hyphal interactions with *Rhizoctonia solani* and *Pythium.* . Microbial Ecology **7:**29-38.

22. **Chet, I., and J. Inbar.** 1994. Biological-control of fungal pathogens. Applied Biochemistry and Biotechnology **48:**37-43.

23. **Choudhary, D. K., and B. N. Johri.** 2009. Interactions of *Bacillus* spp. and plants - with special reference to induced systemic resistance (ISR). Microbiological Research **164:**493-513.

24. **Contreras-Cornejo, H. A., L. Macias-Rodriguez, C. Cortes-Penagos, and J. Lopez-Bucio.** 2009. *Trichoderma virens*, a plant beneficial fungus, enhances biomass production and promotes lateral root growth through an auxin-dependent mechanism in *Arabidopsis*. Plant Physiology **149:**1579-1592.

25. **Cortes, C., A. Gutierrez, V. Olmedo, J. Inbar, I. Chet, and A. Herrera-Estrella.** 1998. The expression of genes involved in parasitism by *Trichoderma harzianum* is triggered by a diffusible factor. Molecular and General Genetics **260:**218-225.

26. **Cramer, R. A., E. K. Schwab, and N. Keller.** 2009. Genetic regulation of *Aspergillus* secondary metabolites and their role in fungal pathogenesis. *In* J. P. Latge and W. J. Steinbach (ed.), *Aspergillus fumigatus* and Aspergillosis. ASM Press, Washington DC.

27. **de Oliveira, A. L., M. Gallo, L. Pazzagli, C. E. Benedetti, G. Cappugi, A. Scala, B. Pantera, A. Spisni, T. A. Pertinhez, and D. O. Cicero.** 2011. The structure of the elicitor cerato-platanin (CP), the first member of the CP fungal protein family, reveals a double psi beta-barrel fold and carbohydrate binding. Journal of Biological Chemistry **286:**17560-17568.

28. **Djonovic, S., M. J. Pozo, and C. M. Kenerley.** 2006. Tvbgn3, a beta-1,6-glucanase from the biocontrol fungus *Trichoderma virens*, is involved in mycoparasitism and control of *Pythium ultimum*. Applied and Environmental Microbiology **72:**7661-7670.

29. **Djonovic, S., Pozo, M.J., Dangott, L.J., Howell, C.R., and Kenerley, C.M.** 2006. Sm1, a proteinaceous elicitor secreted by the biocontrol fungus *Trichoderma virens* induces plant defense responses and systemic resistance. Molecular Plant-Microbe Interactions **19:**838-853.

30. **Djonovic, S., Vargas, W.A., Kolomiets, M.V., Horndeski, M., Wiest, A., and Kenerley C.M.** 2007. A proteinaceous elicitor Sm1 from the beneficial fungus *Trichoderma virens* is required for induced systemic resistance in maize. Plant Physiology **145:**875-889.

31. **Druzhinina, I., V. Seidle-Seiboth, A. Herrera-Estrella, B. A. Horwitz, C. Kenerley, E. Monte, P. Mukherjee, S. Zeilinger, I. Grigoriev, and C. P.**

Kubicek. 2011. *Trichoderma*: the genomics of opportunistic success. Nature Reviews Microbiology **9:**749-759.

32. **Durrant, W. E., and X. Dong.** 2004. Systemic acquired resistance. Annual Review of Phytopathology **42:**185-209.

33. **Einhauer, A., and A. Jungbauer.** 2001. The FLAG (TM) peptide, a versatile fusion tag for the purification of recombinant proteins. Journal of Biochemical and Biophysical Methods **49:**455-465.

34. **Engelberth, J., T. Koch, G. Schuler, N. Bachmann, J. Rechtenbach, and W. Boland.** 2001. Ion channel-forming alamethicin is a potent elicitor of volatile biosynthesis and tendril coiling. Cross talk between jasmonate and salicylate signaling in lima bean. Plant Physiology **125:**369-377.

35. **Espino, J. J., G. Gutierrez-Sanchez, N. Brito, P. Shah, R. Orlando, and C. Gonzalez.** 2010. The *Botrytis cinerea* early secretome. Proteomics **10:**3020-3034.

36. **Frias, M., C. Gonzalez, and N. Brito.** 2011. BcSpl1, a cerato-platanin family protein, contributes to *Botrytis cinerea* virulence and elicits the hypersensitive response in the host. New Phytologist **192:**483-495.

37. **Fudal, I., J. Collemare, H. U. Bohnert, D. Melayah, and M. H. Lebrun.** 2007. Expression of *Magnaporthe grisea* avirulence gene ACE1 is connected to the initiation of appressorium-mediated penetration. Eukaryotic Cell **6:**546-554.

38. **Gams, W., and J. Bissett.** 1998. Morphology and identification of *Trichoderma*, p. 1-31. *In* C. P. Kubicek and G. E. Harman (ed.), *Trichoderma & Gliocladium*, vol. 1. Taylor and Francis, Bristol, PA.

39. **Gardiner, D. M., and B. J. Howlett.** 2005. Bioinformatic and expression analysis of the putative gliotoxin biosynthetic gene cluster of *Aspergillus fumigatus*. FEMS Microbiology Letters **248:**241-248.

40. **Ghisalberti, E. L., and K. Sivasithamparam.** 1991. Antifungal antibiotics produced by *Trichoderma* spp. Soil Biology & Biochemistry **23:**1011-1020.

41. **Guerry, P., C. P. Ewing, M. Schirm, M. Lorenzo, J. Kelly, D. Pattarini, G. Majam, P. Thibault, and S. Logan.** 2006. Changes in flagellin glycosylation affect *Campylobacter* autoagglutination and virulence. Molecular Microbiology **60:**299-311.

42. **Guindon, S., J. F. Dufayard, V. Lefort, M. Anisimova, W. Hordijk, and O. Gascuel.** 2010. New algorithms and methods to estimate maximum-likelihood phylogenies: assessing the performance of PhyML 3.0. systematic biology **59:**307-321.

43. **Hanania, U., and A. Avni.** 1997. High-affinity binding site for ethylene-inducing xylanase elicitor on *Nicotiana tabacum* membranes. Plant Journal **12:**113-120.

44. **Harman, G. E.** 2011. Multifunctional fungal plant symbionts: new tools to enhance plant growth and productivity. New Phytologist **189:**647-649.

45. **Harman, G. E.** 2000. Myths and dogmas of biocontrol - changes in perceptions derived from research on *Trichoderma harzianum* T-22. Plant Disease **84:**377-393.

46. **Harman, G. E., C. R. Howell, A. Viterbo, I. Chet, and M. Lorito.** 2004. *Trichoderma* species - opportunistic, avirulent plant symbionts. Nature Reviews Microbiology **2:**43-56.

47. **Harman, G. E., M. A. Obregon, G. J. Samuels, and M. Lorito.** 2010. Changing models for commericialization and implementation of biocontrol in the developing and the developed world. Plant Disease **94:**928-936.

48. **Hopp, T. P., K. S. Prickett, V. L. Price, R. T. Libby, C. J. March, D. P. Cerretti, D. L. Urdal, and P. J. Conlon.** 1988. A short polypeptide marker sequence useful for recombinant protein identification and purification. Bio-Technology **6:**1204-1210.

49. **Howell, C. R., and R. D. Stipanovic.** 1995. Mechanisms in the biocontrol of *Rhizoctonia solani*-induced cotton seedling disease by *Gliocladium virens*: antibiotics. Biol Control **85:**469-472.

50. **Howell, C. R., and R. D. Stipanovic.** 1984. Phytotoxicity to crop plants and herbicidal effects on weeds of viridiol produced by *Gliocladium virens*. Phytopathology **74:**1346-1349.

51. **Howell, C. R., R. D. Stipanovic, and R. D. Lumsden.** 1993. Antibiotic production by strains of *Gliocladium virens* and its relation to the biocontrol of cotton seedling disease. Biocontrol Science and Technology **3:**435-441.

52. **Humphris, S. N., A. Bruce, E. Buultjens, and R. E. Wheatley.** 2002. The effects of volatile microbial secondary metabolites on protein synthesis in *Serpula lacrymans*. FEMS Microbiology Letters **210:**215-219.

53. **Humphris, S. N., R. E. Wheatley, and A. Bruce.** 2001. The effects of specific volatile organic compounds produced by *Trichoderma* spp. on the growth of wood decay basidiomycetes. Holzforschung **55:**233-237.

54. **Hynes, J., C. T. Muller, T. H. Jones, and L. Boddy.** 2007. Changes in volatile production during the course of fungal mycelial interactions between *Hypholoma fasciculare* and *Resinicium bicolor*. Journal of Chemical Ecology **33:**43-57.

55. **Ihle, N. T., R. Williams, S. Chow, W. Chew, M. I. Berggren, G. Pain-Murrieta, D. J. Halter, P. Wipf, R. Abraham, L. Kirkpatrick, and G. Powis.** 2004. Molecular pharmacology and antitumor activity of PX-866, an novel inhibitor of phosphoinositide-3-kinase signalling. Molecular Cancer Therapy **3:**763-772.

56. **Insam, H., and M. S. A. Seewald.** 2010. Volatile organic compounds (VOCs) in soils. Biology and Fertility of Soils **46:**199-213.

57. **Jeong, J. S., T. K. Mitchell, and R. A. Dean.** 2007. The *Magnaporthe grisea* snodprot1 homolog, MSPI, is required for virulence. FEMS Microbiology Letters **273:**157-165.

58. **Jones, R. W., and J. G. Hancock.** 1987. Conversion of viridin to viridiol by viridin-producing fungi. Canadian Journal of Microbiology **33:**963-966.

59. **Keller, N., and T. Hohn.** 1997. Metabolic pathway gene clusters in filamentous fungi. Fungal Genetics and Biology **21:**17-29.

60. **Keller, N. P., G. Turner, and J. W. Bennett.** 2005. Fungal secondary metabolism [mdash] from biochemistry to genomics. Nat Rev Micro **3:**937-947.

61. **Khaldi, N., F. T. Seifuddin, G. Turner, D. Haft, W. C. Nierman, K. H. Wolfe, and N. D. Fedorova.** 2010. SMURF: genomic mapping of fungal secondary metabolite clusters. Fungal Genetics and Biology **47:**736-741.

62. **Krause, F.** 2006. Detection and analysis of protein-protein interactions in organellar and prokaryotic proteomes by native gel electrophoresis: (membrane) protein complexes and supercomplexes. Electrophoresis **27:**2759-2781.

63. **Kubicek, C. P., A. Herrera-Estrella, V. Seidl-Seiboth, D. A. Martinez, I. S. Druzhinina, M. Thon, S. Zeilinger, S. Casas-Flores, B. A. Horwitz, P. K. Mukherjee, M. Mukherjee, L. Kredics, L. D. Alcaraz, A. Aerts, Z. Antal, L. Atanasova, M. G. Cervantes-Badillo, J. Challacombe, O. Chertkov, K. McCluskey, F. Coulpier, N. Deshpande, H. von Dohren, D. J. Ebbole, E. U.**

Esquivel-Naranjo, E. Fekete, M. Flipphi, F. Glaser, E. Y. Gomez-Rodriguez, S. Gruber, C. Han, B. Henrissat, R. Hermosa, M. Hernandez-Onate, L. Karaffa, I. Kosti, S. Le Crom, E. Lindquist, S. Lucas, M. Lubeck, P. S. Lubeck, A. Margeot, B. Metz, M. Misra, H. Nevalainen, M. Omann, N. Packer, G. Perrone, E. E. Uresti-Rivera, A. Salamov, M. Schmoll, B. Seiboth, H. Shapiro, S. Sukno, J. A. Tamayo-Ramos, D. Tisch, A. Wiest, H. H. Wilkinson, M. Zhang, P. M. Coutinho, C. M. Kenerley, E. Monte, S. E. Baker, and I. V. Grigoriev. 2011. Comparative genome sequence analysis underscores mycoparasitism as the ancestral life style of *Trichoderma*. Genome Biology **12:**15.

64. **Kubicek, C. P., M. Komon-Zelazowska, and I. S. Druzhinina.** 2008. Fungal genus *Hypocrea*/*Trichoderma*: from barcodes to biodiversity. Journal of Zhejiang University-Science B **9:**753-763.

65. **Kulmburg, P., M. Mathieu, C. Dowzer, J. Kelly, and B. Felenbok.** 1993. Specific binding-sites in the *alcr* and *alcr* promoters of the ethanol regulon for the CREA repressor mediating carbon catabolite repression in *Aspergillus nidulans*. Molecular Microbiology **7:**847-857.

66. **Kupfahl, C., T. Heinekamp, G. Geginat, T. Ruppert, A. Härtl, H. Hof, and A. A. Brakhage.** 2006. Deletion of the gliP gene of *Aspergillus fumigatus* results in loss of gliotoxin production but has no effect on virulence of the fungus in a low-dose mouse infection model. Molecular Microbiology **62:**292-302.

67. **Lamba, P., S. Sharma, G. D. Munshi, and S. K. Munshi.** 2008. Biochemical changes in sunflower plants due to seed treatment/spray application with biocontrol agents. Phytoparasitica **36:**388-399.

68. **Larkin, M. A., G. Blackshields, N. P. Brown, R. Chenna, P. A. McGettigan, H. McWilliam, F. Valentin, I. M. Wallace, A. Wilm, R. Lopez, J. D. Thompson, T. J. Gibson, and D. G. Higgins.** 2007. Clustal W and clustal X version 2.0. Bioinformatics **23:**2947-2948.

69. **Lee, S.-J., and B. Ahn.** 2009. Comparison of volatile components in fermented soybean pastes using simultaneous distillation and extraction (SDE) with sensory characterisation. Food Chemistry **114:**600-609.

70. **Leite, B., and R. L. Nicholson.** 1993. A volatile self-inhibitor from *Colletotrichum graminicola*. Mycologia **85:**945-951.

71. **Linder, M., G. R. Szilvay, T. Nakari-Setala, H. Soderlund, and M. Penttila.** 2002. Surface adhesion of fusion proteins containing the hydrophobins HFBI and HFBII from *Trichoderma reesei*. Protein Science **11:**2257-2266.

72. **Linder, M. B.** 2009. Hydrophobins: proteins that self assemble at interfaces. Current Opinion in Colloid & Interface Science **14:**356-363.

73. **Linder, M. B., G. R. Szilvay, T. Nakari-Setala, and M. E. Penttila.** 2005. Hydrophobins: the protein-amphiphiles of filamentous fungi. FEMS Microbiology Reviews **29:**877-896.

74. **Lorito, M., S. L. Woo, M. Dambrosio, G. E. Harman, C. K. Hayes, C. P. Kubicek, and F. Scala.** 1996. Synergistic interaction between cell wall degrading enzymes and membrane affecting compounds. Molecular Plant-Microbe Interactions **9:**206-213.

75. **Lorito, M., S. L. Woo, G. E. Harman, and E. Monte.** 2010. Translation research on *Trichoderma*: from 'omics to the field. Annual Review of Phytopathology **48:**395-417.

76. **Lumsden, R. D., J. F. Walter, and C. P. Baker.** 1996. Development of *Gliocladium virens* for damping-off disease control. Canadian Journal of Plant Pathology-Revue Canadienne de Phytopathologie **18:**463-468.

77. **Luti, S., F. Martellini, C. Comparini, P. Bettini, B. Pantera, A. Scala, G. Cappugi, and L. Pazzagli.** 2011. Functional characterization of cerato-platanin, a non-catalytic fungal PAMP involved in the canker stain disease. FEBS Journal **278:**316-316.

78. **Lynch, J. M., and A. J. Moffat.** 2005. Bioremediation - prospects for the future application of innovative applied biological research. Annals of Applied Biology **146:**217-221.

79. **Maldonado, A. M., P. Doerner, R. A. Dixon, C. J. Lamb, and R. K. Cameron.** 2002. A putative lipid transfer protein involved in systemic resistance signalling in *Arabidopsis*. Nature **419:**399-403.

80. **Marchler, G., C. Schuller, G. Adam, and H. Ruis.** 1993. A *Saccaromyces cerevisiae* UAS element controlled by protein kinase-A activitates transcription in response to a variety of stress conditions. EMBO Journal **12:**1997-2003.

81. **Marianayagam, N., M. Sunde, and J. Matthews.** 2004. The power of two: protein dimerization in biology. Trends in Biochemical Sciences **29:**618-625.

82. **McNeal, K. S., and B. E. Herbert.** 2009. Volatile organic metabolites as indicators of soil microbial activity and community composition shifts. Soil Sci. Soc. Am. J. **73:**579-588.

83. **Melin, E., and S. Krupa.** 1971. Studies on ectomycorrhizae of pine. 2. Growth inhibition of mycorrhizal fungi by volatile organic constituents of *Pinus silvestris* (Scots pine) roots. Physiologia Plantarum **25:**337-340.

84. **Miller, J. H.** 1972. Experiments in Molecular Genetics, Cold Spring Harbor, Cold Spring Harbor, New York.

85. **Minerdi, D., S. Bossi, M. L. Gullino, and A. Garibaldi.** 2009. Volatile organic compounds: a potential direct long-distance mechanism for antagonistic action of *Fusarium oxysporum* strain MSA 35. Environmental Microbiology **11:**844-854.

86. **Moran-Diez, E., R. Hermosa, P. Ambrosino, R. E. Cardoza, S. Gutierrez, M. Lorito, and E. Monte.** 2009. The ThPG1 endopolygalacturonase is required for the *Trichoderma harzianum*-plant beneficial interaction. Molecular Plant-Microbe Interactions **22:**1021-1031.

87. **Mukherjee, M., B. A. Horwitz, P. D. Sherkhane, R. Hadar, and P. K. Mukherjee.** 2006. A secondary metabolite biosynthesis cluster in *Trichoderma virens*: evidence from analysis of genes underexpressed in a mutant defective in morphogenesis and antibiotic production. Current Genetics **50:**193-202.

88. **Mukherjee, P. K., and C. M. Kenerley.** 2010. Regulation of morphogenesis and biocontrol properties in *Trichoderma virens* by a VELVET protein, Vel1. Applied and Environmental Microbiology **76:**2345-2352.

89. **Mukherjee, P. K., A. Wiest, N. Ruiz, A. Keightley, M. E. Moran-Diez, K. McCluskey, Y. F. Pouchus, and C. M. Kenerley.** 2011. Two classes of new peptaibols are synthesized by a single non-ribosomal peptide synthetase of *Trichoderma virens*. Journal of Biological Chemistry **286:**4544-4554.

90. **Neilands, J. B.** 1995. Siderophores - structure and function of microbial iron transport compounds. Journal of Biological Chemistry **270:**26723-26726.

91. **Nemcovic, M., L. Jakubikova, I. Viden, and V. Farkas.** 2008. Induction of conidiation by endogenous volatile compounds in *Trichoderma* spp. FEMS Microbiology Letters **284:**231-236.

92. **Nurnberger, T., and B. Kemmerling.** 2009. PAMP-triggered basal immunity in plants, p. 1-38. *In* L. C. VanLoon (ed.), Plant Innate Immunity, vol. 51. Academic Press Ltd-Elsevier Science Ltd, London.

93. **Oostendorp, M., W. Kunz, B. Dietrich, and T. Staub.** 2001. Induced disease resistance in plants by chemicals. European Journal of Plant Pathology **107:**19-28.

94. **Osbourn, A.** 2010. Secondary metabolic gene clusters: evolutionary toolkits for chemical innovation. Trends in Genetics **26:**449-457.

95. **Pazzagli, L., Cappugi, G., Manao, G., Camici, G., Santini A., and Scala, A.** 1999. Purification, characterization, and amino acid sequence of cerato-platanin, a new phytotoxic protein from *Ceratocystis fimbriata f.sp. platani*. The Journal of Biological Chemistry **274:**24959-24964.

96. **Pazzagli, L., C. Zoppi, L. Carresi, B. Tiribilli, F. Sbrana, S. Schiff, T. A. Pertinhez, A. Scala, and G. Cappugi.** 2009. Characterization of ordered aggregates of cerato-platanin and their involvement in fungus-host interactions. Biochimica Et Biophysica Acta-General Subjects **1790:**1334-1344.

97. **PE Applied Biosystems.** 2001. Sequence detector user bulletin 2. PE Applied Biosystems, 1-36.

98. **Peberdy, J. F.** 1994. Protein secretion in filamentous fungi - trying to understand a highly productive black box. Trends in Biotechnology **12:**50-57.

99. **Pozo, M. J., J. M. Baek, J. M. Garcia, and C. M. Kenerley.** 2004. Functional analysis of tvsp1, a serine protease-encoding gene in the biocontrol agent *Trichoderma virens*. Fungal Genetics and Biology **41:**336-348.

100. **Quinones, B., G. Dulla, and S. E. Lindow.** 2005. Quorum sensing regulates exopolysaccharide production, motility, and virulence in *Pseudomonas syringae*. Molecular Plant-Microbe Interactions **18:**682-693.

101. **Ravagnani, A., L. Gorfinkiel, T. Langdon, G. Diallinas, E. Adjadj, S. Demais, D. Gorton, H. N. Arst, and C. Scazzocchio.** 1997. Subtle hydrophobic interactions between the seventh residue of the zinc finger loop and the first base of an HGATAR sequence determine promoter-specific recognition by the *Aspergillus nidulans* GATA factor AreA. EMBO Journal **16:**3974-3986.

102. **Reino, J. L., R. F. Guerro, R. Hernandez-Galan, and I. G. Collado.** 2008. Secondary metabolites from species of the biocontrol agent *Trichoderma*. Phytochemistry Review **7:**89-123.

103. **Rispail, N., and A. Di Pietro.** 2009. *Fusarium oxysporum* Ste12 controls invasive growth and virulence downstream of the fmk1 MAPK cascade. Molecular Plant-Microbe Interactions **22:**830-839.

104. **Ron, M., and A. Avni.** 2004. The receptor for the fungal elicitor ethylene-inducing xylanase is a member of a resistance-like gene family in tomato. Plant Cell **16:**1604-1615.

105. **Rosenberg, I., B. J. Cherayil, K. J. Isselbacher, and S. Pillai.** 1991. MAC-2-binding glycoproteins - putative ligands for a cytosolic beta-galactoside lectin. Journal of Biological Chemistry **266:**18731-18736.

106. **Rosewich, U. L., and H. C. Kistler.** 2000. Role of horizontal gene transfer in the evolution of fungi. Annual Review of Phytopathology **38:**325-363.

107. **Salas-Marina, M. A., M. A. Silva-Flores, E. E. Uresti-Rivera, E. Castro-Longoria, A. Herrera-Estrella, and S. Casas-Flores.** 2011. Colonization of *Arabisopsis* roots by *Trichoderma atroviride* promotes growth and enhances systemic disease resistance through jasmonic acid/ethylene and salicylic acid pathways. European Journal of Plant Pathology **131:**15-26.

108. **Sambrook, J., E. F. Fritsch, and T. Maniatis.** 1989. Molecular Cloning: A Laboratory Manual. Cold Spring Harbor Laboratory Press, Cold Spring Harbor, NY.

109. **Scala, A., L. Pazzagli, C. Comparini, A. Santini, S. Tegli, and G. Cappugi.** 2004. Cerato-platanin, an early-produced protein by *Ceratocystis fimbriata* f. sp. *platani*, elicits phytoalexin synthesis in host and non-host plants. Journal of Plant Pathology **86**.

110. **Schirmbock, M., M. Lorito, Y. L. Wang, C. K. Hayes, I. Arisanatac, F. Scala, G. E. Harman, and C. P. Kubicek.** 1994. Parallel formation and synergism of hydrolytic enzymes and peptaibol antibiotics, molecular mechanisms involved in the antagonistic action of *Trichoderma harzianum* against phytopathogenic fungi. Applied and Environmental Microbiology **60:**4364-4370.

111. **Schmitt, I., and H. T. Lumbsch.** 2009. Ancient horizontal gene transfer from bacteria enhances biosynthetic capabilities of fungi. Plos ONE **4:**1-8.

112. **Schuster, A., and M. Schmoll.** 2010. Biology and biotechnology of *Trichoderma*. Appl Microbiol Biotechnol **87:**787-799.

113. **Segarra, G., E. Casanova, M. Aviles, and I. Trillas.** 2010. *Trichoderma asperellum* strain T34 controls Fusarium wilt disease in tomato plants in soilless culture through competition for iron. Microbial Ecology **59:**141-149.

114. **Segarra, G., S. Van der Ent, I. Trillas, and C. M. J. Pieterse.** 2009. MYB72, a node of convergence in induced systemic resistance triggered by a fungal and a bacterial beneficial microbe. Plant Biology **11:**90-96.

115. **Seidl, V., M. Marchetti, R. Schandl, G. Allmaier, and C. P. Kubicek.** 2006. Epl1, the major secreted protein of *Hypocrea atroviride* on glucose, is a member of a strongly conserved protein family comprising plant defense response elicitors. FEBS Journal **273:**4346-4359.

116. **Shoresh, M., and G. E. Harman.** 2008. The molecular basis of shoot responses of maize seedlings to *Trichoderma harzianum* T22 inoculation of the root: a proteomic approach. Plant Physiology **147:**2147-2163.

117. **Shoresh, M., G. E. Harman, and F. Mastouri.** 2010. Induced systemic resistance and plant responses to fungal biocontrol agents. Annual Review of Phytopathology **48:**41-43.

118. **Shoresh, M., I. Yedidia, and I. Chet.** 2005. Involvement of jasmonic acid/ethylene signaling pathway in the systemic resistance induced in cucumber by *Trichoderma asperellum* T203. Phytopathology **95:**76-84.

119. **Sivasithamparam, K., and E. L. Ghisalberti.** 1998. Secondary metabolism in *Trichoderma* and *Gliocladium*, p. 139-191. *In* C. P. Kubicek and G. E. Harman (ed.), *Trichoderma* and *Gliocladium*. Taylor & Francis Inc.: Bristol, PA.

120. **Solovyov, A., and H. F. Gilbert.** 2004. Zinc-dependent dimerization of the folding catalyst, protein disulfide isomerase. Protein Science **13:**1902-1907.

121. **Splivallo, R., U. Fischer, C. Gobel, I. Feussner, and P. Karlovsky.** 2009. Truffles regulate plant root morphogenesis via the production of auxin and ethylene. Plant Physiology **150:**2018-2029.

122. **Stoppacher, N., B. Kluger, S. Zeilinger, R. Krska, and R. Schuhmacher.** 2010. Identification and profiling of volatile metabolites of the biocontrol fungus *Trichoderma atroviride* by HS-SPME-GC-MS. Journal of Microbiological Methods **81:**187-193.

123. **Strobel, G.** 2006. *Muscodor albus* and its biological promise. Journal of Industrial Microbiology & Biotechnology **33:**514-522.

124. **Strobel, G. A., E. Dirkse, J. Sears, and C. Markworth.** 2001. Volatile antimicrobials from *Muscodor albus*, a novel endophytic fungus. Microbiology **147:**2943-2950.

125. **Tao, L., and J. H. Yu.** 2009. AbaA and WetA govern distinct stages of *Aspergillus fumigatus* development. Microbiology **157:**313-326.

126. **Terry, L. A., and D. C. Joyce.** 2004. Elicitors of induced disease resistance in postharvest horticultural crops: a brief review. Postharvest Biology and Technology **32:**1-13.

127. **Tilburn, J., S. Sarkar, D. A. Widdick, E. A. Espeso, M. Orejas, J. Mungroo, M. A. Penalva, and H. N. Arst.** 1995. The *Aspergillus* PacC zinc-finger transcription factor mediates regulation of both acid-expressed and alkaline-expressed genes by ambient pH. EMBO Journal **14:**779-790.

128. **Torkkeli, M., R. Serimaa, O. Ikkala, and M. Linder.** 2002. Aggregation and self-assembly of hydrophobins from *Trichoderma reesei*: Low-resolution structural models. Biophysical Journal **83:**2240-2247.

129. **Vargas, W. A., F. K. Crutcher, and C. M. Kenerley.** 2011. Functional characterization of a plant-like sucrose transporter from the beneficial fungus *Trichoderma virens*. Regulation of the symbiotic association with plants by sucrose metabolism inside the fungal cells. New Phytologist **189:**777-789.

130. **Vargas, W. A., Djonovic, S., Sukno, S.A., and Kenerley, C.M.** 2008. Dimerization controls the activity of fungal elicitors that trigger systemic resistance in plants. The Journal of Biological Chemistry **283:**19804-19815.

131. **Vargas, W. A., J. C. Mandawe, and C. M. Kenerley.** 2009. Plant-derived sucrose is a key element in the symbiotic association between *Trichoderma virens* and maize plants. Plant Physiology **151:**792-808.

132. **Vinale, F., K. Sivasithamparam, E. L. Ghisalberti, R. Marra, M. J. Barbetti, H. Li, S. L. Woo, and M. Lorito.** 2008. A novel role for *Trichoderma* secondary metabolites in the interactions with plants. Physiological and Molecular Plant Pathology **72:**80-86.

133. **Viterbo, A., and I. Chet.** 2006. TasHyd1, a new hydrophobin gene from the biocontrol agent *Trichoderma asperellum*, is involved in plant root colonization. Molecular Plant Pathology **7:**249-258.

134. **Viterbo, A., J. Inbar, Y. Hadar, and I. Chet.** 2007. Plant disease biocontrol and induced resistance via fungal mycoparasites. *In* C. P. Kubicek and I. Druzhinina (ed.), The Mycota IV: Environmental and Microbial Relationships. Springer, Heidelberg, Germany.

135. **Viterbo, A., A. Wiest, Y. Brotman, I. Chet, and C. Kenerley.** 2007. The 18mer peptaibols from *Trichoderma virens* elicit plant defense responses. Molecular Plant Pathology **8:**737-746.

136. **Vogel, H. J.** 1956. A convenient growth medium for *Neurospora* (Medium N). Microbiol. Genet. Bull. **13:**42-43.

137. **Weindling, R., and O. H. Emerson.** 1936. The isolation of a toxic substance from the culture filtrate of *Trichoderma*. Phytopathology **26:**1068-1070.

138. **Wenke, K., M. Kai, and B. Piechulla.** 2010. Belowground volatiles facilitate interactions between plant roots and soil organisms. Planta **231:**499-506.

139. **Westholm, J. O., N. Nordberg, E. Muren, A. Ameur, J. Komorowski, and H. Ronne.** 2008. Combinatorial control of gene expression by the three yeast repressors Mig1, Mig2 and Mig3. Bmc Genomics **9:**15.

140. **Wheatley, R., C. Hackett, A. Bruce, and A. Kundzewicz.** 1997. Effect of substrate composition on production of volatile organic compounds from *Trichoderma* spp. inhibitor to wood decay fungi. International Biodeterioration and Biodegradation **39:**199-205.

141. **Wiest, A., A. Viterbo, I. Chet, and C. Kenerley.** 2005. Analysis of the *Trichoderma virens* NRPS gene, tex1: expression and effect on biocontrol. Phytopathology **95:**S111-S111.

142. **Wilson, L. M., A. Idnurm, and B. J. Howlett.** 2002. Characterization of a gene (sp1) encoding a secreted protein from *Leptosphaeria maculans*, the blackleg pathogen of *Brassica napus*. Molecular Plant Pathology **3:**487-493.

143. **Wipf, P., D. J. Minion, R. J. Hlater, M. I. Berggren, C. B. Ho, G. G. Chiang, L. Kirkpatrick, R. Abraham, and G. Powis.** 2004. Synthesis and biological evaluation of synthetic viridin derived from C (20)-heteroalkylation of the steroidal PI-3-kinase inhibitor wortmannin. Organic Biomolecular Chemistry **2:**1911-1920.

144. **Woo, S. L., F. Scala, M. Ruocco, and M. Lorito.** 2006. The molecular biology of the interactions between *Trichoderma* spp., phytopathogenic fungi, and plants. Phytopathology **96:**181-185.

145. **Xu, B. W., J. R. Wild, and C. M. Kenerley.** 1996. Enhanced expression of a bacterial gene for pesticide degradation in a common soil fungus. Journal of Fermentation and Bioengineering **81:**473-481.

146. **Yang, Y. Y., H. J. Zhang, G. J. Li, W. Li, X. E. Wang, and F. M. Song.** 2009. Ectopic expression of MgSM1, a Cerato-platanin family protein from *Magnaporthe grisea*, confers broad-spectrum disease resistance in *Arabidopsis*. Plant Biotechnology Journal **7:**763-777.

147. **Yedidia, I., N. Benhamou, and I. Chet.** 1999. Induction of defense responses in cucumber plants (*Cucumis sativus* L.) by the biocontrol agent *Trichoderma harzianum*. Applied and Environmental Microbiology **65:**1061-1070.

148. **Yedidia, I., N. Benhamou, Y. Kapulnik, and I. Chet.** 2000. Induction and accumulation of PR proteins activity during early stages of root colonization by the mycoparasite *Trichoderma harzianum* strain T-203. Plant Physiology and Biochemistry **38:**863-873.

149. **Yedidia, I., M. Shoresh, Z. Kerem, N. Benhamou, Y. Kapulnik, and I. Chet.** 2003. Concomitant induction of systemic resistance to *Pseudomonas spingae* pv. *lachrymans* in cucumber by *Trichoderma asperellum* (T-203) and accumulation of phytoalexins. Applied and Environmental Microbiology **69:**7343-7353.

150. **Yedidia, I., A. K. Srivastva, Y. Kapulnik, and I. Chet.** 2001. Effect of *Trichoderma harzianum* on microelement concentrations and increased growth of cucumber plants. Plant and Soil **235:**235-242.

151. **Yin, W. B., and N. P. Keller.** 2011. Transcriptional regulatory elements in fungal secondary metabolism. Journal of Microbiology **49:**329-339.

152. **Yu, J. H., and N. Keller.** 2005. Regulation of secondary metabolism in filamentous fungi, p. 437-458, Annual Review of Phytopathology, vol. 43. Annual Reviews, Palo Alto.

153. **Zipfel, C., G. Kunze, D. Chinchilla, A. Caniard, J. D. G. Jones, T. Boller, and G. Felix.** 2006. Perception of the bacterial PAMP EF-Tu by the receptor EFR restricts *Agrobacterium*-mediated transformation. Cell **125:**749-760.

VITA

Name:	Frankie Kay Crutcher
Address:	Department of Plant Pathology and Microbiology Texas A&M University, College Station, TX 77843-2132
Email Address:	fkc@tamu.edu
Education:	2006-B.S. Montana State University, Major: Plant Biotechnology 2011-Ph.D. Texas A&M University, Major: Genetics